POST-TRANSCRIPTIONAL REGULATION BY microRNAS IN PREGNANCY AND PARTURITION

APPROVED BY SUPERVISORY COMMITTEE

Carole R. Mendelson, Ph.D.

Alexander Pertsemlidis, Ph.D.

Mala Mahendroo, Ph.D.

Eric N. Olson, Ph.D.

Ellen S. Vitetta, Ph.D.

DEDICATION

I would like to thank my family for their unrelenting support throughout all my schooling. I thank my parents, who have engrained in me both the confidence to approach the seemingly impossible and the skills to solve such challenges creatively. I thank my brother and sister, who are my greatest friends and have saved me on so many occasions. I thank my grandparents, who have taught me discipline and respect for a job well done. I also thank Mr. Israel Solon (Greenhill School), Dr. Christine Buchanan (Southern Methodist University), Dr. David Crews (The University of Texas at Austin), Dr. Amelia Eisch, Dr. Ellen Vitetta, and Dr. Iowna Stroynowski (UT Southwestern), who took the time to teach me basic biology and who inspired my interest in biomedical research. I thank my thesis advisor, Dr. Carole Mendelson, for her mentorship in lab and in life. From her obvious passion for science, to her dedication to improving the community, to her life as mother of four, she somehow does it all and has been an amazing role model. I also thank the Medical Scientist Training Program, whose support has kept me motivated and fascinated by all aspects of biology and medicine. Finally, I thank my husband and secret weapon, Will, without whom this work would not have been as enjoyable or even possible, and my children, Amber and Sawyer, who bring meaning to my universe and inspire me to dedicate myself to helping others less fortunate.

POST-TRANSCRIPTIONAL REGULATION BY microRNAS IN PREGNANCY AND PARTURITION

by

NORA EDWARDS RENTHAL

DISSERTATION

Presented to the Faculty of the Graduate School of Biomedical Sciences

The University of Texas Southwestern Medical Center at Dallas

In Partial Fulfillment of the Requirements

For the Degree of

DOCTOR OF PHILOSOPHY

The University of Texas Southwestern Medical Center at Dallas

Dallas, Texas

September, 2010

POST-TRANSCRIPTIONAL REGULATION BY microRNAS IN PREGNANCY AND PARTURITION

NORA EDWARDS RENTHAL, Ph.D.

The University of Texas Southwestern Medical Center at Dallas, 2010

CAROLE R. MENDELSON, Ph.D.

Throughout most of pregnancy, uterine quiescence is maintained by increased progesterone receptor (PR) transcriptional activity, while spontaneous labor is initiated/facilitated by a concerted series of biochemical events that activate inflammatory pathways and negatively impact PR function. In this study, we uncovered a new regulatory pathway whereby miRNAs serve as hormonally-modulated and conserved mediators of contractile gene regulation in the pregnant uterus from mouse to human. Using miRNA and gene expression microarray

analyses of uterine tissues, we identified a conserved family of miRNAs, the miR-200 family, that is highly induced at term in both mice and humans, as well as two coordinately downregulated targets, zinc finger E-box binding homeobox proteins, ZEB1 and ZEB2, which act as transcriptional repressors. We also observed upregulation of the miR-200 family and downregulation of ZEB1 and ZEB2 in two different mouse models of preterm labor. We further demonstrated that ZEB1 is directly upregulated by the action of P_4/PR at the *ZEB1* promoter. Excitingly, we observed that ZEB1 and ZEB2 inhibited expression of the contraction-associated genes, *oxytocin receptor* and *connexin-43* and blocked oxytocin-induced contractility in human myometrial cells. Together, these findings implicate the miR-200 family and their targets ZEB1 and ZEB2 as novel P_4/PR-mediated regulators of uterine quiescence and contractility during pregnancy and labor, and shed new light on the molecular mechanisms involved in preterm birth.

TABLE OF CONTENTS

PRIOR PUBLICATIONS

RESEARCH ARTICLES

1. **Edwards NA**, Kriegsfeld L, Crews D. (2004) Neural substrates for sexual and thermoregulatory behavior in the male leopard gecko, Eublepharis macularius. *Brain Research* 10;1029(1):77-83.

2. Russo SJ, Bolanos CA, Theobald DE, Decarolis N, Renthal W, Kumar A, Winstanley, CA, **Renthal NE**, Wiley, MD, Self DW, Russell DS, Neve RL, Eisch AJ, Nestler EJ. (2006) IRS2-Akt pathway in midbrain dopamine neurons regulates behavioral and cellular responses to opiates. *Nature Neuroscience.* 10:93-9.

3. **Renthal NE**, Chen CC, Williams KC, Gerard RD, Prange-Kiel J, Mendelson CR. (2010) The miR-200 family and targets, ZEB1 and ZEB2, modulate uterine quiescence and contractility during pregnancy and labor. *Proceedings of the National Academy of Sciences*. 107(48): 20828-20833.

4. **Renthal NE**, Guidry PA, Shanmuganad S, Renthal W, Stroynowski I. (2011) Isoforms of the nonclassical class I MHC antigen H2-Q5 are enriched in brain and encode Qdm peptide. Immunogenetics. 63(1): 57-64.

PUBLISHED ABSTRACTS

1. **Renthal NE,** Mendelson CR. Regulation of Inflammatory and Contractile Genes by miRNAs during Pregnancy and Labor. *91st Annual Meeting of The Endocrine Society Abstracts 2009.*
2. **Renthal NE,** Mendelson CR. Regulation of Inflammatory and Contractile Genes by miRNAs during Pregnancy and Labor. *Texas Forum for Reproductive Sciences Abstracts 2009.*
3. **Renthal NE,** Mendelson CR The miR-200/429 Family serves as a Potent Regulator of Myometrial Contractile Gene Expression during Pregnancy and Labor. *Keystone Symposium - RNA Silencing: Mechanism, Biology and Application Abstracts 2010.*
4. **Renthal NE,** Mendelson CR. The miR-200/429 Family Serves as a Potent Regulator of Myometrial Contractile Gene Expression during Pregnancy and Labor. *Texas Forum for Reproductive Sciences Abstracts 2010.*
5. **Renthal NE**, Chen CC, Gerard RD, Mendelson CR. The miR-200/429 Family Serves as a Potent Regulator of Myometrial Contractile Gene Expression during Pregnancy and Labor. Endocrine Reviews 31: 3, Supplement 1, June 2010.

LIST OF FIGURES

CHAPTER 1 – Introduction

CHAPTER 2- SECTION 1 – A Role for MicroRNAs in the Timing of Labor

CHAPTER 2- SECTION 2 –miR-200s Regulate ZEB1 & ZEB2 Expression

CHAPTER 2- SECTION 3 –Conservation of the miR-200 / ZEB Relationship

CHAPTER 2- SECTION 4 – miR-200 / ZEBs in Models of Preterm Labor

CHAPTER 2- SECTION 5 –Hormonal Regulation of miR-200s and ZEBs

CHAPTER 2- SECTION 6 – Inhibition of Contractile-Associated Genes and Contraction by miR-200s and ZEBs

APPENDIX: Year One of Graduate Training – Brain-Expressed Isoforms of the Nonclassical Class I MHC Antigen Encode Qdm Peptide

LIST OF TABLES

LIST OF APPENDICES

LIST OF DEFINITIONS

Abbreviation	Definition
20α-HSD	20α-Hydroxysteroid Dehydrogenase
β-gal	Beta-galactosidase
CCL-2	Chemoattractant Protein 1
ChIP	Chromatin Immunoprecipitation
COX-1	Cyclooxygenase-1
COX-2	Cyclooxygenase-2
CRH	Corticotropin Releasing Hormone
CtBP	C-terminal binding protein
CXN-43	Connexin-43
dpc	Days post coitum
EMT	Epithelial-mesenchymal transition
Exp5	Exportin-5
FBS	Fetal Bovine Serum
FDR	False Discovery Rate
HEK-293	Human Embryonic Kidney 293 Cells
HLA	Human Leukocyte Antigen
hTERT-HM	Human telomerase reverse transcriptase-Immortalized Myometrial Cells
IFNγ	Interferon gamma
IHC	Immunohistochemistry
IκB	Inhibitor of kappa B
ISH	In Situ Hybridization

LPS	Lipopolysaccharide
MHC	Major Histocompatibility Complex
miRNA	microRNA
NF-κB	Nuclear factor kappa B
OXTR	Oxytocin Receptor
P_4	Progesterone
PGHS-1	Prostaglandin H Synthetase 1
PGHS-2	Prostaglandin H Synthetase 2
PIR-B	Paired immunoglobulin like receptor-B
PR	Progesterone Receptor
PRKO	Progesterone receptor knockout mice
qRT-PCR	Quantitative Real-Time Polymerase Chain Reaction
RISC	RNA-Induced Silencing Complex
SP-A	Surfactant Protein-A
TAP2	Transporter Associated with Antigen Processing 2
TM	Transmembrane Domain
UTR	Untranslated Region
WT	Wild Type
ZEB1	Zinc Finger E-Box-Binding Homeobox 1
ZEB2	Zinc Finger E-Box-Binding Homeobox 2

CHAPTER 1
Introduction

The Dilemma of Preterm Birth

Premature birth, defined as birth before 37 completed weeks gestation, is the leading cause of neonatal morbidity and mortality in developed countries (Mendelson, 2009). The delivery of infants before 30 weeks gestation is associated with high levels of perinatal mortality and morbidity, including increased incidence of respiratory distress syndrome, intraventricular hemorrhage, patent ductus arteriosus, necrotizing enterocolitis, infection, jaundice, anemia, and a host of other diseases. Furthermore, in addition to immeasurable emotional and social costs, neonatal intensive care in the United States alone costs at least $26 billion a year, according to the Institute of Medicine of the National Academies.

Despite advances in the care of low birth weight infants, which currently allow for the recovery of premature babies born as early as 24 weeks gestation (Jobe, 2010), the rates of preterm birth in the United States have been steadily increasing to a current level of 12.3% of all births annually (Martin et al., 2007), suggesting that advances in our ability to care for premature infants postnatally have far outpaced advances in obstetrics to maintain the length of gestation for at least 38 weeks.

As over half a million women annually in the United States and more than 1.5 million women worldwide could benefit from treatment to postpone the onset of labor, the development of more effective uterine tocolytic agents remains a pressing objective for the medical and scientific community. In particular, the control of myometrial excitability has important therapeutic implications for patients at risk of preterm labor. However, the signaling mechanisms that maintain uterine quiescence during pregnancy and promote increased uterine contractility leading to labor at term and preterm remain incompletely defined (Mendelson, 2009). It is our hope that an increased understanding of the molecular and physiological mechanisms underpinning the genesis and pathogenesis of human labor will serve to aid in the identification of novel therapeutics to modulate myometrial contractility.

Multiple Pathways in the Initiation of Parturition

While the mechanisms that lead to term and preterm labor have yet to be fully identified, several molecules have long been understood to play an important role in the maintenance of pregnancy and the timing of mammalian parturition. Various pathways- endocrine, inflammatory, and mechanical- have been shown to regulate the timing of parturition (Figure 1-1.1). The endocrine cascade leading to parturition includes an increase in maternal estrogens, an increase in the metabolism of progesterone, and changes in PR function. One mechanism by which the actions of progesterone and estrogen are thought to regulate parturition is through their potent effects on the inflammatory pathway.

Preterm and term labor are associated with an inflammatory response in both the fetal (amniotic fluid and fetal membranes) and maternal (myometrium, endometrium, and cervix) compartments. This is exemplified by observations of neutrophil and macrophage infiltration into the myometrium, cervix, and fetal membranes during term and preterm labor (Cox et al., 1997, Osman et al., 2003). It is thought that these invading immune cells then secrete cytokines and chemokines (Romero et al., 2007), resulting in the activation of proinflammatory transcription factors, such as NF-κB, in the myometrium (Condon et al., 2006, Condon et al., 2004), cervical epithelium (Elliott et al., 2001) and amniotic

membranes (Allport et al., 2001, Lee et al., 2005). Indeed, increased proinflammatory cytokines, such as IL-1β, IL-6, and IL-8, have been observed in the amniotic fluid during preterm and term labor an (Osman et al., 2003, Thomson et al., 1999, Condon et al., 2004). Then, activated NF-kB increases expression of contraction-associated genes, including the prostaglandin F2α receptor (PGF2R) (Olson, 2003), the gap junction protein, connexin-43 (CXN-43) (Chow and Lye, 1994), the oxytocin receptor (OXTR) (Fuchs et al., 1984), and COX-2 (Soloff et al., 2004). In preterm labor, intrauterine and intraamniotic infection may provide the stimulus for increased amniotic fluid interleukins and inflammatory cell migration (Cherouny et al., 1993). While at term, mechanical stretch (Shynlova et al., 2008, Sooranna et al., 2004) caused by the growing fetus, withdrawal of P4/PR function, increased production of estrogens, as well as signals produced by the developing fetus near term (Condon et al., 2004, Shaw and Renfree, 2001, Challis et al., 2000, Mitchell et al., 1984), may promote production of chemokines leading to neutrophil and macrophage migration and up-regulation of inflammatory response pathways.

Progesterone, elevated throughout gestation, acts to maintain uterine quiescence by inhibiting activation of the uterine inflammatory response and by blocking the production of chemokines that promote

chemotaxis of immune cells. For example, P_4/PR inhibits expression of the prostanoid synthesis enzyme, cyclooxygenase-2 (COX-2), in myometrial cells through direct interaction of PR with NF-κB p65 (Kalkhoven et al., 1996) and by P_4-induced expression of the NF-κB inhibitor, IκBα (Hardy et al., 2006, Miller and Hunt, 1998). The action of progesterone to antagonize NF-κB function may have far reaching effects on the maintenance of uterine quiescence because, as previously mentioned, NF-κB can bind directly to the promoters of genes that mediate increased uterine contractility, including PGF2R (Olson, 2003), CXN-43 (Chow and Lye, 1994), OXTR (Fuchs et al., 1984), and COX-2 (Soloff et al., 2004).

In both mice and humans, early pregnancy is supported by the production of progesterone from the corpus luteum of the ovary. In humans, there occurs a luteo-placental switch by the second trimester, after which the major source of circulating progesterone becomes the placenta, where the production of progesterone rapidly dwarfs that of the ovary. The timing of the luteo-placental shift appears to be varied in different species (Csapo, 1969). As compared to humans, in mice, progesterone continues to be synthesized by the corpus luteum throughout the entirety of pregnancy, and thus, it is thought that luteolysis

triggers progesterone withdrawal and contributes to the initiation of labor in this species.

By contrast, the placenta provides the vast majority of progesterone at term in humans. Moreover, in women, circulating maternal progesterone levels remain elevated until birth (Tulchinsky et al., 1972), leading investigators to hypothesize that a functional progesterone withdrawal acts to initiate labor in women. Functional progesterone withdrawal occurs as a consequence of several coordinated mechanisms, each decreasing sensitivity of the uterus to progesterone at term. These mechanisms include inflammation-induced repression of PR by NF-κB (Kalkhoven et al., 1996), changes in PR coactivator levels (Condon et al., 2003), alterations in PR isoform ratios (Merlino et al., 2007), and the catabolism of progesterone in the uterus into inactive compounds (Lee et al., 2008b). Via their coordinated action on PR functionality in the myometrium at term, each of these mechanisms is capable of decreasing myometrial responsiveness to progesterone, permitting the activation of pathways blocked by progesterone throughout pregnancy.

Despite differences at term in progesterone regulation between mouse and human, the importance of progesterone to all species of gestating animals cannot be underestimated. Luteectomy (removal of the corpus luteum) during early pregnancy in both mice and humans results in

early abortion (Csapo et al., 1973, Abel and Hollingsworth, 1986), while antagonism of the progesterone receptor by RU486 results in the premature initiation of labor (Cadepond et al., 1997, Spitz and Bardin, 1993, Dudley et al., 1996).

At the same time as we observe a decline in P_4/PR function, estrogen, known to increase dramatically at term, acts to enhance inflammatory pathways within the maternal uterus (Mesiano et al., 2002). For example, estrogen is known to facilitate the secretion of immunoglobulin and recruitment of macrophages into the uterine lumen, a process which can be inhibited by progesterone (Sullivan and Wira, 1984, Wira and Sandoe, 1977, De and Wood, 1990). The antagonistic effect of progesterone on estrogen-induced macrophage and neutrophil migration fails to occur in mice with a deletion of the *PR* gene (*PRKO* mice) and is, therefore, PR dependent (Tibbetts et al., 1999). Furthermore, *PRKO* mice manifest a massive uterine inflammatory response upon estrogen (Tibbetts et al., 1999) or estrogen plus progesterone treatment (Lydon et al., 1995). Thus, the balance of an estrogen to progesterone ratio may be an important factor in determining the timing of labor (Mesiano, 2004, Mesiano et al., 2002).

The mechanical pathway is one in which the growing fetus imposes tension on the uterine wall inducing biochemical and molecular changes

within the myometrium. Changes imposed by uterine stretch result in signaling pathways that are integrated with both the hormonal and inflammatory pathways leading to labor. For example, it has been shown that stretch can enhance the monocyte chemoattractant activity of uterine myocytes via the action of monocyte chemoattractant protein-1 (CCL-2) (Shynlova et al., 2008). Myometrial stretch was also found to increase the synthesis of prostaglandins in the uterus (Sooranna et al., 2004).

In addition to mechanical signals triggered by the growing fetus, several investigations point to the fact that hormonal and developmental signals from the fetus may serve as triggers of parturition. Findings from our laboratory suggest that surfactant protein-A (SP-A), which is increasingly secreted by the fetal lung into the amniotic fluid near term, may provide an important signal for the initiation of labor (Condon et al., 2004). Shown to be increased by proinflammatory stimuli (Islam and Mendelson, 2002), SP-A synthesis by the fetal lung reaches maximal levels just before birth (Mendelson and Boggaram, 1990). Evidence for the ability of SP-A to initiate labor comes from studies in which mice injected with purified SP-A undergo premature parturition, whereas mice treated with intraamniotic, SP-A-depleting antibody delivered viable pups one day late (20.5 days post-coitum [dpc]) (Condon et al., 2004).

Increased cortisol production by the fetal adrenal gland, due to maturation of the hypothalamic-pituitary-adrenal axis at term, has also been suggested to serve a role in the initiation of labor (Liggins et al., 1973). Elevated fetal cortisol enhances expression of *COX-2*, leading to increased production of prostaglandins. Interestingly, fetal cortisol may also increase maturation of the fetal lung and its capacity to synthesize surfactant (Liggins, 1969).

Lastly, it has also been suggested that fetal-derived corticotropin-releasing hormone (CRH) may play a role in the initiation of labor (Florio et al., 2002, Torricelli et al., 2007). CRH is a peptide produced by the hypothalamus that controls function of the pituitary-adrenal axis in response to stress. CRH is also secreted in increasing amounts by the placenta late in pregnancy. Increased fetal-derived CRH is inhibited by progesterone (Jones et al., 1989, Karalis et al., 1996) and has been proposed to upregulate placental synthesis of estrogens, which oppose the action of P_4/PR to maintain uterine quiescence.

CRH also is developmentally induced in the bronchiolar epithelium of fetal mouse lung, proceeding the developmental induction of SP-A. Interestingly, induction of *SP-A* is delayed in *CRH*-deficient mice (Muglia et al., 1999), indicating that CRH may contribute to the initiation of labor by

enhancing production fetal cortisol and/or by stimulating lung maturation and the production of SP-A.

The integration of these pathways- mechanical, endocrine, and inflammatory- acts to increase the expression of a cadre of downstream effectors that mediate the physical contraction of the uterine myometrium. Termed “contraction-associated genes,” these effectors include Na^{+} and Ca^{2+} ion channels that control myometrial excitability, the gap junction protein, connexin-43 (CXN-43), which enhance myocyte connectivity and receptors for uterotonic agonists such as oxytocin and stimulatory prostaglandins.

The essential nature of these downstream contraction-associated genes is underscored by findings from a number of studies. In the uterus, gap junctions serve as specialized conduits between myometrial cells that allow direct intercellular communication via the passive intercellular diffusion of molecules of up to 1 kDa (Kumar and Gilula, 1996). By facilitating the exchange of metabolites, second messengers, and ions between cells, gap junctions facilitate electrical communication between coupled myocytes (Willecke et al., 2002), thus facilitating the coordinated contractile activity of myometrial cells. The importance of gap junctions in the laboring uterus is highlighted by the fact that CXN-43 is highly upregulated at term in both mouse and human (Chow and Lye, 1994,

Orsino et al., 1996). In addition, labor is delayed in mice lacking CXN-43 (Doring et al., 2006).

Oxytocin, which is produced in the supraoptic and paraventricular nuclei of the hypothalamus, interacts with G-protein-coupled receptors in the breast and uterus to induce contraction of mammary myoepithelial and uterine smooth muscle cells (Fuchs, 1995, Fuchs et al., 1995, Riemer and Heymann, 1998). During late gestation, oxytocin receptors (OXTR) are significantly induced in the myometrium in all mammalian species (Fuchs, 1995, Zingg et al., 1995). Treatment of animals with oxytocin significantly augments uterine contractility and hastens the progression of labor in both humans and mice (Imamura et al., 2000, Kobayashi et al., 1999, Douglas et al., 2002). Conversely, treatment with OXTR antagonists delays parturition in humans and rodents (Antonijevic et al., 1995, Goodwin et al., 1994). However, the role of oxytocin and the OXTR in normal parturition is uncertain, since oxytocin gene knockout mice undergo parturition and give birth to live young (Young et al., 1996, Nishimori et al., 1996), and mice deficient in the OXTR manifest normal timing and duration of parturition (Takayanagi et al., 2005). These unexpected phenotypes may be due to a functional redundancy of the oxytocin/OXTR signaling system and/or to compensatory upregulation of other uterotonic systems, such as COX-2/prostaglandins.

Prostaglandins also play a direct role in the stimulation of uterine contractility. Prostaglandins are synthesized from arachidonic acid by the enzyme prostaglandin H synthetase (PGHS). There are two forms of PGHS, termed cyclooxygenase-1 or COX-1 (PGHS-1) and COX-2 (PGHS-2). While it is generally thought that COX-1 is the constitutive form and COX-2, the inducible form of the enzyme, both players are thought to aid in the initiation of term and/or preterm labor (Tsuboi et al., 2003, Reese et al., 2000).

Evidence for a role of prostaglandins in the initiation of labor comes from the fact that prostaglandin levels are increased before and during labor in the uterus and amniotic membranes (Olson et al., 1983b, Skinner and Challis, 1985) and that administration of prostaglandins is used clinically to induce human labor (Agnew and Turner, 2009). Furthermore, prostaglandin levels are decreased by progesterone and increased by estrogens (Olson et al., 1983a, Smith and Kelly, 1987, Siler-Khodr et al., 1996, Ishihara et al., 1995), further highlighting the respective roles of these hormones in pregnancy and parturition. Increased cytokine production may also result in an increase in prostaglandin synthesis (Pomini et al., 1999), implicating prostaglandin-induced uterine contractility as a mechanism by which intrauterine infection results in premature labor.

Thus, coordinated uterine contractility at term and preterm results from the activation of multiple pathways which converge on the myometrium. These include progesterone withdrawal, estrogen-induced inflammatory responses, and increases in ion channels, oxytocin receptors, and gap junction proteins. Once activated, the myometrium can optimally respond to several key ligands, namely, increased oxytocin and prostaglandins, uterine agonists that drive the myometrial contractions required for delivery of the fetus.

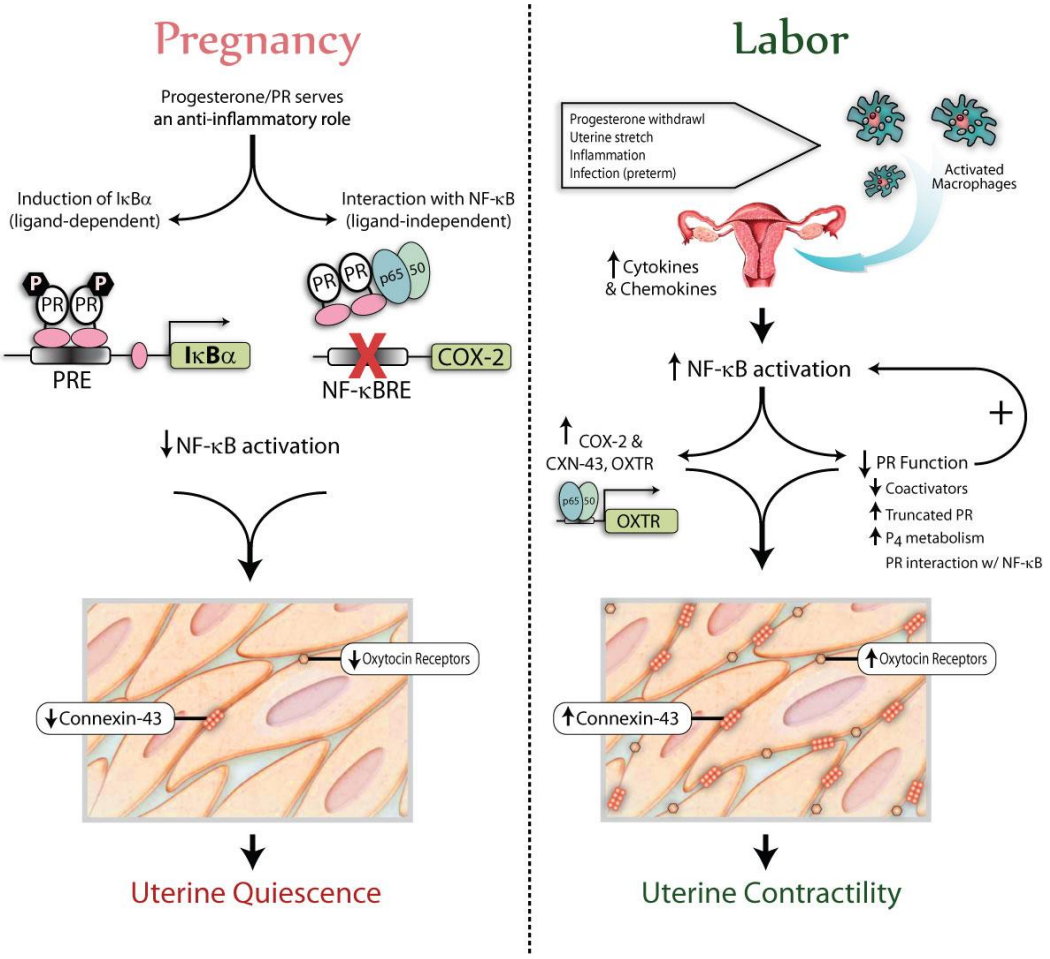

Figure 1-1.1. Mechanisms for regulation of uterine quiescence during pregnancy and induction of uterine contractility in preterm and term labor. During pregnancy, the uterus is maintained in a quiescent state by the action of progesterone/PR, which blocks activation of the inflammatory transcription factor, NF-κB. PR acts in a ligand-dependent manner to up-regulate expression of the NF-κB inhibitor IκBα in myometrial cells. Alternatively, PR acts in a dominant ligand-independent manner to block NF-κB activation, DNA binding, and transactivation of contractile genes within the uterus. Labor can be initiated preterm as a result of bacterial infection, resulting in enhanced migration of macrophages to the maternal uterus with release of cytokines/chemokines and activation of NF-κB. However, at term, activated NF-κB directly acts to increase expression of contractile genes and causes an impairment of PR function. These concerted events culminate in a further increase in NF-κB activation and expression of contraction-associated genes, CXN-43 and OXTR, leading to labor.

MicroRNAs in Female Reproduction

MicroRNAs (miRNAs) are short ~22 nucleotide RNAs that function to inhibit gene translation in a broad range of biological processes, and have been shown to modulate intracellular signaling pathways involved in development and disease (Bartel, 2009). In fact, it was recently demonstrated that the majority of all human genes are under the control of at least one miRNA, if not more (Friedman et al., 2009).

miRNAs are encoded throughout the genome and may be independently transcribed or found as clusters, expressed from the same promoter (Lim et al., 2003a, Lee and Ambros, 2001, Lau et al., 2001, Lagos-Quintana et al., 2001, Lim et al., 2003b). The excision and activation of active single-stranded miRNAs from precursor transcripts occurs through a multi-step process, which entails transcription, hairpin release, export from the nucleus to the cytoplasm, Dicer processing, and strand selection by the RNA-induced silencing complex (RISC) (Figure 1-1.2).

miRNAs are initially expressed as part of transcripts termed primary miRNAs (pri-miRNAs) (Lee et al., 2002). They are transcribed by RNA Polymerase II, and include 5' caps and 3' poly(A) tails (Smalheiser, 2003, Cai et al., 2004). The miRNA portion of the pri-miRNA transcript likely forms a hairpin with signals for dsRNA-specific nuclease cleavage.

The dsRNA-specific ribonuclease, Drosha, digests the pri-miRNA in the nucleus to release hairpin, precursor miRNA (pre-miRNA) (Lee et al., 2003). Pre-miRNAs appear to be approximately 70 nt RNAs with 1–4 nt 3' overhangs, 25–30 bp stems, and relatively small loops. Drosha also generates either the 5' or 3' end of the mature miRNA, depending on which strand of the pre-miRNA is selected by RISC (Lee et al., 2003).

Exportin-5 (Exp5) is responsible for export of pre-miRNAs from the nucleus to the cytoplasm (Yi et al., 2003) and has been shown to bind directly and specifically to a two-nucleotide overhang left by Drosha at the 3’ end of the correctly processed pre-miRNA hairpin (Kim, 2004). Exp5 is required for miRNA biogenesis, with a probable role in coordination of nuclear and cytoplasmic processing steps (Yi et al., 2003, Lund et al., 2004).

Dicer is a member of the RNase III superfamily and has been implicated in RNA interference pathways from plants to humans. Once in the cytoplasm, Dicer cleaves the pre-miRNA approximately 19 bp from the Drosha cut site (Lee et al., 2003, Yi et al., 2003). The resulting double-stranded RNA has 1–4 nucleotide 3’ overhangs at either end (Lund et al., 2004). Classically, only one of the two strands becomes the mature, RISC-associated miRNA (named miR-XX), derived from either the leading or lagging strand of the pri-miRNA transcript, while the other strand is

either degraded, or expressed to a lesser extent (named miR-XX*) (Hutvagner and Zamore, 2002). In some cases, both strands of the pri-miRNA become fully mature miRNAs, incorporated into the RISC. In this case, miRNAs are termed miR-XX-3p and miR-XX-5p. Selection of the active strand from the dsRNA appears to be based primarily on the stability of the termini of the two ends of the dsRNA (Khvorova et al., 2003, Schwarz et al., 2003). The strand with lower stability base pairing of the 2–4 nucleotides at the 5' end of the duplex preferentially associates with RISC and thus becomes the active miRNA (Schwarz et al., 2003).

Once associated with the RISC, the active miRNA inhibits translation or promotes mRNA degradation by annealing to complementary sequences in the 3′ untranslated regions (UTR) of target mRNA. miRNAs contain a short stretch of 6–8 nucleotides at their 5′ ends which form perfect Watson–Crick pairing to their target mRNAs, termed the “seed” sequence. While miRNAs are highly conserved among species, the seed match is especially conserved throughout evolution, since it is the region of the miRNA most important for target binding. Individual miRNAs typically target dozens of mRNAs, which often encode proteins with related functions in a physiologic or pathologic process. Thus, although the inhibitory effects of a particular miRNA on an individual mRNA target are generally modest, their combined effects on multiple

mRNAs can evoke strong biological responses, particularly by targeting transcription factors and, thus affecting several levels of regulation within the cell (Ambros, 2004).

Recently, it has been shown that miRNAs play especially powerful roles in vascular smooth muscle cells and in female reproduction, where they have been implicated in proliferation, differentiation, and hormone responsiveness (Albinsson et al., 2010, Creighton et al., 2010).

Little is known about the roles that miRNAs play in the uterus during female reproduction, and even less is understood about miRNAs in the induction of labor. It has been shown that deletion of Dicer1 causes malformations of the uterus; uteri from *Dicer1fl/fl;Amhr2Cre/+* mice were less than one-half the normal length and diameter, and one-third the weight of uteri from wild-type females (Hong et al., 2008, Nagaraja et al., 2008). In addition, histologic examination indicated a decreased smooth muscle layer and decreased presence of uterine glands (Hong et al., 2008, Nagaraja et al., 2008). While indicative of the importance of miRNAs to global uterine form and function, these studies shed relatively little light on the individual roles of miRNAs in various specific reproductive functions.

Only a handful of more specific studies have been conducted to investigate the role of miRNAs in female fertility, as summarized in Table

1-1, and none to date has investigated a role for miRNA regulation of the maintenance of pregnancy and induction of parturition. Because of this, and the fact that miRNAs function in several systems as hormonally-regulated modulators of gene expression, we were prompted to investigate their roles in P_4/PR regulation of contraction-associated genes during pregnancy and labor. Our investigations have uncovered the important role of a family of miRNAs, the miR-200 family, known to target repressive transcription factors, ZEB1 and ZEB2.

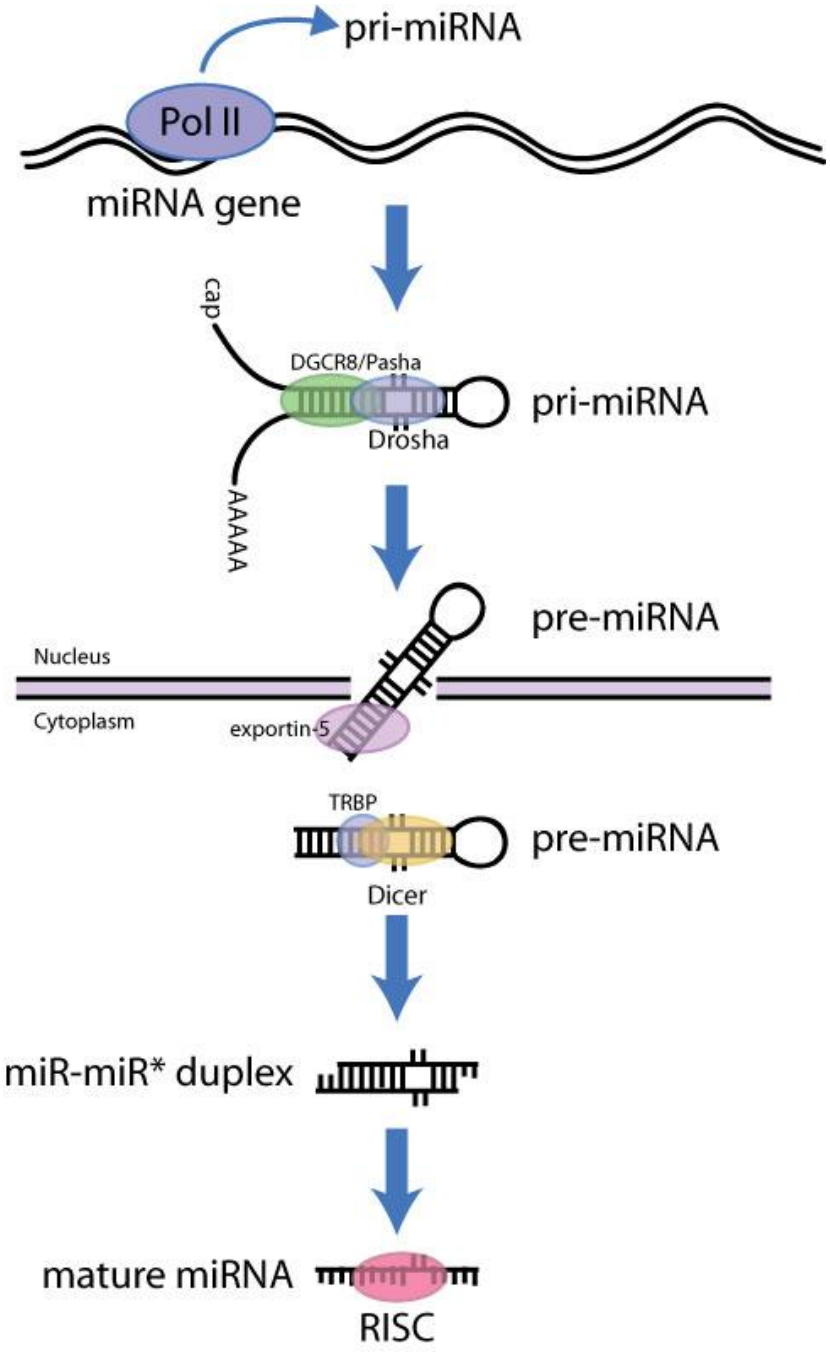

Figure 1-1.2. Diagram of miRNA processing. Shown are the basic players involved in miRNA processing, from the pri-miRNA transcribed by polymerase II to the mature miRNA incorporated into the RNA Induced Silencing Complex (RISC).

TABLE 1-1.1. Investigations of microRNAs in the Uterus

Process	Citation
Embryo Implantation	(Chakrabarty et al., 2007)
Endometriosis	(Pan et al., 2007)
Embryo Implantation	(Hu et al., 2008)
Uterine Development	(Hong et al., 2008)
Uterine Development	(Nagaraja, Andreu-Vieyra et al. 2008)
Cervical Carcinoma	(Lee et al., 2008a)
Cervix after Labor	(Hassan et al., 2010)
Endometrium during the Estrous Cycle	(Kuokkanen et al., 2010)

The MicroRNA-200 Family

The miR-200 family of miRNAs map to two clusters in the mouse and human genomes, each less than 2000 bp in length (Figure 1-1.3). The first cluster (Figure 1-1.3, upper) contains miR-429, miR-200a, and miR-200b and is located in chromosome 4 of the mouse and 1 of the human. Analysis of expression of this cluster reveals that all three members are co-expressed, suggesting that they are driven by a common promoter (Korpal et al., 2008). The second cluster (Figure 1-1.3, lower) consists of miR-200c and miR-141 and is located in a 500-bp region of chromosome 6 in mouse and chromosome 12 in human. The five miR-200 family members contain very similar seed sequences, with the seed sequence of miR-200b/c/429, AAUACUG, differing by only one nucleotide from the seed sequence of miR-200a/141, AACACUG (Figure 1-1.3). Most importantly, there is near-complete homology between members of the miR-200 family in mouse and human, which cluster identically, and differ in their mature sequence only by 2 nucleotides in the 3' region of miR-429 (Figure 1-1.3). Because of their homology and seed sequence identity, members of the miR-200 family bind and repress a highly similar set of mRNA targets in mouse and human (Park et al., 2008).

Prior studies have shown that the miR-200 family plays a strong role in development and cancer metastasis. miR-200s act to maintain the

epithelial phenotype of cells (Korpal et al., 2008, Park et al., 2008, Gregory et al., 2008). This occurs through direct targeting of ZEB1 and ZEB2, which act as transcriptional repressors of E-cadherin and promote epithelial-mesenchymal transition (EMT), the initiating step of cancer metastasis (Gibbons et al., 2009). Consequently, the miR-200 family has been shown to inhibit EMT (Gregory et al., 2008, Korpal et al., 2008). Likewise, several investigations have shown the miR-200 family to be downregulated in metastatic cancers (Gee et al., Gregory et al., 2008).

In the present study, we show that members of the miR-200 family in both mouse and human uterus are significantly induced during late gestation, repress ZEB1 and ZEB2, and mediate myometrial contractility.

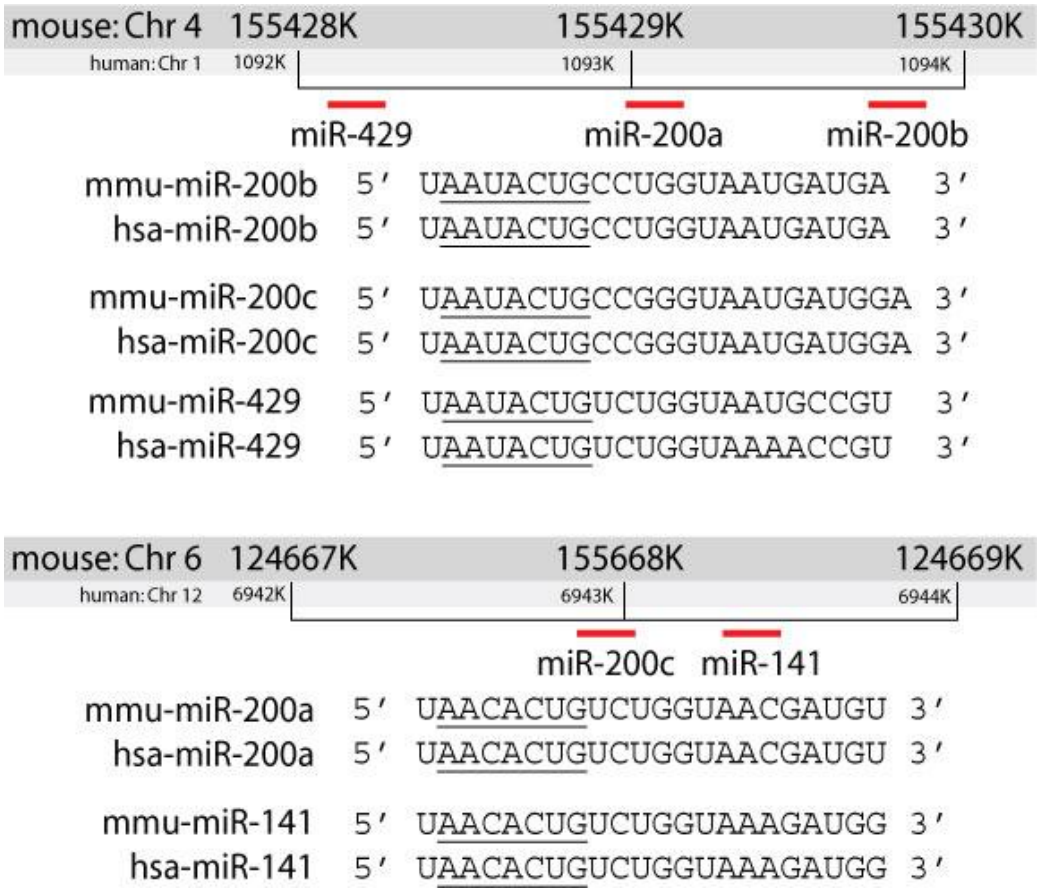

Figure 1-1.3. Chromosomal location and mouse-human homology of members of the miR-200 family. Seed sequences for each miRNA are underlined.

The Repressive Transcription Factors, ZEB1 and ZEB2

Members of the ZEB family of transcription factors are essential players during normal embryonic development, particularly muscle differentiation, during which they induce EMT, a process that reorganizes epithelial cells to become migratory mesenchymal cells (Miyoshi et al., 2006, Postigo and Dean, 1999, Sekido et al., 1994). For this reason, they have also been identified as key players in many types of cancer, where cancer cells acquire invasive and metastatic properties by exploiting EMT-inducing transcription factors (Comijn et al., 2001, Eger et al., 2005, Haddad et al., 2009, Spoelstra et al., 2006).

Expressed highly in tissues of smooth muscle origin, and particularly uterus (Hurt et al., 2008), the ZEB family members are structurally similar, containing two zinc-finger-binding domains, a central repression region including C-terminal binding protein (CtBP) and Smad-interacting domains, and N- and C-terminal p300-interacting domains (van Grunsven et al., 2001, Verschueren et al., 1999). Both family members, ZEB1/dEF1 and ZEB2/SIP1, can repress transcription by directly binding to E-box-binding sequences (5'-CAC(C/G)(T/G)(G/T)-3') located in various gene promoters (Sekido et al., 1994, Remacle et al., 1999). The list of ZEB targets includes genes coding for cell junctions, including adherens junctions, demsosomes, and gap junctions (Vandewalle et al., 2005).

The structure of the ZEB1 and ZEB2 proteins are highly similar in key regions, indicating their ability to target similar gene promoters. On the other hand, the 5'-flanking regions of the *ZEB1* and *ZEB2* gene differ markedly, suggesting their differential regulation (van Grunsven et al., 2001, Nelles et al., 2003). Despite their structural similarity, therefore, ZEB1 and ZEB2 are likely to be regulated by distinct stiumli, acting on their dissimilar promoters.

As mentioned above, members of the miR-200 family directly bind (Figure 1-1.4) and downregulate expression of ZEB1 and ZEB2 (Korpal et al., 2008, Christoffersen et al., 2007, Park et al., 2008, Hurteau et al., 2007, Gregory et al., 2008). Furthermore, the ZEB1 and ZEB2 transcription factors, in turn, downregulate expression of the miR-200 family (Burk et al., 2008, Bracken et al., 2008). Taken together, the actions of miR-200s and ZEBs direct a double-negative feedback loop. This reciprocal repression maintains stable levels miR-200s and ZEB1 and ZEB2 within the cell, yet retains the ability to switch the player that is dominant at any given time. This is exemplified by transforming growth factor beta (TGF-β) induced EMT, where cells switch from expressing high levels of miR-200s to high levels of ZEBs (Bracken et al., 2008), as well as the current investigation, where progesterone withdrawal leading to labor

triggers a decline in ZEB1 and ZEB2, and the induction of the miR-200 family.

The current studies have elucidated a role for the miR-200 family and its reciprocal targets, ZEB1 and ZEB2, in the regulation of contraction-associated genes, CXN-43 and OXTR. Our investigations have revealed that the miR-200 family is significantly upregulated at term in both mouse and human myometrium, coordinated with a downregulation in ZEB1 and ZEB2 in these same tissues. Furthermore, we have implicated ZEB1 as a direct target of progesterone induction, providing a novel pathway by which progesterone acts to maintain uterine quiescence to term.

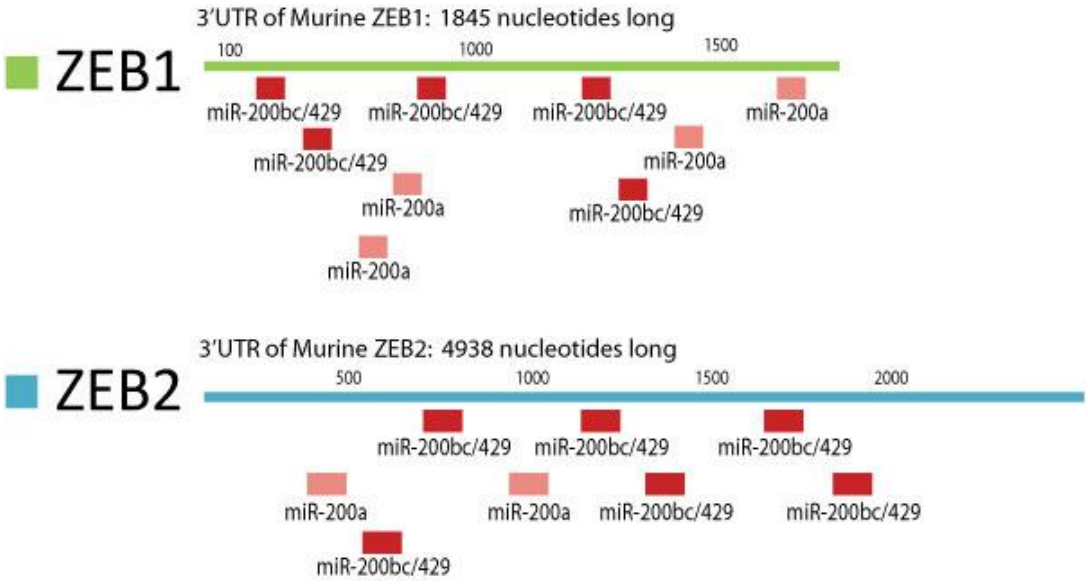

Figure 1-1.4. Diagram depicting the known, experimentally validated binding sites for members of the miR-200 family within the 3'UTR of murine ZEB1 and ZEB2 (Park et al., 2008; Gregory et al. 2008).

CHAPTER 2- Section 1.
A Role for MicroRNAs in the Timing of Labor

Introduction and Experimental Design

In an effort to identify miRNAs that mediate myometrial transition to a contractile phenotype in preparation for labor, we performed microarray analysis to compare the miRNA expression profile in RNA from isolated myometrium of mice at 15.5 days post-coitum (dpc) compared to mice at 18.5 dpc, just hours before the initiation of labor. Eighteen mice from each time point were sacrificed and myometrial tissues enriched by careful dissection. After performing analysis for RNA quality control and quantification, RNA from mice sacrificed at each time point were pooled equally according to concentration into three groups of 6 uteri each from eighteen 15.5 dpc versus three pools of 6 uteri each from eighteen 18.5 dpc pregnant mice (Figure 2-1.1). RNA samples were then subject to further quality control testing by LC Sciences (Houston, Texas), before amplification and hybridization of our samples to microRNA microarray.

In order to minimize false positive findings on our microarray, we chose to perform analysis on three separate two-color chips (Figure 2-1.2), with each chip profiling the miRNA expression of a different pool of 6 mice at 15.5 dpc versus 6 mice at 18.5 dpc. In order to reduce false

positives and improve our statistical power, we included a total of 36 mice for analysis, and performed our arrays in triplicate.

Upon receipt of our array data from LC Sciences, each target that proved statistically significant across all three chips was examined by qRT-PCR on RNA from the same and independently collected samples. Furthermore, temporal expression profiles were conducted to determine more specifically the timing of induction of each regulated miRNA.

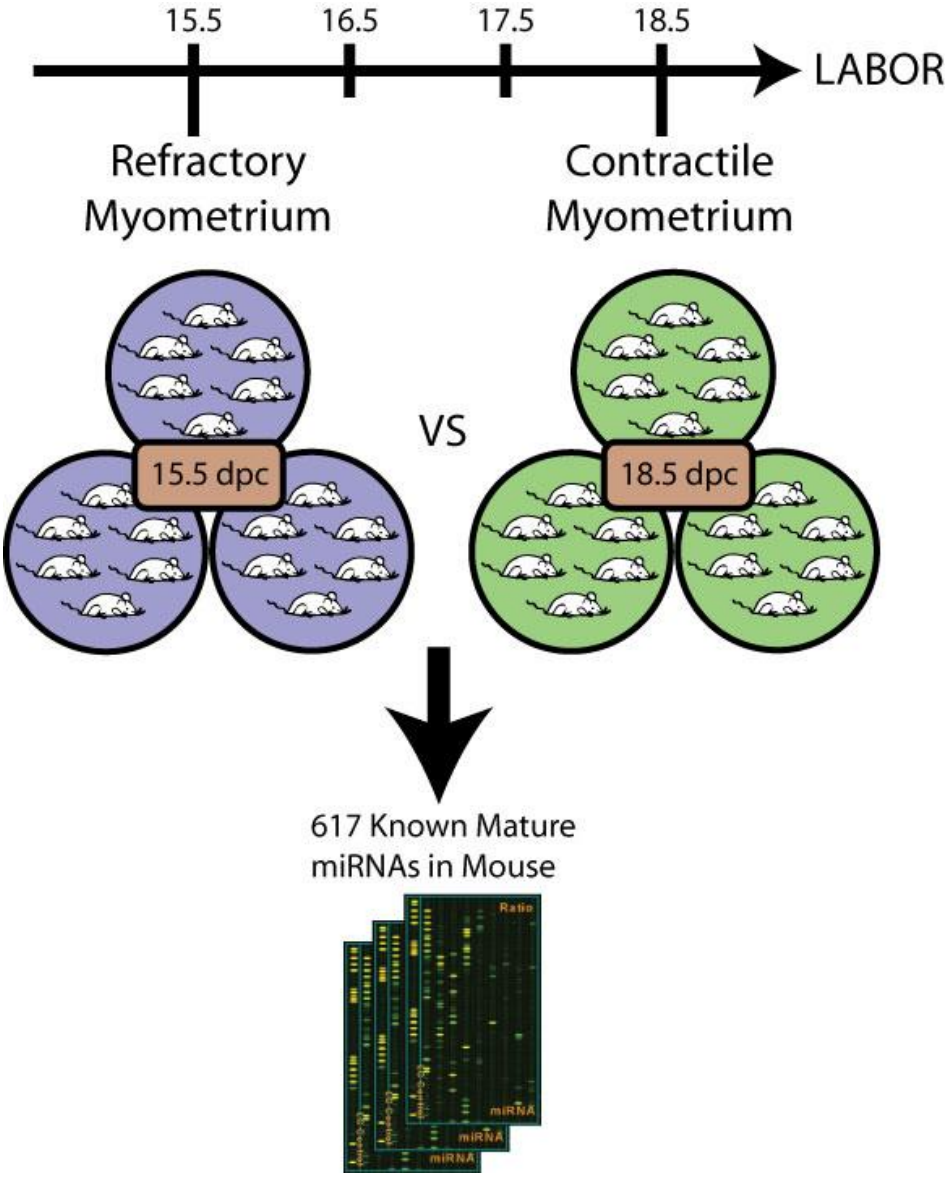

Figure 2-1.1. MicroRNA Microarray Experimental Design. Myometrial RNA from eighteen mice at 15.5 dpc was pooled equally according to concentration into three groups of 6 uteri each. Myometrial RNA from eighteen 18.5 dpc mice was similarly pooled into three groups of 6 uteri each, and analyzed by triplicate two-color microarray for the 617 known mature murine microRNAs (miRbase v12.0).

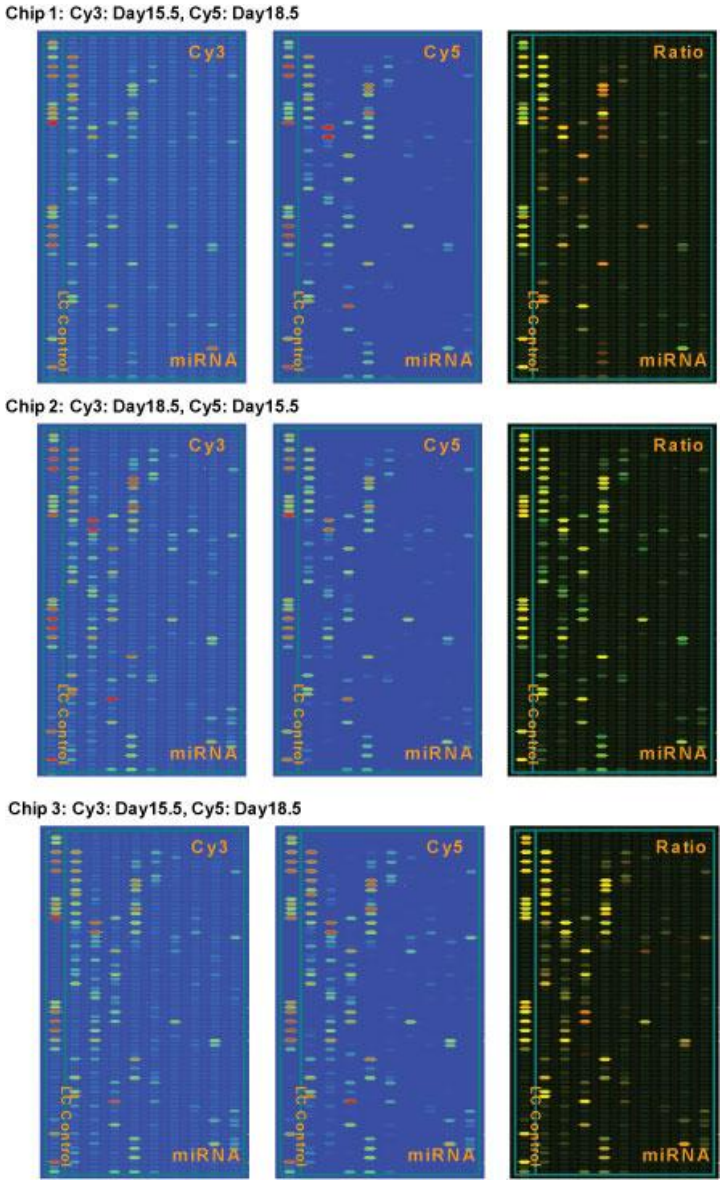

Figure 2-1.2. Raw Data from MicroRNA Microarray Chips. To analyze the ratio of expression between 15.5 dpc and 18.5 dpc, we conducted three two-color microarrays, in which each biological sample pool was hybridized with either Cy3 or Cy5 and the ratio of these two signals was compared. Dye-balancing was conducted such that each time point was labeled at least once with Cy3 and once with Cy5. This strategy of alternate labeling ensures an automatic correction of any potential gene-specific labeling bias.

Results: Regulation of the miR-200 Family in Late Gestation

The results from our miRNA microarray revealed five miRNAs, whose expression profiles were statistically different between 15.5 dpc and 18.5 dpc: miR-155, miR-182, miR-200b, miR-429, and miR-669a (Figure 2-1.3). Of these, only miR-155, miR200b, and miR-429 were expressed at high levels (signal intensity >500) and each of these were confirmed by qRT-PCR (Figure 2-1.4). Among the highly regulated and highly expressed miRNAs, two of the miRNAs we identified, miR-200b and miR-429, belong to a family of miRNAs, the miR-200 family. Although miR-200b and miR-429 were identified by application of the most stringent statistical criteria, upon further analysis, all five members of the miR-200 family were found to be upregulated between 15.5 dpc and 18.5 dpc to some extent across all three chips (Figure 2-1.5). Interestingly, the three members of the miR-200 family showing the most dramatic upregulation, miR-429, miR-200a, and miR-200b, are all are expressed as a single cluster within the mouse and human genomes: the miR200b-a-429 cluster on chromosome 4 in the mouse and chromosome 1 in the human (Figure1-1.3). Because miR-200b and miR-429 showed significant increases in expression between 15.5 dpc and term by microarray, we chose these two miRNAs to profile throughout the course of all our investigations.

In situ hybridization for miR-200b revealed expression of miR-200b, localized to the myometrium of the pregnant mouse uterus at term (18.5 dpc) (Figure 2-1.6A). Temporal expression analysis of miR-200b and miR-429 by qRT-PCR confirmed the upregulation seen in our microarray findings in an independent cohort of animals and revealed a significant increase in expression of these two miR-200 family members, beginning at 17.5 dpc (Figure 2-1.6B).

A.

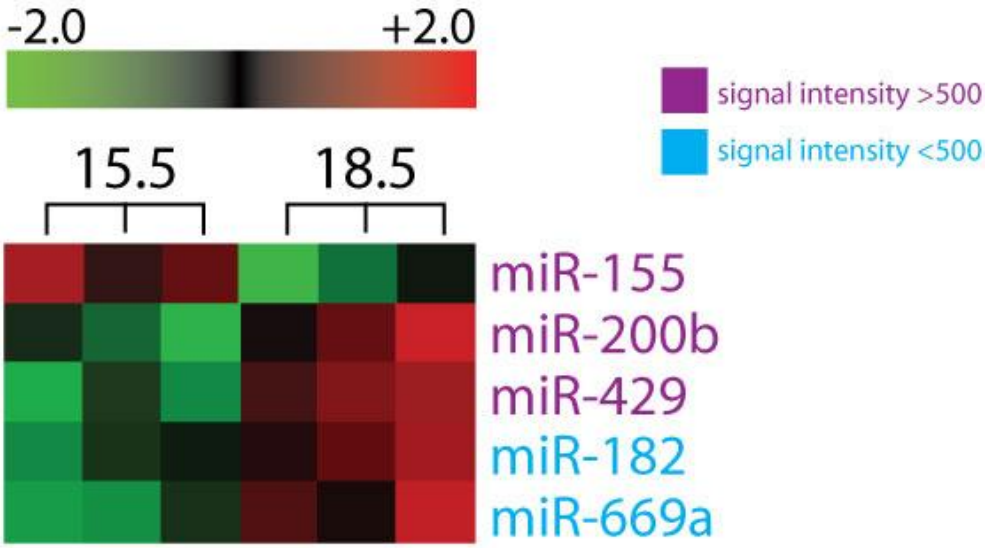

B.

Reporter Name	p-value	15.5 dpc Mean Signal Intensity	18.5 dpc Mean Signal Intensity	Log2 (18.5/15.5)
mmu-miR-429	9.97E-03	591	1,797	1.60
mmu-miR-155	3.60E-02	530	142	-1.90
mmu-miR-200b	4.99E-02	3,509	7,240	1.05
mmu-miR-182	4.56E-02	77	160	1.06
mmu-miR-669a	3.68E-02	12	31	1.33

Figure 2-1.3. MicroRNA Microarray Revealed 5 Genes Significantly Regulated at Term (A) Heatmap comparing miRNA expression between 15.5 and 18.5 dpc (n=18 per group) for the miRNAs significantly regulated at term. miR-155 was downregulated at 18.5 dpc, while miR-429, miR-200b, miR-182, miR-669a were all upregulated. **(B)** Among the significantly regulated genes, only miR-155, miR-429, and miR-200b were expressed with a signal intensity of greater than 500. Student's t-test ($p<0.05$).

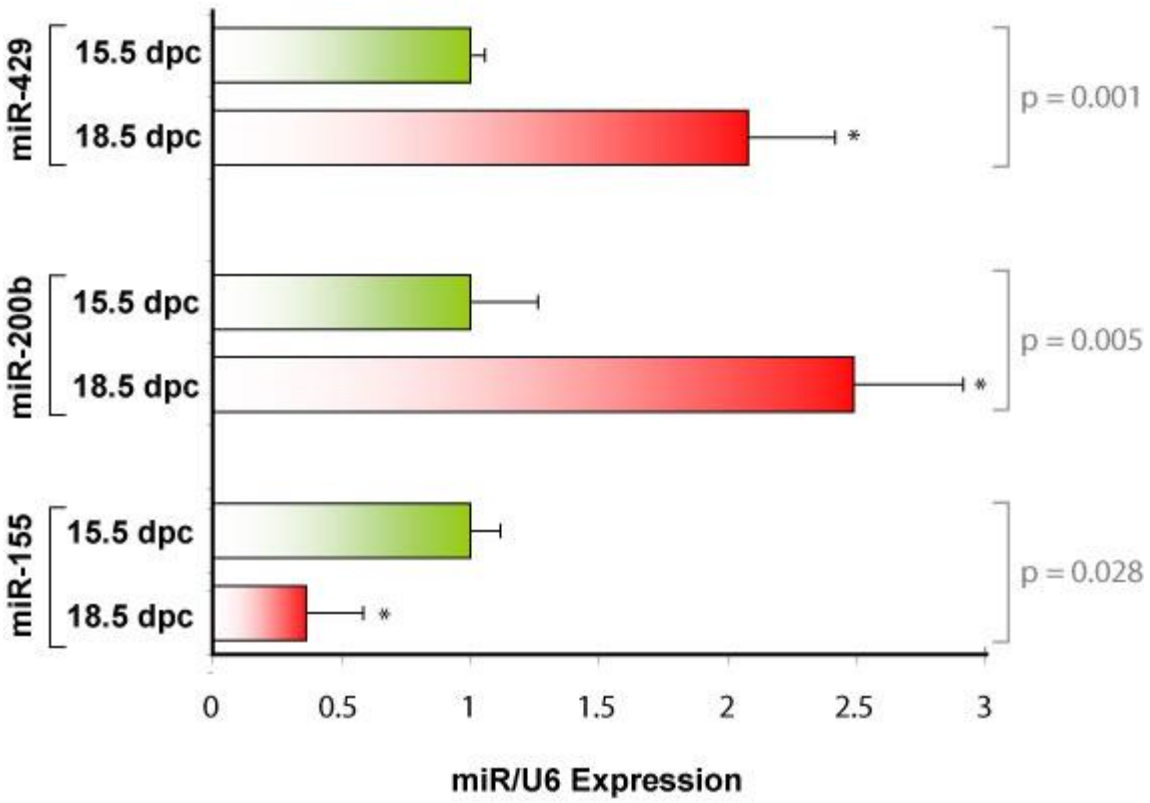

Figure 2-1.4. qRT-PCR Confirmed Regulation of All 3 Highly Expressed, Significantly Regulated miRNAs. qRT-PCR was used to confirm upregulation of both miR-200b and miR-429, and downregulation of miR-155. Expression of each miRNA was determined by qRT-PCR, normalized to U6, and expressed as fold change, as compared to 15.5 dpc. Data are the mean ± SEM of 18 tissue samples per goup. Murine myometrial samples used for confirmation were the same as those examined by microarray (n=18 per group). Student's t-test ($p<0.05$).

A.

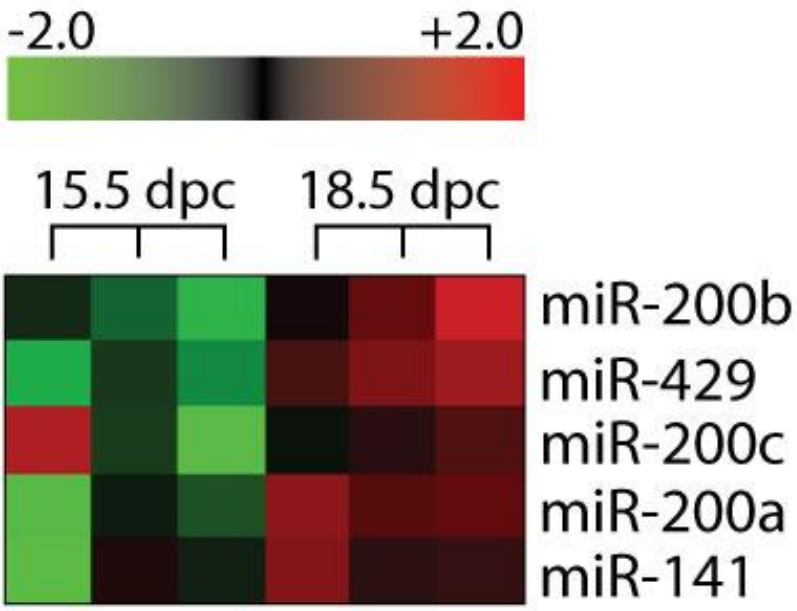

B.

Reporter Name	p-value	15.5 dpc Mean Signal Intensity	18.5 dpc Mean Signal Intensity	Log2 (18.5/15.5)
mmu-miR-429	9.97E-03	591	1,797	1.60
mmu-miR-200b	4.99E-02	3,509	7,240	1.05
mmu-miR-200c	5.86E-01	8,930	10,025	0.17
mmu-miR-200a	7.38E-02	386	1,086	1.49
mmu-miR-141	9.71E-02	96	160	0.74

Figure 2-1.5. Microarray analyses reveal a significant upregulation of the miR-200 family in the murine uterus at term. (A) Heatmap comparing miRNA expression between 15.5 and 18.5 dpc (n=18 per group) for the all members of the miR-200 family. As mentioned above, two members of this family were found to be significantly upregulated at term: miR-200b and miR-429 ($p<0.05$). (B) All members of the miR-200 family increase in their expression to some extent at 18.5 dpc, with members of the miR-200b-a-429 cluster increasing most robustly.

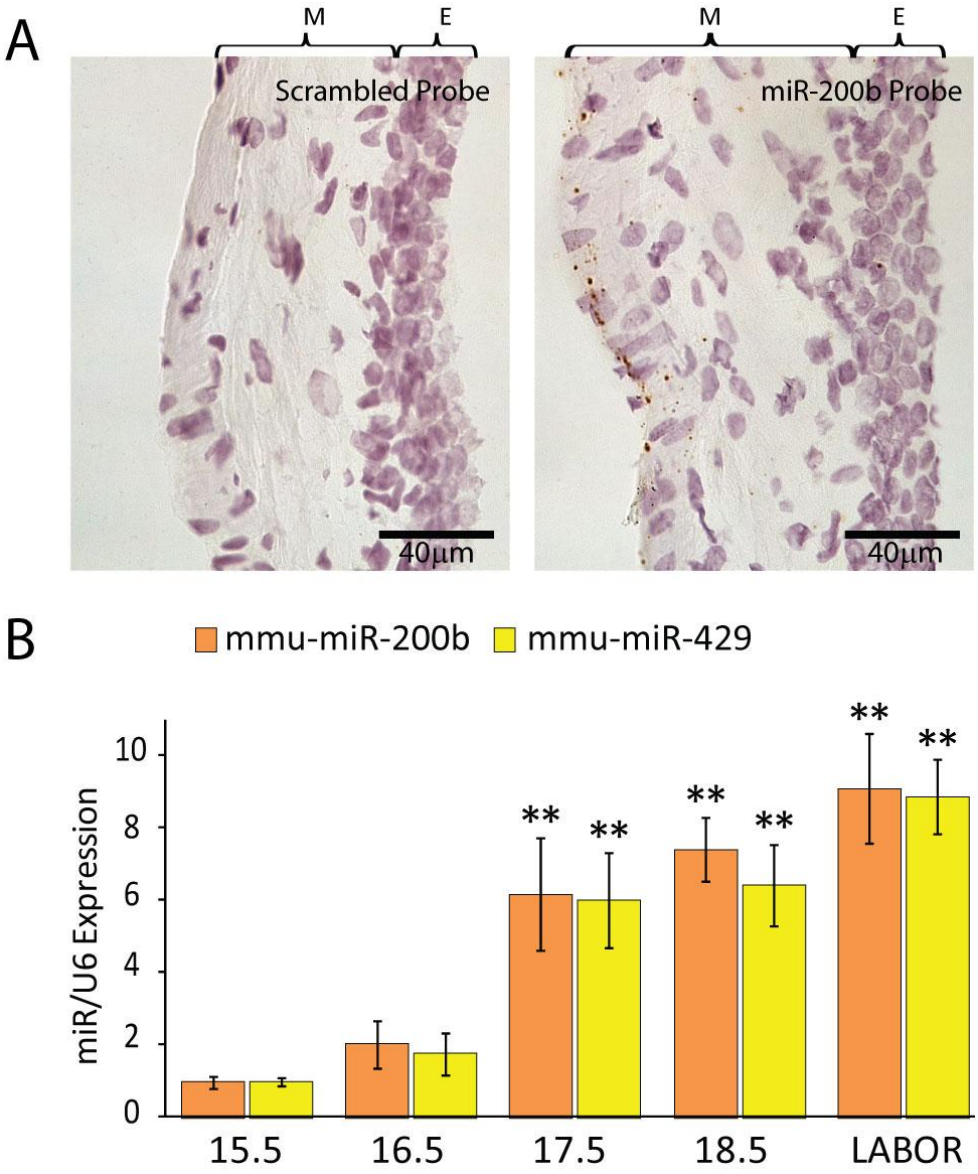

Figure 2-1.6: Mature miR-200b/429 are Significantly Upregulated in Pregnant Mouse Myometrium Beginning at 17.5 dpc. (A) Myometrial localization of miR-200b was determined by in situ hybridization (ISH) using LNA-modified DIG-labeled probes. ISH was performed on uteri from pregnant mice at 18.5 dpc. M: Myometrium, E: Endometrium. **(B)** Expression of each miRNA was determined by qRT-PCR, normalized to U6, and expressed as fold increase over 15.5 dpc. Mean ± SEM values are shown. One-way ANOVA, miR-200b: $F(4,20)=14.82$, $p<0.0001$; miR-429: $F(4,20)=17.49$, $p<0.0001$. Multiple comparison test compared to 15.5 dpc: *$p<0.05$, **$p<0.01$. Murine myometrial samples used for this analysis were distinct from those examined by microarray. n = 10 mice each for 15.5 dpc and laboring groups, 5 each for 16.5-18.5dpc.

Discussion

There are several noteworthy points that arise from our finding that miR-200b and miR-429 are upregulated across late gestation. The first is that all members of this family appear to be similarly upregulated. Members of the miR-200 family contain identical or nearly identical seed sequences (Figure 1-1.3), and thus target a highly similar pool of mRNAs. One would infer, therefore, that if this miRNA family is playing an important role in the physiology of parturition, consistent regulation of its targets between all members of the miRNA family would be beneficial.

The second interesting finding from our initial investigations of the miR-200 family comes out of our observation that the miR-200s appear to be statistically upregulated beginning at 17.5 dpc. This time point during late gestation marks an important transition for the maternal uterus in its switch from a quiescent to contractile phenotype, and corresponds to such changes as the decline in circulating progesterone observed prior to parturition in murine pregnancy (Virgo and Bellward, 1974).

With these two major findings in mind, our next aim was to determine the specific targets of the miR-200 family during late gestation and to dissect the role of these genes in the uterus, during the progression of the myometrium from quiescence to contraction.

Materials and Methods

Mice and Murine Tissue Collection. All animal protocols were approved by the Institutional Animal Care and Use Committee of the University of Texas Southwestern Medical Center. Eight-week-old, timed-pregnant ICR/CD1 females were purchased from Harlan Laboratories. Timed-pregnancies were achieved by housing females with males overnight, beginning at 1800h. Mice found to have vaginal plugs at 0600 h were considered to be 0.5 dpc.

For qRT-PCR, uterine tissues were isolated from pregnant mice at 15.5, 16.5, 17.5 and 18.5 dpc and upon delivery of the first pup (labor). The uterus was slit open lengthwise, cleared of all embryonic material and maternal decidua, and further enriched for myometrium by sterile scraping and blotting with a paper towel (Figure 2-1.7). The remaining myometrial tissue was washed in 1x PBS and flash frozen for subsequent protein and mRNA analysis.

For in situ hybridization (ISH) of the uterus, pregnant mice at 18.5 dpc were deeply anesthetized with an injection of a ketamine-xylazine-acepromazine mixture and transcardially perfused with 4% paraformaldehyde in PBS. The uteri were dissected and pups and placental material removed, leaving the uterus intact. Tissues were

embedded in O.C.T. tissue-tek. 16 μm thick sections were cut on a cryotome and stored at -80˚C.

miRNA Microarray Analysis. miRNA microarray assay was performed using a service provider (LC Sciences). Eighteen murine uteri at 15.5 dpc and an equal number of mice at 18.5 dpc were pooled into 3 groups of 6 animals for each gestational time point, and two-color chips were run in triplicate. The assay was initiated with 5 μg of total RNA per sample, which was size fractionated using a YM-100 Microcon centrifugal filter (Millipore); isolated small RNAs (< 300 nt) were 3'-extended with poly(A) polymerase. An oligonucleotide tag was ligated to the poly(A) tail for later fluorescent dye staining with either Cy3 or Cy5 dyes. Two different tags were used for 15.5 dpc and 18.5 dpc samples and dye-swapping was conducted, alternating every other chip, to avoid dye bias. Hybridization was performed overnight on a μParaflo microfluidic chip using a micro-circulation pump (Atactic Technologies). Each detection probe consisted of a chemically modified nucleotide coding segment complementary to target miRNA (miRBase v12.0) or other RNA control sequence. The detection probes were made by in situ synthesis using PGR (photogenerated reagent) chemistry. The hybridization melting temperatures were balanced and hybridization images were collected

using a laser scanner (GenePix 4000B, Molecular Device) and digitized using Array-Pro image analysis software (Media Cybernetics). Data were analyzed by first subtracting the background and then normalizing signals using a LOWESS filter (Locally-weighted Regression). As we conducted two-color experiments, the ratio of the two sets of detected signals (log2 transformed, balanced) and p-values of the t-test were calculated across all three chips; differentially detected signals were those with $p < 0.05$.

In Situ Hybridization. In situ detection of miR-200b was performed on 16-μm frozen tissue sections of whole uterus from paraformaldehyde perfused 18.5 dpc pregnant mice. Sections were stored at -80C until use. Before hybridization, sections were dried for 10 min at room temperature, followed by 10 min at 50C. Slides were then fixed in 4% paraformaldehyde and acetylated in acetic anhydride/triethanolamine, each followed by washes in PBS. Sections were then prehybridized in hybridization solution (50% formamide, 5× SSC, 500 μg/mL yeast RNA, 0.1% Tween, 50 μg/mL heparin) at 48°C for 30 min. 25 micromolar DIG-labeled probe (LNA-modified oligonucleotide, Exiqon) complementary to miR-200b or scrambled (negative control) was hybridized to the sections for 2 h at 48°C. After post-hybridization washes in increasing stringencies of SSC at 54°C, in situ hybridization signals were detected using anti-DIG-

Horseradish Peroxidase (HRP) antibody (Roche cat#11207733910) and a tyramide signal amplification system (Perkin Elmer) according to the manufacturer's instructions. Slides were counterstained with hematoxylin.

qRT-PCR Analysis of mmu-miR-155, mmu-miR-200b, and mmu-miR-429. cDNA was reverse transcribed from total RNA using specific miRNA primers from the TaqMan microRNA assays and reverse transcription kit (Applied Biosystems). PCR products were amplified from cDNA samples using the TaqMan microRNA assay (Applied Biosystems). Mouse miRNAs were detected with the following primers and probes: Applied Biosystems mmu-miR-155 Assay ID# 002571, Applied Biosystems mmu-miR-200b Assay ID# 002251, and Applied Biosystems mmu-miR-429 Assay ID# 001077. U6 snRNA was used as an internal control for each reaction, using Applied Biosystems U6 snRNA Assay ID # 001973. PCR for each sample was set up in triplicate, using a miRNA-specific TaqMan probe and TaqMan Universal PCR Master Mix (Applied Biosystems) on an ABI Prism 7700 Detection System (Applied Biosystems). miRNA expression was normalized using U6 snRNA.

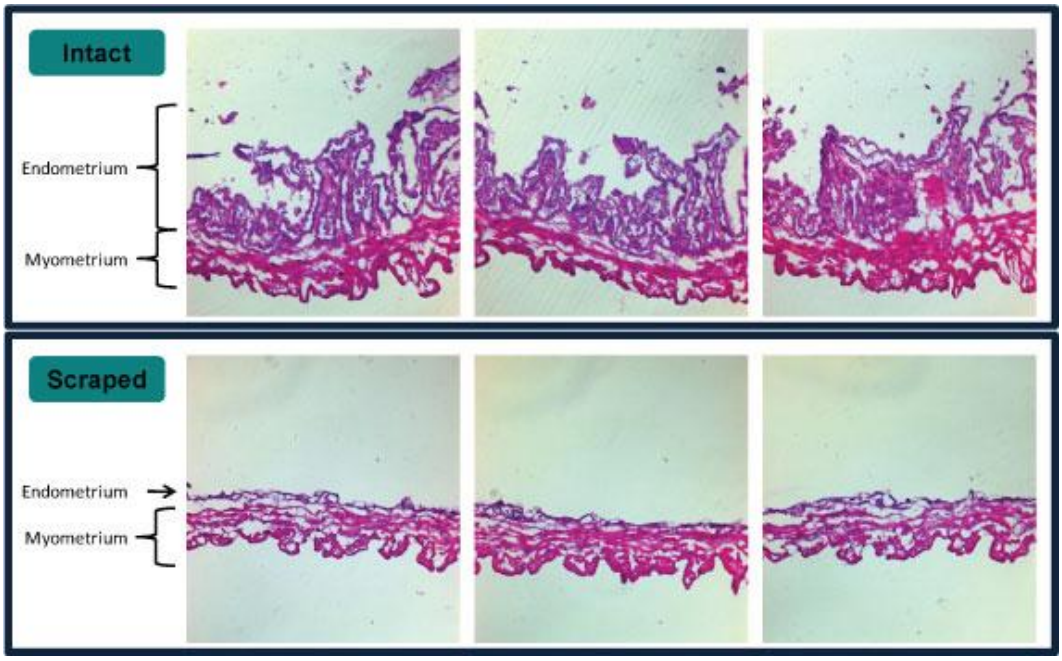

Figure 2-1.7. Histology Illustrating Myometrial Enrichment in Scraped and Blotted Uterine Dissections. Upon dissection, the uterus was cleared of all embryonic material and maternal decidua (Upper Panel). To achieve optimal isolation of murine myometrium, dissected uteri were further enriched for myometrium specifically by sterile scraping and blotting with a paper towel (Lower Panel).

CHAPTER 2- SECTION 2
miR-200s Regulate ZEB1 & ZEB2 Expression

Experimental Design

Because members of the miR-200 family are predicted to target over 609 different mRNA transcripts (Target Scan), we performed a gene expression microarray in order to most efficiently narrow the pool of genes potentially regulated by miR-200b/429 during pregnancy and labor. For these experiments, we compared sets of genes downregulated by microarray, with genes assigned the strongest miR-200b/c/429 context scores by the TargetScan prediction algorithm (Lewis et al., 2005, Grimson et al., 2007).

Those putative miR-200b/429 targets found to be regulated with the highest context scores on microarray were then evaluated by qRT-PCR across late gestation in murine uterus to investigate whether expression of the target was inversely correlated with expression of miR-200b/429 (*i.e.* that expression would decrease significantly beginning at 17.5 dpc and decline to term). Following these investigations, we then confirmed the miRNA/target relationship in TERT-immortalized myometrial smooth muscle cells (hTERT-HM), employing miRNA mimic overexpression.

Results: ZEB1/ZEB2 are Suppressed by miR-200s in the Uterus

Nearly 2000 genes were found to be downregulated on our gene expression microarray, comprising several gene regulatory pathways, including cellular movement and inflammatory pathways (Figure 2-2.1). Of these downregulated genes, 60 were predicted by Target Scan to be targets of the miR-200 family (Figure 2-2.2). Upon examination of these 60 targets (Table 3-1), ZEB1 and ZEB2 mRNAs were predicted to be the strongest targets of the miR-200 family, with 5 and 6 confirmed binding sites in their 3'UTRs, respectively (Figure 1-1.4) (Park et al., 2008, Christoffersen et al., 2007, Korpal et al., 2008, Gregory et al., 2008). For this reason, we chose to further investigate ZEB1 and ZEB2 and the potential relevance of these transcription factors in the progression of the myometrium to labor.

As shown in Section 1, miR-200b/429 were found to be upregulated in the pregnant mouse uterus beginning at 17.5 dpc (Figure 2-1.6). We next sought to compare these data to the temporal expression of ZEB1 and ZEB2 in the mouse myometrium during late gestation, from 15.5 dpc to labor. By qRT-PCR analysis, we found that the increase seen in miR-200 family expression was correlated with a significant decline in ZEB1 and ZEB2 gene expression, beginning at 17.5 dpc (Figure 2-2.3A). Via immunoblot analysis, we also found ZEB1 protein to be significantly

decreased in the murine uterus during late gestation, declining to barely detectable levels in tissues from laboring mice (Figure 2-2.3B). Several attempts to quantify ZEB2 protein *in vivo* with commercially available antibodies proved unsuccessful.

In light of these encouraging data, we next sought to further confirm the miR-200/ZEB relationship in the uterine myometrium. While previous studies indicate that miR-200 family members downregulate expression of ZEB1 and ZEB2 in a variety of cells and cell lines (Park et al., 2008, Christoffersen et al., 2007, Gregory et al., 2008, Korpal et al., 2008), this relationship had not previously been investigated in uterine myometrium. To explore regulation of ZEB1 and ZEB2 by members of the miR-200 family in uterine myocytes, we transfected mimics of miR-200b and miR-429 into an immortalized human myometrial cell line (hTERT-HM). Transfection of miR-200b/429 mimics into hTERT-HM cells resulted in a significant reduction in endogenous ZEB1 and ZEB2 expression within 24 h (Figure 2-2.4A). Furthermore, adenoviral transduction of the miR-200b-a-429 cluster into hTERT-HM cells also resulted in suppressed endogenous ZEB1 and ZEB2 expression (Figure 2-2.4B).

We next sought to ask whether the reciprocally repressive relationship reported elsewhere between the miR-200 family and ZEBs (Burk et al., 2008, Bracken et al., 2008) might play a role in the

myometrium. To address this question, primary cultures of mouse myocytes were transduced with recombinant adenoviruses for ZEB1 or ZEB2 and examined for levels of endogenous miR-200b and miR-429. As determined by qRT-PCR, expression of miR-200b/429 was repressed by both ZEB1 and ZEB2 adenoviral mediated overexpression (Figure 2-2.4C & D).

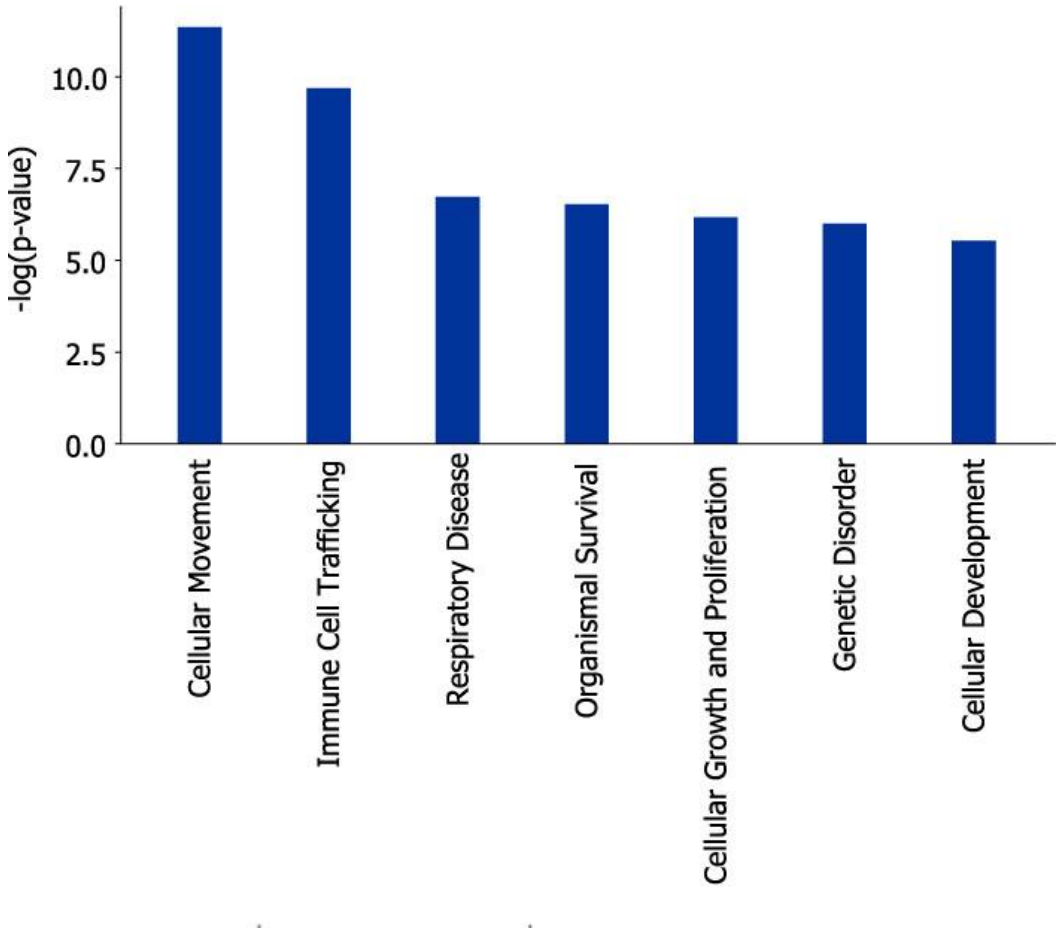

Figure 2-2.1. The Top 7 Most Regulated Gene Networks at Term by Gene Expression Microarray. Normalized microarray data were analyzed by use of Ingenuity Pathways Analysis to detect common gene networks regulated between 15.5 dpc and 18.5 dpc on microarray. The top seven most regulated pathways are shown. Interestingly, ZEB1 and ZEB2 belong to the category "Cellular Movement," which was found to be the most highly regulated network in the uterine myometrium at term, closely followed by "Immune Cell Trafficking."

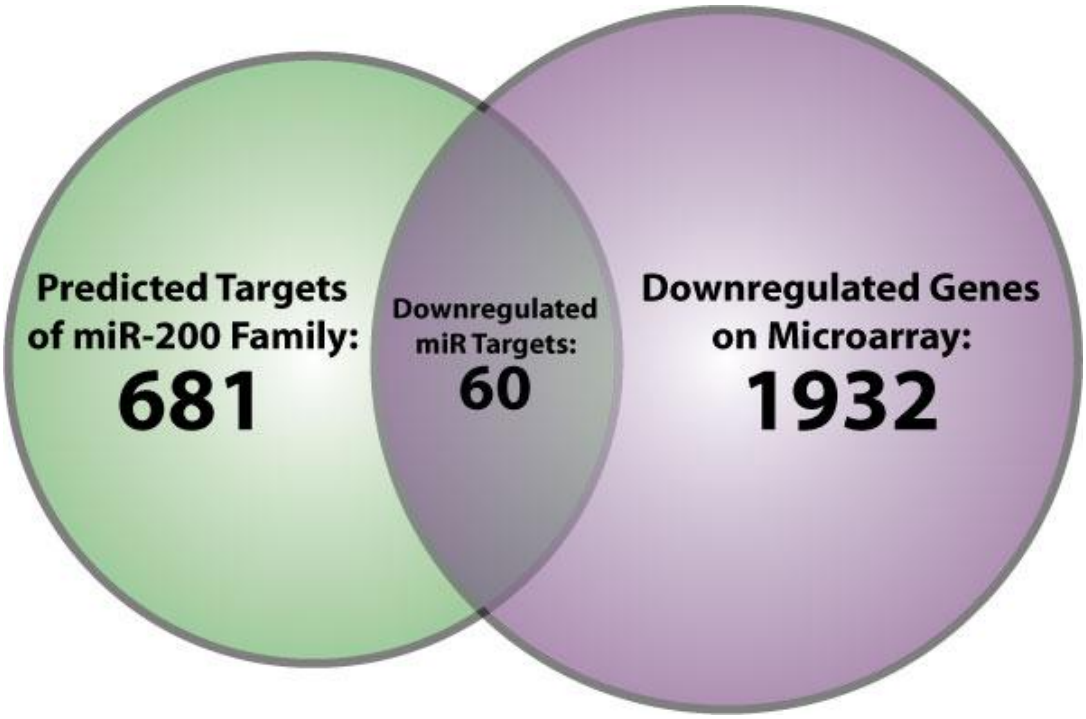

Figure 2-2.2. Diagram Depicting the 60 Genes Predicted to be Targets of the miR-200 Family and Downregulated on Microarray. Targetscan predicts that 681 genes may be directly targeted by members of the miR-200 family and nearly 2000 genes were found to be downregulated on our gene expression microarray. Taking the intersection of these two data sets, 60 genes were found to be targets of the miR-200 family and downregulated on microarray.

TABLE 2-2.1. Targets of miR-200 Family Downregulated by Microarray

GENE SYMBOL	E18/E15	FOLD mRNA CHANGE	GENE NAME	# miR binding sites	miR binding score	miR binding rank
Zeb2	0.6696	-1.5	zinc finger E-box binding homeobox 2	**6**	-1.72	1
Zeb1	0.5970	-1.7	zinc finger E-box binding homeobox 1	**5**	-1.22	2
Crtap	0.5739	-1.7	cartilage associated protein	**1**	-0.72	14
Lcorl	0.4099	-2.4	ligand dependent nuclear receptor corepressor-like	**2**	-0.66	21
Lhfp	0.4462	-2.2	lipoma HMGIC fusion partner	**1**	-0.64	26
Pkd1	0.5548	-1.8	polycystic kidney disease 1 homolog	**2**	-0.63	28
Slc5a3	0.4072	-2.5	solute carrier family 5 (inositol transporters), member 3	**1**	-0.52	68
St6galnac5	0.5412	-1.8	ST6-N-acetylgalactosaminide alpha-2,6-sialyltransferase 5	**1**	-0.52	73
Lass6	0.4283	-2.3	LAG1 homolog, ceramide synthase 6	**1**	-0.5	81
Olfr558	0.6250	-1.6	olfactory receptor 558	**1**	-0.49	90
Ets1	0.5583	-1.8	E26 avian leukemia oncogene 1, 5' domain	**2**	-0.49	93
Arhgap20	0.4825	-2.1	Rho GTPase activating protein 20	**1**	-0.49	94
Scd2	0.6235	-1.6	stearoyl-Coenzyme A desaturase 2	**1**	-0.46	115
Sesn1	0.4141	-2.4	sestrin 1	**1**	-0.44	132
Sema6d	0.5908	-1.7	sema domain, transmembrane domain (TM), and cytoplasmic domain, (semaphorin) 6D	**1**	-0.43	141
Nog	0.3510	-2.8	noggin	**1**	-0.43	145
Pcsk2	0.6819	-1.5	proprotein convertase subtilisin/kexin type 2	**1**	-0.41	157
Pcdh19	0.5735	-1.7	protocadherin 19	**2**	-0.4	158
Ccnyl1	0.6201	-1.6	cyclin Y-like 1	**1**	-0.4	161
Kcnd2	0.0904	-11.1	potassium voltage-gated channel, Shal-related family, member 2	**1**	-0.39	167
Lamc1	0.3381	-3.0	laminin, gamma 1	**1**	-0.38	172
Frmd4a	0.3740	-2.7	FERM domain containing 4A	**1**	-0.36	197
Sfxn1	0.4802	-2.1	sideroflexin 1	**1**	-0.36	199
Lrp1	0.5043	-2.0	low density lipoprotein receptor-related protein 1	**1**	-0.35	200
Abat	0.4276	-2.3	4-aminobutyrate aminotransferase	**1**	-0.35	214
Ank1	0.3023	-3.3	ankyrin 1, erythroid	**1**	-0.34	217
Fyn	0.4562	-2.2	Fyn proto-oncogene	**1**	-0.34	221
Nptx1	0.0244	-41.0	neuronal pentraxin 1	**1**	-0.33	230
Clic4	0.4681	-2.1	chloride intracellular channel 4	**1**	-0.31	252

Glis2	0.6336	-1.6	GLIS family zinc finger 2	**1**	-0.3	265
Syvn1	0.6909	-1.4	synovial apoptosis inhibitor 1, synoviolin	**1**	-0.3	269
Arl5a	0.6580	-1.5	ADP-ribosylation factor-like 5A	**1**	-0.29	286
Cish	0.5693	-1.8	cytokine inducible SH2-containing protein	**1**	-0.29	287
Prkcb1	0.3408	-2.9	protein kinase C, beta 1	**1**	-0.28	309
Ngef	0.4335	-2.3	neuronal guanine nucleotide exchange factor	**1**	-0.27	310
Golim4	0.5961	-1.7	golgi integral membrane protein 4	**1**	-0.27	321
Reck	0.5852	-1.7	reversion-inducing-cysteine-rich protein with kazal motifs	**1**	-0.26	334
Ddx26b	0.4277	-2.3	DEAD/H (Asp-Glu-Ala-Asp/His) box polypeptide 26B	**1**	-0.26	342
Anln	0.4383	-2.3	anillin, actin binding protein (scraps homolog, Drosophila)	**1**	-0.25	347
Gli3	0.4665	-2.1	GLI-Kruppel family member GLI3	**1**	-0.25	353
Snai2	0.5649	-1.8	snail homolog 2 (Drosophila)	**1**	-0.23	369
Rgl1	0.4542	-2.2	ral guanine nucleotide dissociation stimulator,-like 1	**1**	-0.23	378
Scn3b	0.5716	-1.7	sodium channel, voltage-gated, type III, beta	**1**	-0.22	395
Schip1	0.5121	-2.0	schwannomin interacting protein 1	**1**	-0.22	401
Tln1	0.6354	-1.6	talin 1	**2**	-0.22	402
Coro1c	0.6882	-1.5	coronin, actin binding protein 1C	**1**	-0.22	403
Gfi1	0.4617	-2.2	growth factor independent 1	**1**	-0.21	412
Chst2	0.6432	-1.6	carbohydrate sulfotransferase 2	**1**	-0.21	421
Senp5	0.5440	-1.8	SUMO/sentrin specific peptidase 5	**1**	-0.2	434
Cntfr	0.4788	-2.1	ciliary neurotrophic factor receptor	**1**	-0.19	446
Ahnak	0.4546	-2.2	AHNAK nucleoprotein (desmoyokin)	**1**	-0.19	450
Plxna2	0.2521	-4.0	plexin A2	**1**	-0.19	464
Asph	0.2669	-3.7	aspartate-beta-hydroxylase	**1**	-0.18	472
Thex1	0.6175	-1.6	three prime histone mRNA exonuclease 1	**1**	-0.17	479
Cblb	0.5476	-1.8	Casitas B-lineage lymphoma b	**1**	-0.17	480
Sec61a2	0.6558	-1.5	Sec61, alpha subunit 2 (S. cerevisiae)	**1**	-0.17	482
Nedd4l	0.6446	-1.6	neural precursor cell expressed, developmentally down-regulated gene 4-like	**1**	-0.16	506
Arl2bp	0.6168	-1.6	ADP-ribosylation factor-like 2 binding protein	**1**	-0.14	528
Hnf1b	0.4001	-2.5	HNF1 homeobox B	**1**	-0.14	536
Calu	0.5659	-1.8	calumenin	**1**	-0.12	555

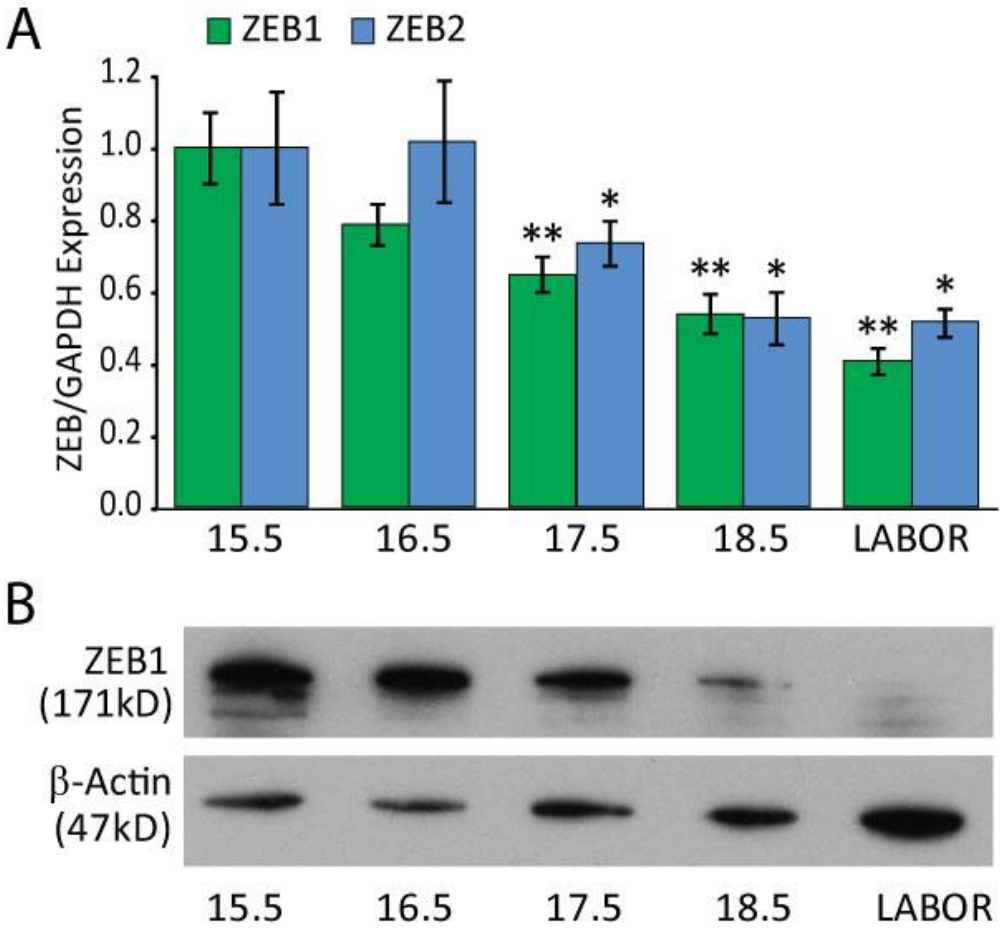

Figure 2-2.3. ZEB1 and ZEB2 mRNA and Protein are Coordinately Downregulated During Late Gestation with Upregulation of the miR-200 Family. (A) ZEB1 and ZEB2 mRNA are downregulated across late gestation in the mouse myometrium, beginning at 17.5 dpc. Expression of each mRNA was determined by qRT-PCR, normalized to GAPDH, and expressed as fold change from 15.5 dpc. Mean ± SEM values are shown. One-way ANOVA, ZEB1: $F(4,20)=12.71$, $p<0.0001$; ZEB2: $F(4,20)=5.37$, $p=0.004$. Multiple comparison test compared to 15.5 dpc: *$p<0.05$, **$p<0.01$, n = 10 mice each for 15.5 dpc and laboring groups, 5 each for 16.5-18.5dpc. (B) ZEB1 protein in nuclear extracts of murine myometrium mirrors the decline in ZEB1 mRNA. β-actin was used as a loading control. Immunoblot shown is representative of 3 independent gestational series of mice. Densitometry analysis of all 3 series revealed a significant decrease in ZEB1 protein between 15.5 dpc and labor. Student's t-test, *$p<0.05$, n = 3 mice per group.

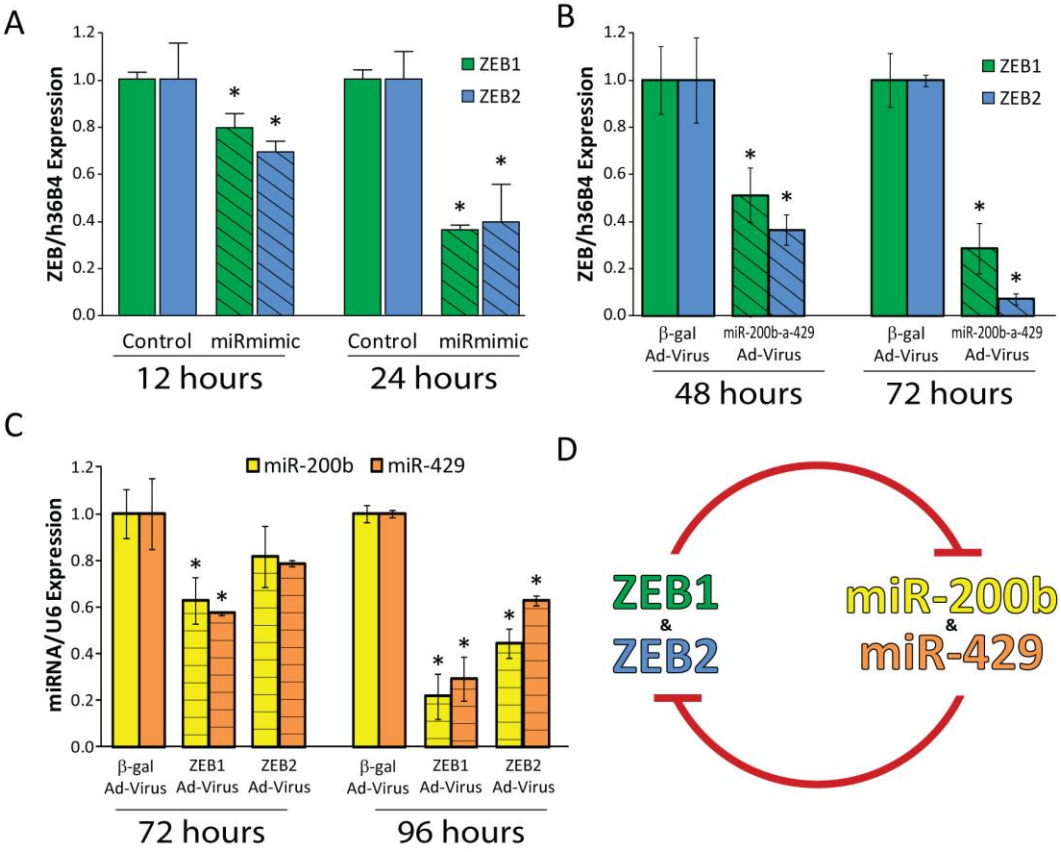

Figure 2-2.4. ZEB1 and ZEB2 are Reciprocally Repressive Targets of the miR-200 Family in Myometrial Cells. **(A)** Transfection of hTERT-HM cells with miRmimics of miR-200b/429 causes a significant reduction in endogenous ZEB1 and ZEB2 at both 12h and 24 h. **(B)** Adenoviral transduction of the miR-200b-a-429 cluster into hTERT-HM cells replicates our findings with miR-200b/429 miRmimics to suppress expression of ZEB1 and ZEB2. **(C)** Primary cultures of mouse myocytes transduced with recombinant adenovirus for ZEB1 or ZEB2 showed suppressed levels of endogenous miR-200b and miR-429. This confirms the reciprocally repressive relationship reported between the miR-200 family and ZEBs. Levels of each mRNA/miRNA were determined by qRT-PCR, normalized to h36B4/U6, and expressed as fold change as compared to non-targeting RNA oligo transfected or β-gal transduced controls. Data are the means ± SD of three replicate experiments. Student's t-test, *p<0.05. **(D)** Diagram depicting the repressive relationship between ZEB1 and ZEB2 and the miR-200 family.

Discussion

These data establish the presence of the miR-200/ZEB relationship in murine myometrium during late gestation. Interestingly, ZEB1 has previously been observed to be expressed in myometrium (Hurt et al., 2008) and regulated by estrogen and progesterone (Spoelstra et al., 2006). Hurt et al. profiled ZEB1 expression patterns in a wide variety of human tissues and found ZEB1 to be highly expressed in the uterus, second only to another tissue enriched in smooth muscle, the bladder. Spoelstra et al. showed that ovariectomized mice treated with progesterone displayed increased expression of ZEB1 in the myometrium, but whether this was a direct action of PR on the ZEB1 promoter was not explored directly.

Our investigations implicate ZEB1 and ZEB2, both shown to be downregulated at term and in labor, as inhibitors of miR-200b/429 in the myometrium by both miRmimic transfection and recombinant adenoviral overexpression of the miR-200b-a-429 cluster. While both methodologies confirm a repression of endogenous ZEB1 and ZEB2 by members of the miR-200 family, recombinant adenoviral overexpression of the miR-200b-a-429 cluster produced more robust downregulation of ZEB1 and ZEB2, perhaps due to the increased transduction efficiency of this assay, and/or due to the presence of miR-200a.

As stated earlier, the ZEB family of transcription factors acts to repress genes by directly binding to E-box (CACCT) sequences in their promoter regions and recruiting corepressors, such as CtBP (Postigo and Dean, 1999). Because of their role as transcriptional repressors and their relatively high expression in the myometrium until term, we hypothesized that ZEB1 and ZEB2 may inhibit the expression of genes important in the initiation of parturition. Because ZEB1 has been found to inhibit IL-2 (Wang et al., 2009), and ZEB2 is known to inhibit connexin-26 (Vandewalle et al., 2005), we hypothesized that ZEB1 and ZEB2 may repress either inflammatory or contraction-associated genes, and thereby serve to maintain uterine quiescence until term.

Materials and Methods

Gene Expression Microarray Analysis. Gene expression microarray analysis was performed on 3 pooled samples of murine uteri at 15.5 dpc and an equal number of pooled samples at 18.5 dpc. Each pool was comprised of uterine tissues from 6 mice (total 18 mice) for each gestational time point. RNA quality was assessed using a 2100 Bioanalyzer (Agilent), and RIN values were >9.3. 260/280 values were >1.85. After quality and purity were confirmed, 200 ng of total RNA was amplified and labeled by the UT Southwestern Microarray Core Facility at the McDermott Center for Human Growth and Development using the TotalPrep RNA Amplification kit (Illumina/Ambion). 1.5 µg of cRNA from each sample was hybridized to Illumina Mouse 6-V1.1 microarrays using standard procedures. All microarray chips were Illumina Mouse V6-1.1 whole genome arrays. Specific information about these chips can be found at www.illumina.com. The raw expression array data were extracted using BeadStudio v2.0 (Illumina). The data were background subtracted and median normalized. The data were then analyzed by t-test and false discovery rate (FDR).

Ingenuity Analysis. Normalized quantitative data sets were analyzed by use of Ingenuity Pathways Analysis (Ingenuity Systems, version 7.6

(www.ingenuity.com) to detect common pathways and gene networks regulated between 15.5 dpc and 18.5 dpc on microarray.

qRT-PCR Analysis of Murine ZEB1 & ZEB2. RNA was deoxyribonuclease treated (Invitrogen) and 2 µg were reverse-transcribed using the Superscript III reverse transcription kit (Invitrogen). Gene expression analysis was conducted using SYBR Green (Applied Biosystems) on an ABI Prism 7700 Detection System (Applied Biosystems). Expression of murine ZEB1 and ZEB2 were determined using forward and reverse primers detailed in Table 2-2.2 (synthesized by Integrated DNA Technologies). Murine GAPDH was used as an internal control (Table 2-2.2). qPCR cycling conditions were 50°C for 2 min and 95°C for 10 min, followed by 40 cycles of 95°C for 15 sec and 60°C for 1 min. The cycle threshold was set at a level at which the exponential increase in PCR amplification was approximately parallel between all samples. All primer sets produced amplicons of the expected size and sequence. Relative gene expression was calculated using the $\Delta\Delta$Ct method.

Immunoblot Analysis. Immunoblots were conducted on nuclear extracts of hTERT-HM cells or flash frozen myometrial tissues. Cells or tissues

were lysed in NE-PER extraction reagent (Pierce, cat# 78833) according to the manufacturer's instructions. Protein concentration was determined by a Bradford assay (Pierce cat# 23225). Equivalent amounts of protein were added to 2X Laemmli Buffer and samples were heated to 95C for 10 min, loaded on 10% SDS-polyacrylamide gels, run at 70-110 volts and transferred to a polyvinylidene difluoride (PVDF) membrane. Membranes were incubated in blocking buffer, comprised of Tris-buffered saline (0.15 M NaCl, 0.05 M Tris-HCl [pH 8.0], 0.05% [vol/vol] Tween 20) containing 3% nonfat dry milk for 60 min at room temperature before addition of primary antibodies. Antibodies directed against ZEB1 (generous gift of Douglas Darling, University of Louisville (Darling et al., 2003)) were diluted in blocking buffer (1:2500). β-Actin (Abcam), diluted in blocking buffer (1:5000) was used as a loading control. Primary antibodies were incubated with membranes overnight at 4C with rocking. Membranes were washed 4 times with Tris-Buffered Saline Tween-20 (TBS-T) for 5 min each at room temperature. Horseradish peroxidase-conjugated goat anti-rabbit IgG, used as a secondary antibody (Zymed Invitrogen cat# 62-1820) was diluted in blocking buffer (1:6,000) and incubated with membranes for 60 min. Membranes were washed 4 times in TBST for 5 min each and visualized using SuperSignal West Pico Chemiluminescent substrate (Thermo Scientific, Rockford, IL) according to the

manufacturer's protocol. Quantitative measurement of immunoblots was performed using Image J (http://rsb.info.nih.gov/ij/index.html).

Cell Culture and miRNA Mimic Studies. hTERT-immortalized human myometrial (hTERT-HM) cells (Condon et al., 2002) were maintained in DMEM-F12 (Gibco) with 10% fetal bovine serum. Upon reaching approximately 75% confluency, hTERT-HM cells were trypsinized, counted, appropriately diluted, plated and transfected with HiPerFect Transfection Reagent (Qiagen), according to the manufacturer's instructions for transfection of smooth muscle cells. Briefly, 5×10^5 hTERT-HM cells plated in 2 ml culture medium per well of a 6-well plate were transfected upon plating with miRNA mimics for both miR-200b and miR-429 (to achieve a final mimic concentration of 10 nM for each miRNA). Cells were allowed to adhere to culture dishes in the presence of miR mimics and harvested at 12 h and 24 h post-transfection for subsequent qRT-PCR analysis.

Isolation of Primary Mouse Myometrial Cells. Primary cultures of myometrial SMCs were prepared using a variation of a method previously described (Shynlova et al., 2002, Mollard et al., 1986). Non-pregnant, female ICR mice were injected subcutaneously with 50 μg 17β-estradiol (Sigma, diluted in 10%

ethanol: 90% sesame oil). Twenty-four hours post-injection, uteri were excised and placed in Buffer A [Hanks Basic Salt Solution (HBSS) pH 7.4 containing 0.098 g/L $MgSO_4$ and 0.185 g/L $CaCl_2$, 25 mM HEPES, 100 U/ml penicillin-streptomycin (Gibco, Grand Island, N.Y., USA) and 2.5 μg/ml amphotericin B (Sigma)]. The uteri horns were cleaned of fat, minced, and washed three times with Buffer B (Buffer A without Mg^{2+} or Ca^{2+}). Enzymatic digestion of the tissue was performed at 37°C with agitation (100 rev/min) for 30 min by adding 10 mL per gram of tissue of 1 mg/ml collagenase type II (Sigma), 0.15 mg/ml deoxyribonuclease I (DNase I, Boehringer Manheim), 0.1 mg/ml soybean trypsin inhibitor, 10% FBS (Cansera, Rexdale, Ontario), and 1 mg/ml BSA (Sigma) in Buffer B. Following incubation, the uterine cells were gently titurated for 1-2 min to aid enzymatic dispersion. Equal amounts (v/v) of buffer B supplemented with 10% FBS was added and the mixture was passed through a cell strainer (40 μm) and stored on ice. Fresh enzyme mix was added to the remaining undigested tissue, and the incubation-aspiration process repeated a total of five to six times. The first cell solution was discarded since it contains mostly debris and damaged cells, and the rest of the solutions were combined. Dissociated cells were collected by centrifugation (200 g for 15 min) and the cell pellet was resuspended in sterile, phenol red-free DMEM (Gibco) supplemented with 10% FBS, 25 mM HEPES, 100 U/ml Penicillin/Streptomycin and 2.5 μg/ml Amphotericin B. To selectively enrich for uterine myocytes, the freshly isolated cell mixture was subjected to a differential attachment technique (Kasten, 1975), whereby dissociated cells were pre-plated on polystyrene dishes for 30-45 min at 37°C to

allow quickly adhering non-myocytes (mostly fibroblasts) to attach to the bottom of the dish. Following attachment of these cells, the supernatant containing the more slowly adhering myometrial smooth muscle cells was collected. Cell numbers and viability were assessed by trypan blue exclusion using a Countess Automated Cell Counter (Invitrogen) prior to plating in 60mm dishes at a density of $3x10^6$ cells per dish. Media was changed 24 hours after plating and every other day thereafter. Cells were used on days 2-5 following isolation.

Adenoviral Transduction. hTERT-HM cells or primary mouse myometrial cells were plated in 30 mm dishes at 500,000 cells per well. Twenty-four hours later, recombinant adenoviruses overexpressing ZEB1, ZEB2, the miR-200b-a-429 cluster, or β-galactosidase were added in a minimal volume of medium (1 ml DMEM:F12/well) at a multiplicity of infection (MOI) of 85-500 pfu/cell. After overnight infection, the cells were washed once with PBS, fed with complete medium and harvested 48-96 h later. Cells overexpressing β-galactosidase were used to assess transduction efficiency (Fig. 2-6.3A) and as a negative control for non-specific effects of adenoviral infection.

Table 2-2.2. Primer sets used in Sybr Green qRT-PCR

Mouse:	
ZEB1-F	GCTGGCAAGACAACGTGAAAG
ZEB1-R	GCCTCAGGATAAATGACGGC
ZEB2-F	GGGACAGATCAGCACCAAAT
ZEB2-R	GACCCAGAATGAGAGAAGCG
CXN-43-F	TCCAAGGAGTTCCACCACTT
CXN-43-R	TGGAGTAGGCTTGGACCTTG
OXTR-F	TTCTTCGTGCAGATGTGGAG
OXTR-R	TGTAGATCCATGGGTTGCAG
COX2-F	CAGCCAGGCAGCAAATCC
COX2-R	ACATTCCCCACGGTTTTGAC
20αHSD-F	GTACAAGCCTGTGTGCAACCA
20αHSD-R	CAGTAGGCCAGCAGCTTGCT
GAPDH-F	TTCTTCGTGCAGATGTGGAG
GAPDH-R	TGTAGATCCATGGGTTGCAG

Human:	
ZEB1-F	GATGATGAATGCGAGTCAGATGC
ZEB1-R	CTGGTCCTCTTCAGGTGCC
ZEB2-F	AACAACGAGATTCTACAAGCCTC
ZEB2-R	TCGCGTTCCTCCAGTTTTCTT
CXN-43-F	TGGATTCAGCTTGAGTGCTG
CXN-43-R	GGTCGCTCTTTCCCTTAACC
OXTR-F	TTCTTCGTGCAGATGTGGAG
OXTR-R	CAGCATGTAGATCCAGGGGT
36B4-F	TGCATCAGTACCCCATTCTATCA
36B4-R	AAGGTGTAATCCGTCTCCACAGA

CHAPTER 2- SECTION 3
Conservation of the miR-200 / ZEB Relationship

Experimental Design

Because of reports sighting major differences between murine and human gestation and parturition (Mitchell and Taggart, 2009), one of our main aims in investigating miRNA regulation of gene expression in pregnancy was to identify novel, conserved pathways, common to mice and women. As one of the defining features of miRNAs is their broad conservation across species, we hypothesized that the miR-200 family and ZEBs may play similar roles in both murine and human myometrium. All 5 members of the miR-200 family are known to be expressed in both species, and are similarly clustered in each (Figure 1-1.2).

To investigate whether expression of the miR-200 family and ZEB1 and ZEB2 during pregnancy and labor are conserved from mouse to human, we conducted qRT-PCR analysis of RNA from myometrial biopsies of women at term, either not in labor or in labor.

Results: The miR-200/ZEB Relationship is Conserved from Mouse to Human

Supporting our hypothesis that the miR-200/ZEB relationship may play a role in pregnancy in mouse and human, the miR-200 family was found to be significantly upregulated (Figure 2-3.1A) and ZEB1 and ZEB2 downregulated in laboring human myometrium, as compared to myometrium of non-laboring women at term (Figure 2-3.1B). Consistent with the RNA data, protein expression of ZEB1 was also significantly downregulated at term in human myometrial samples as measured by Western blotting (Figure 2-3.1C). These data indicate that the miR-200 family and ZEB1/2 are similarly regulated in both mice and humans during labor.

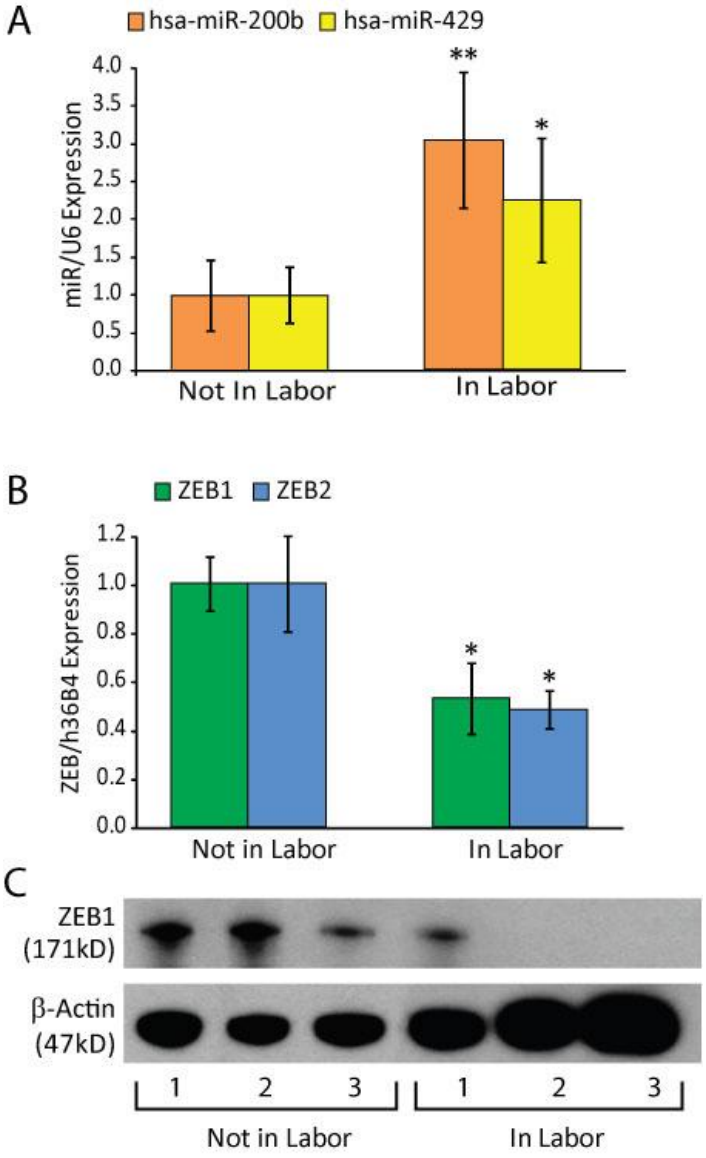

Figure 2-3.1. The miR-200/ZEB Relationship is Conserved from Mouse to Human. miR-200b/429 was significantly upregulated (A) and ZEB1 and ZEB2 mRNA significantly downregulated (B) in laboring human myometrium (IL), as compared to non-laboring (NIL) controls. Expression of each miRNA/mRNA was determined by qRT-PCR, normalized to U6/h36B4, and expressed as-fold increase over NIL. Mean ± SEM values are shown. Student's t-test, *$p<0.05$, $n=14$ for IL, $n=23$ for NIL. (C) ZEB1 protein expression was decreased in nuclear extracts of myometrium from women IL. β-actin was used as a loading control. Immunoblot shown is representative of 3 replicate experiments. Densitometry analysis of all blots comparing IL to NIL revealed a significant decrease in ZEB1 protein in labor. Student's t-test, *$p<0.05$, $n = 9$ per group.

Discussion

Our findings that miR-200b/429 and ZEB1 and ZEB2 are regulated in the same manner from mouse to human are extremely exciting and open the possibility that ZEB1 and ZEB2, already known to be highly enriched in human uterus (Hurt et al., 2008), may play a role in the maintenance of uterine quiescence during human gestation.

These findings also lend support to our use of the mouse as a model to further investigate the function of the miR-200 family and its targets, ZEB1 and ZEB2, during gestation and parturition. As pregnant human myometrial samples at various stages of pregnancy are rare, the ability to study gene regulation in the murine myometrium dramatically improves our ability to conduct more mechanistic investigations.

Materials and Methods

Human Subjects and Tissue Acquisition. Lower uterine segment myometrial tissues were biopsied at term from pregnant women undergoing cesarean section. Informed consent was obtained in writing from each woman before surgery using protocols approved by the Institutional Review Board of University of Texas Southwestern Medical Center in accordance with the Donors Anatomical Gift Act of the State of Texas. Myometrial biopsies were collected from two groups of subjects: 1) pregnant women who underwent cesarean section before the onset of labor at term with no evidence of infection; 2) pregnant women in active labor at term who underwent cesarean section. Myometrial smooth muscle was dissected from each biopsy, flash frozen in liquid nitrogen, and stored at –80 C for subsequent protein and mRNA analysis.

qRT-PCR Analysis of hsa-miR-200b, and hsa-miR-429. Reverse transcription and TaqMan qPCR (Applied Biosystems) were performed as described in Section 1 with the following primers and probes: Applied Biosystems hsa-miR-200b Assay ID# 002251, Applied Biosystems hsa-miR-429 Assay ID# 001024, and Applied Biosystems U6 snRNA Assay ID # 001973.

qRT-PCR Analysis of Human ZEB1 & ZEB2. RNA was deoxyribonuclease treated (Invitrogen), Superscript III reverse transcribed (Invitrogen), and subjected to SYBR Green PCR (Applied Biosystems), as described in Section 2. Expression of human ZEB1 and ZEB2 was determined using forward and reverse primers detailed in Table 2-2.2. Human 36B4 was used as an internal control (Table 2-2.2).

Immunoblot Analysis. Immunoblots for ZEB1 were conducted on nuclear extracts of flash frozen myometrial tissues from term human patients, as detailed in Section 2.

CHAPTER 2- SECTION 4
miR-200 / ZEBs in Models of Preterm Labor

Experimental Design

Because of our encouraging data demonstrating a clear reciprocal relationship of the miR-200 family and its targets, ZEB1 and ZEB2, during pregnancy and labor, we wanted to determine whether similar changes in miR-200b/429 and ZEB1 and ZEB2 expression were associated with preterm labor. To explore this, we evaluated two mouse models of preterm labor induced at 15.5 dpc, a time point prior to the observed changes in expression of miR-200b/429, ZEB1 and ZEB2, and contraction-associated genes. Preterm labor was induced either by a single subcutaneous injection of the antiprogestin/antiglucocorticosteroid, RU486 (Dudley et al., 1996, Cadepond et al., 1997) (Figure 2-4.1A), or by intra-amniotic injections of the bacterial endotoxin, lipopolysaccharide (LPS), which acts via toll-like receptors to induce a robust intraamniotic and intrauterine inflammatory cascade (Figure 2-4.1B). RU486 induced labor within 12 h in 7/7 injected mice; LPS induced preterm labor within 12-18 hours in 7/10 injected mice. None of the vehicle-injected mice delivered preterm.

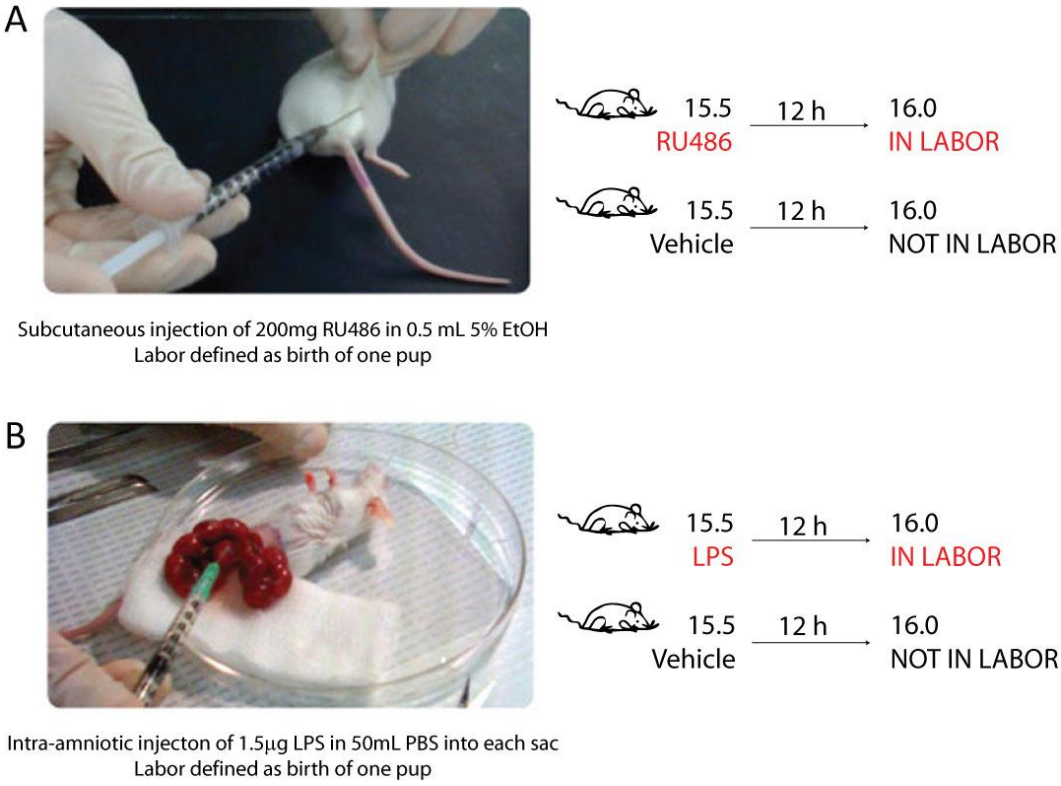

Figure 2-4.1. Experimental Design for Preterm Labor Studies. Two mouse models were utilized for preterm labor studies: a model of intrauterine inflammation and a hormonal model of preterm birth. (A) For the hormonally-induced preterm labor, 15.5 dpc females treated were injected subcutaneously into the flank region with RU486 (200 μg) or sterile 5% EtOH. (B) For the inflammation-induced preterm labor, 15.5 dpc pregnant mice were laparotomized and each amniotic sac was carefully infused with LPS (1.5μg) or sterile PBS. Both models of preterm labor resulted in a high rate of preterm delivery on 16.0 dpc. None of the vehicle-injected mice went into labor prematurely. The mice were sacrificed upon the birth of one pup, and time-matched controls were sacrificed directly afterwards.

Results: miR-200s are Upregulated and ZEBs Downregulated in Preterm Labor

Both RU486 and LPS significantly upregulated miR-200b/429 expression in pregnant mouse myometrium, as compared to vehicle-injected controls (Figure 2-4.2A & Figure 2-4.2B). Consistent with the inverse regulation of miR-200b/429 and ZEB1 and ZEB2 observed during late gestation in mouse and human, both models of preterm labor resulted in markedly decreased expression of ZEB1 and ZEB2 mRNA (Figure 2-4.2C & Figure 2-4.2D). ZEB1 protein was also downregulated in the myometrium of preterm laboring mice (Figure 2-4.2E & Figure 2-4.2F). These findings suggest that alterations in myometrial expression of miR-200b/429 and ZEB1 and ZEB2 may play a role in the induction of both term and preterm labor.

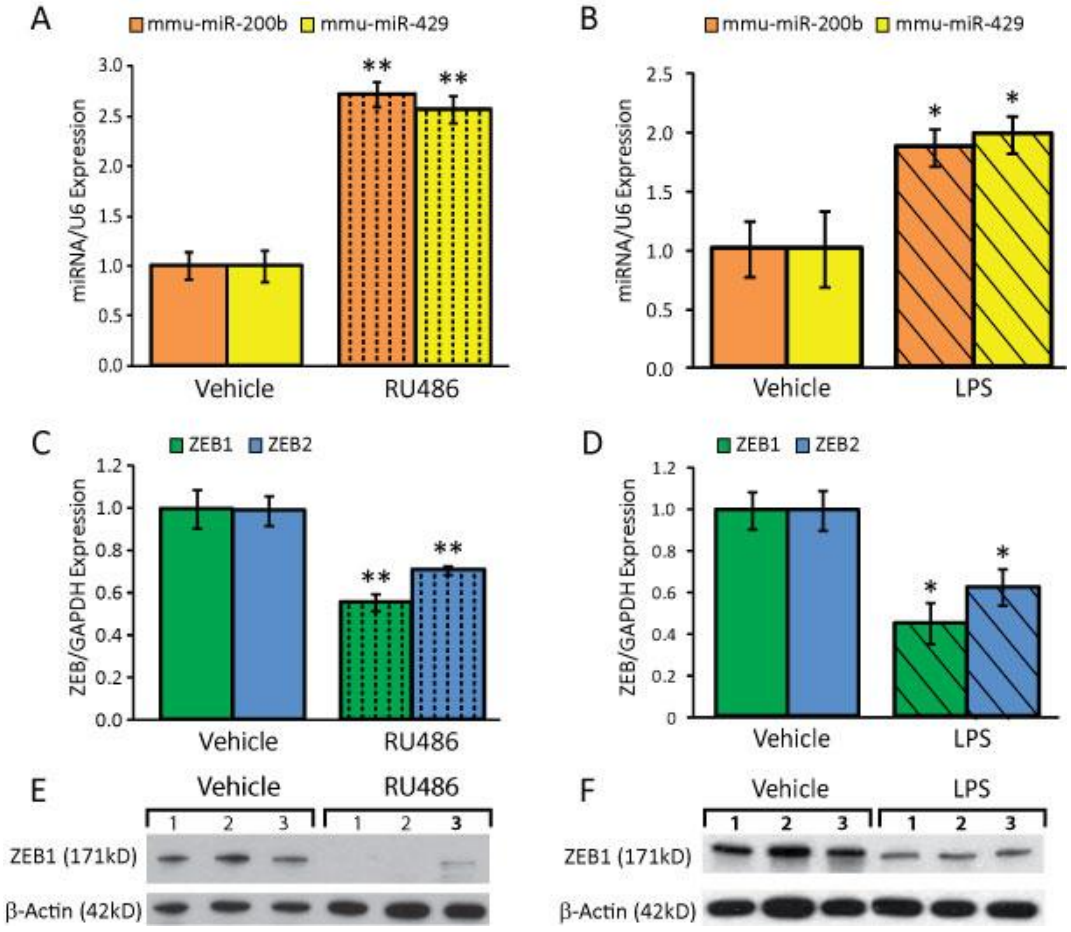

Figure 2-4.2. miR-200b/429 are upregulated and ZEB1 and ZEB2 are downregulated in two models of preterm labor. (A&B) Effects of RU486 treatment (A) or LPS treatment (B) to induce preterm labor. Animals were injected with a single *s.c.* injection of RU486 (200 μg) or intraamniotic injections of 1.5 μg LPS into each sac at 15.5 dpc. Mice were considered in labor upon birth of one pup. (C&D) miR-200b/429 are significantly upregulated in RU486-induced (C) and LPS-induced (D) preterm labor. (E&F) ZEB1 and ZEB2 in the same tissue samples as in C&D are decreased with RU486-induced (E) or LPS-induced (F) preterm labor. Expression of each miRNA/mRNA was determined by qRT-PCR, normalized to U6/GAPDH, and expressed as fold change over vehicle-treated controls. Mean ± SEM values are shown. Student's t-test, *$p<0.05$, **$p<0.01$, n = 7 per group. Experiments were repeated twice with similar results. (G&H) ZEB1 protein expression in nuclear extracts of murine myometrium is decreased in association with RU486-induced (G) or LPS-induced (H) preterm labor. β-actin was used as a loading control. Densitometry analysis of blots comparing uterine nuclear extracts from RU486- and LPS- treated mice to vehicle-injected controls revealed a significant reduction in ZEB1 protein with preterm labor. Student's t-test, *$p<0.05$, n = 7 mice per group.

Discussion

It was our initial hope that by investigating two models of preterm labor, inflammatory (LPS) and hormonal (RU486), we might gain insight into the regulation of the miR-200 family and ZEBs by either inflammation or progesterone withdrawal. However, our finding that both models similarly regulate miR-200s and ZEBs was not unexpected, since inflammation has been shown to decrease circulating progesterone levels (Fidel et al., 1998) and may decrease the functionality of the progesterone receptor (Mendelson, 2009). Therefore, because impaired PR signaling was common to both models of preterm labor, it was of interest to examine the modulation of the miR-200 family and ZEB 1 and 2 by progesterone.

The finding that preterm labor was associated with similar changes in both the miR-200 family and its targets, ZEB1 and ZEB2, to that seen in term labor suggests that these genes may be altered by signaling pathways common to both term and preterm labor. This observation is exciting, not only because it may implicate progesterone withdrawal at term in the regulation of miR-200s and ZEBs, but also because it opens the possibility that therapeutic modulation of either miR-200s or ZEBs could prevent preterm labor.

Materials and Methods

Mice and Murine Tissue Collection. Eight-week-old, timed-pregnant ICR/CD1 females were purchased from Harlan Laboratories (mice were mated and tissues harvested as described in Section 1).

Preterm Labor Studies. Two mouse models were utilized for preterm labor studies: a model of intrauterine inflammation and a hormonal model of preterm birth. For the inflammation-induced preterm labor, 15.5 dpc timed-pregnant ICR/CD1 females were placed briefly under isoflurane anesthesia and subsequently injected (i.p.) with 1.25mL Avertin (tribromoethanol; Sigma). Both uterine horns were gently pulled through a 1-cm midline abdominal incision, and lipopolysaccharide (LPS; Sigma, 1.5μg LPS in 50μL PBS) or sterile PBS (50 μl) was carefully injected through the exposed uterine wall into all amniotic sacs with a sterile 24-gauge, half-inch needle. The uterus was returned to the abdominal cavity, the abdominal muscle wall was closed with ETHICON 5-0 Chromic Gut sutures (Becton Dickinson), and skin was closed by using 9-mm wound clips (AUTOCLIP, Becton Dickinson). The mice were kept under a warming lamp for an hour postoperatively. For the hormonally-induced preterm labor, 15.5 dpc timed-pregnant ICR/CD1 females were placed briefly under isoflurane anesthesia. RU486 (200mg RU486 in 0.5 mL 5%

EtOH, Sigma), or sterile 5% EtOH (0.5 mL) was injected subcutaneously into the flank region of each mouse. Both treatments resulted in a high rate of preterm delivery (12 h post-RU486 and 8-18 h post-LPS treatment), and did not cause maternal mortality (Dudley et al., 1996). None of the vehicle-injected mice went into labor. The mice were sacrificed upon the birth of one pup, and time-matched controls were sacrificed directly afterwards.

qRT-PCR Analysis of mmu-miR-200b and mmu-miR-429. Reverse transcription and TaqMan qPCR (Applied Biosystems) were performed as described in Section 1 with the following primers and probes: Applied Biosystems mmu-miR-200b Assay ID# 002251, Applied Biosystems mmu-miR-429 Assay ID# 001077, and Applied Biosystems U6 snRNA Assay ID # 001973.

qRT-PCR Analysis of Murine ZEB1 & ZEB2. RNA was deoxyribonuclease treated (Invitrogen), Superscript III reverse transcribed (Invitrogen), and SYBR Green PCR (Applied Biosystems) performed as described in Section 2. Expression of murine ZEB1 and ZEB2 were determined using forward and reverse primers detailed in Table 2-2.2. Murine GAPDH was used as an internal control (Table 2-2.2).

Immunoblot Analysis. Immunoblots for ZEB1 were conducted on nuclear extracts of flash frozen myometrial tissues from LPS, RU486, or control treated mice, as detailed in Section 2.

CHAPTER 2- SECTION 5
Hormonal Regulation of miR-200s and ZEBs

Experimental Design

While the mechanisms by which RU486 and LPS induce preterm labor are notably complex, both agents are known to attenuate PR signaling (Fidel et al., 1998). To further investigate whether P_4/PR regulates expression of the miR-200 family or ZEBs directly, we conducted progesterone treatment studies both in pregnant mice and cells in culture.

To investigate the effects of progesterone on expression of the miR-200 family and of ZEB1 and ZEB2 during gestation, mice were injected daily with P_4 on 15.5-18.5 dpc, at a dose known to delay parturition (Hashimoto et al., 2010) (Figure 2-5.1). Uteri from mice treated with daily P_4 were harvested at 19.0 dpc and compared with control mice in labor at the same time point.

Treatment of cultured T47D breast cancer cells with progesterone was also explored. T47D cells were selected for these studies because of their high endogenous expression of PR and consequent sensitivity to progesterone treatment. Cells were treated with progesterone (10^{-7} M) and examined at 12 h and 24 h for expression of ZEB1 and ZEB2, as well as miR-200b and -429.

Direct interaction between the progesterone receptor and the *ZEB1* promoter was investigated in HEK-293 cells, which lack endogenous PR. In these studies, cells were cotransfected with a reporter construct containing 978-bp of *ZEB1* 5'-flanking sequence subcloned upstream of the *luciferase* gene and with an expression vector containing either wild-type (WT) PR-B or PR-B with an inactivating mutation in the DNA-binding domain (mutPR-B_{DBD}). The cells were cultured $\pm$ P_4 (10^{-7} M) for 24 h and assayed for luciferase activity.

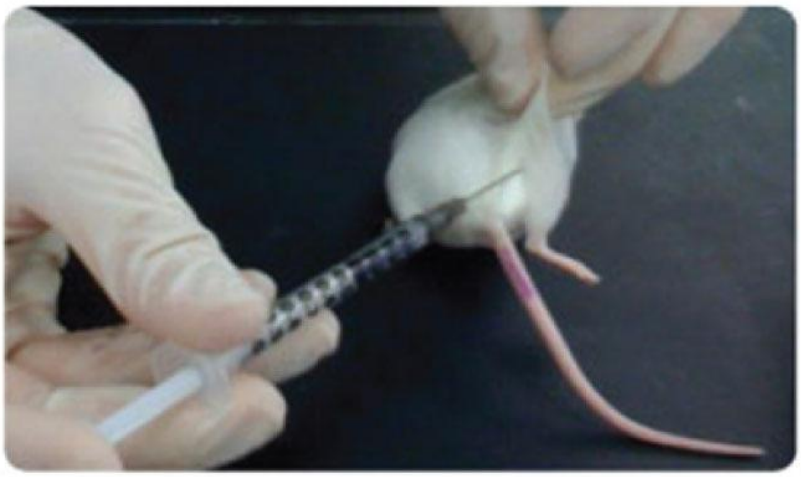

Subcutaneous injection of 1mg P_4 in 0.5mL oil
Labor defined as birth of one pup

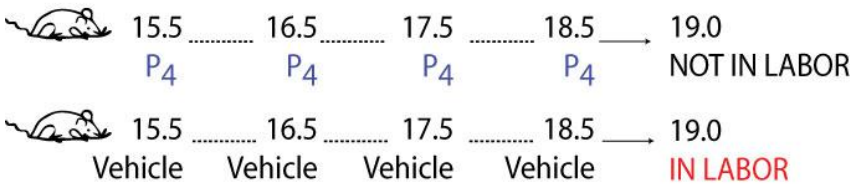

Figure 2-5.1. Experimental Design of Progesterone Treatment Studies. Timed-pregnant ICR/CD1 females were injected subcutaneously each day with progesterone (1μg P_4 in 0.5 mL sesame oil), or with sterile oil (0.5 mL), in the flank region, from 15.5 dpc through 18.5 dpc. Vehicle-injected mice were sacrificed in labor (upon the birth of one pup); time-matched P_4-treated animals were sacrificed directly afterwards. None of the P_4 treated animals progressed to labor at 19.0 dpc.

Results: P_4 acts via the PR to directly induce *ZEB1* Expression with Downstream Effects on ZEB2

P_4 injection had a modest effect to decrease myometrial expression of miR-200b/429 *in vivo*, as compared to vehicle-injected mice (miR-200b expression was reduced to 70% of vehicle treated animals, p = 0.2) (Figure 2-5.2A). By contrast, ZEB1 mRNA (Figure 2-5.2B) and protein (Figure 2-5.2C) levels were significantly increased ($p<0.05$) in myometrium of the P_4 injected mice, while ZEB2 mRNA levels were unaffected (Figure 2-5.2B).

To further investigate the selective induction of ZEB1 by P_4, we conducted experiments in T47D breast cancer cells because of their relatively high levels of expression of endogenous PR. Treatment of the cells with P_4 for 12 or 24 h caused a pronounced induction of ZEB1 mRNA, while no effect of P_4 on ZEB2 expression was evident (Figure 2-5.3). These data recapitulate our findings of the effect of exogenous P_4 treatment *in vivo*.

We next wished to test whether the action of progesterone to induce ZEB1 occurs via the direct result of PR binding to the *ZEB1* promoter. To do this, we cotransfected HEK293 cells with luciferase reporter constructs comprised of the first ~1000-bp of *ZEB1* 5'-flanking sequence fused upstream of *luciferase* and with a PR-B expression

vector. After transfection, the cells were cultured in the absence or presence of progesterone for 24 h. Progesterone treatment had a pronounced effect to upregulate *ZEB1* promoter activity in cells cotransfected with WT PR-B; however, this was blocked in cells cotransfected with mutPR-$B_{DBD,}$ where the PR DNA binding domain was mutated (Figure 2-5.4).

Our findings in pregnant mice and cultured cells (Figures. 2-5.2 and 2-5.3) indicate that P_4 selectively induces ZEB1, but does not have a direct effect to increase ZEB2 expression. Since both ZEB1 and ZEB2 are upregulated in the uterus throughout most of pregnancy, this raises the question as to what factor(s) cause the pregnancy-associated induction of ZEB2. We postulated that P_4 induction of ZEB1 causes suppression of the miR-200 family, which, in turn, relieves suppression of ZEB2, resulting in its subsequent induction. To address this hypothesis experimentally, primary cultures of mouse myometrial cells were infected with recombinant adenoviruses expressing ZEB1 or β-Gal, as control, and ZEB2 mRNA levels were analyzed as a function of time. As shown in Figure 2-5.5, overexpression of ZEB1 resulted in a time-dependent increase in ZEB2 mRNA. These findings may explain why both ZEB1 and ZEB2 are increased in the myometrium during pregnancy, while only ZEB1 is directly upregulated by PR.

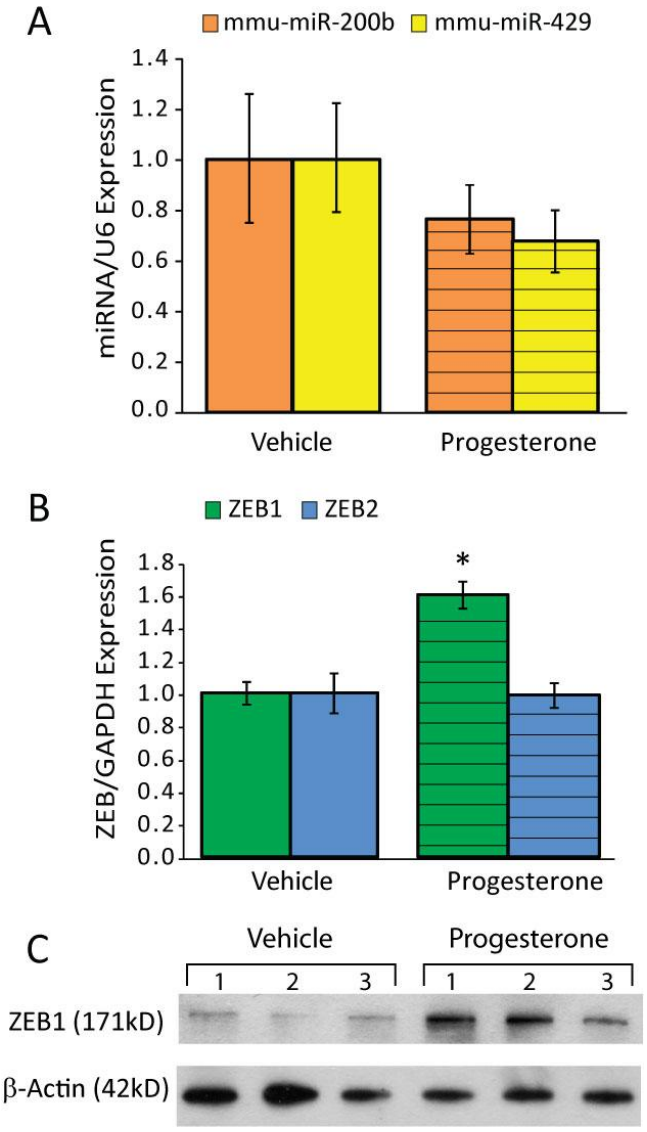

Figure 2-5.2. P_4 Significantly Upregulates ZEB1, but not ZEB2 Expression, and Only Modestly Affects the miR-200 Family in Late Gestation Pregnant Mice. (A) Expression of miR-200b/429 was not significantly inhibited by exogenous P_4 treatment. (B) ZEB1, but not ZEB2 mRNA, was significantly increased by P_4 treatment (same samples as in A) Expression of each miRNA/mRNA was determined by qRT-PCR, normalized to U6/GAPDH, and depicted as fold increase over vehicle-treated controls. Mean ± SEM values are shown. Student's t-test, *$p<0.05$, n = 7 mice per group. Data are representative of three similar experiments. (C) ZEB1 protein in myometrial nuclear extracts is increased by P_4-treatment. β-actin was used as a loading control. Densitometry analysis of blots comparing P_4 treated mice to vehicle controls revealed that P_4 caused a significant increase in ZEB1 protein levels. Student's t-test, *$p<0.05$, n = 7 mice per group.

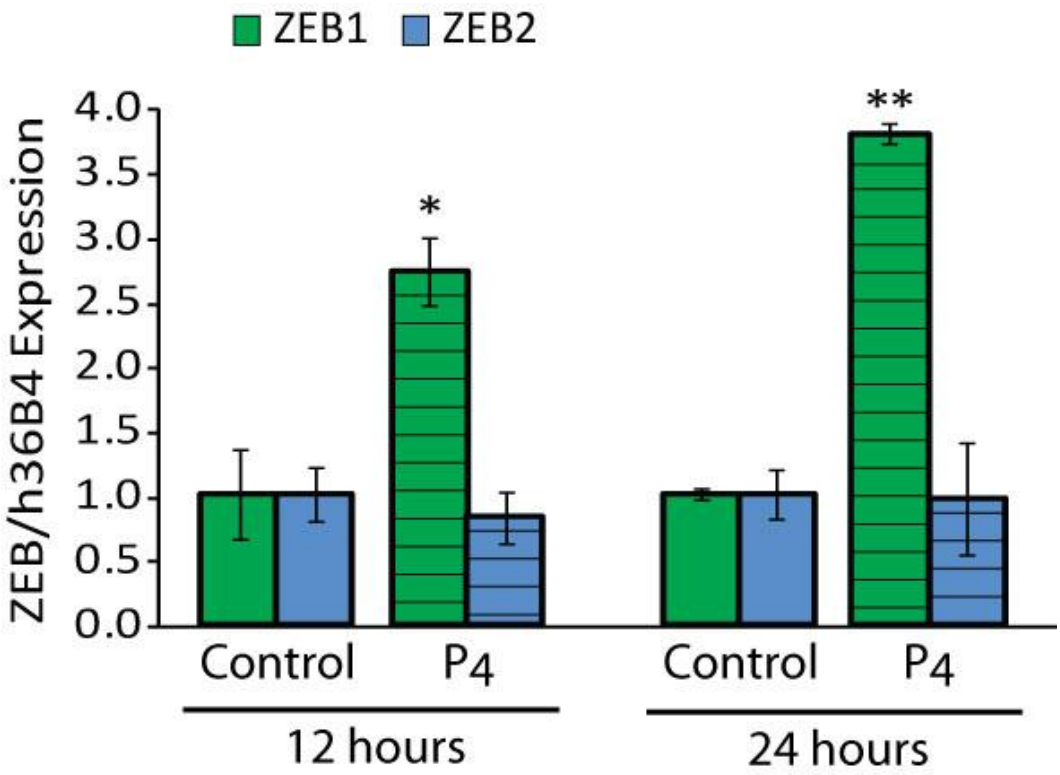

Figure 2-5.3. P_4 Significantly Upregulates ZEB1, but not ZEB2, in T47D Cells. ZEB1, but not ZEB2, mRNA levels are induced in T74D cells treated with 10^{-7} M P_4 for 12 or 24 h. Expression of each gene was determined by qRT-PCR, normalized to h36B4, and expressed as fold increase over vehicle-treated control cells. Data are the means ± SD from three replicate experiments. Student's t-test, *p<0.05, **p<0.01.

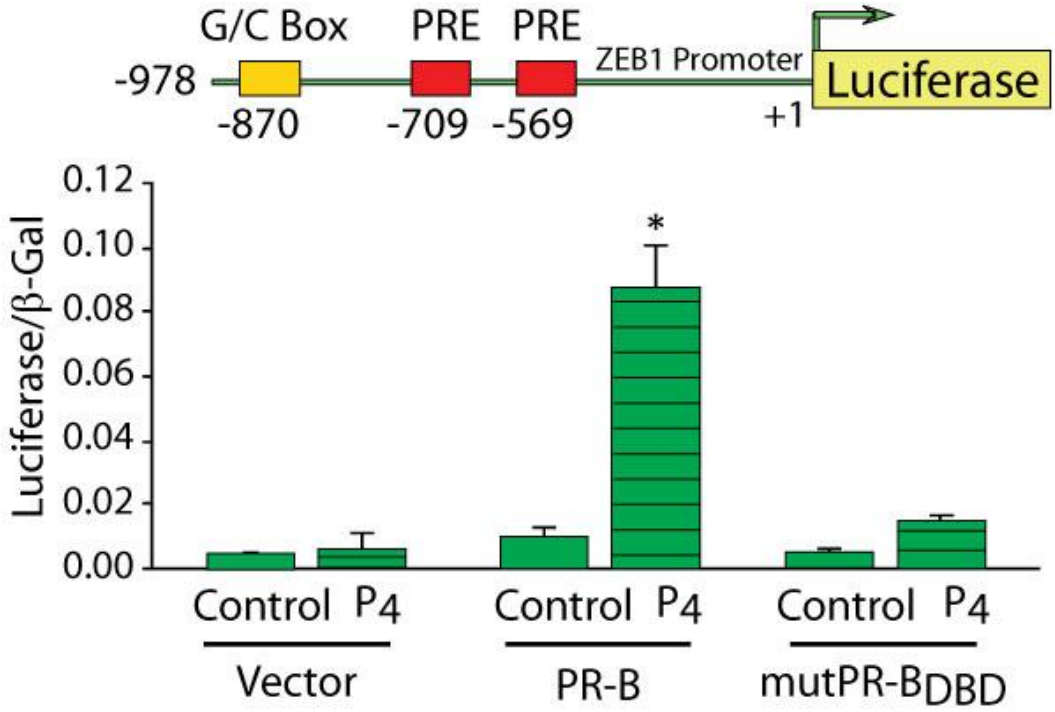

Figure 2-5.4. ZEB1 is Induced by P_4 via Direct Binding of PR to the *ZEB1* Promoter. P4 acting via PR induces *ZEB1* promoter activity. HEK293 cells were transiently transfected with a *ZEB1-Luc* reporter construct containing 978-bp of 5'-flanking sequence from the *hZEB1* gene and with empty expression vector (control) or with a *CMV* expression vector for the mouse PR-B isoform (mPR-B), with or without a mutation in the DNA-binding domain (mutPR-B_{DBD}). The cells were cultured ± P_4 (10^{-7} M) for 24 h and luciferase activity was assayed, normalized to β-gal, and expressed as fold increase over vector-transfected control cells. Data depict the means ± SD of three replicate experiments. Student's t-test, *p<0.05.

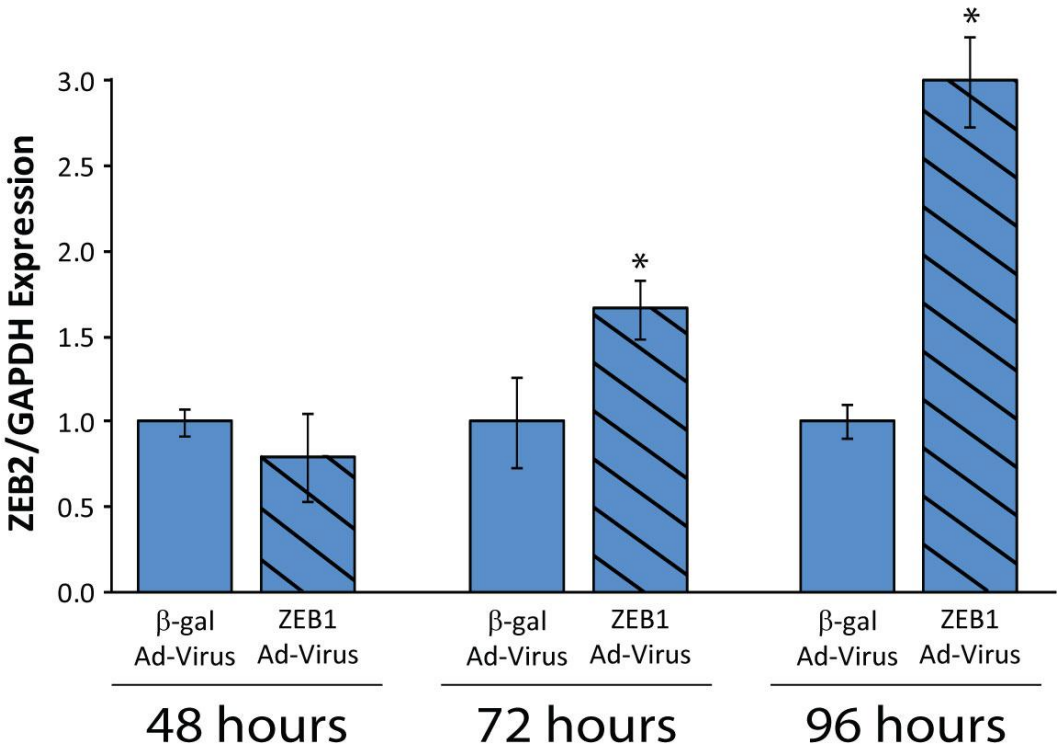

Figure 2-5.5. Overexpression of ZEB1 Causes Induction of ZEB2 mRNA Expression in Primary Mouse Myometrial Cells. Recombinant adenoviral transduction of ZEB1 into primary murine myometrial cells results in induction of endogenous after 72 hours. Expression of ZEB2 was determined by qRT-PCR, normalized to GAPDH, and expressed as fold increase over β-gal-transduced control cells. Data depict the means ± SD of two replicate experiments. Student's t-test, *$p<0.05$.

Discussion

These data provide strong evidence to suggest that *ZEB1* is a direct PR target gene. Based on these findings, we hypothesize that during pregnancy, P_4/PR increases expression of ZEB1 by direct binding to the ZEB1 promoter. From our findings in myometrial cells (Figure 2-2.4C) and those of others in different cell types, it is known that increased expression of ZEB1, in turn, acts to suppress the miR-200 family. We suggest that the increased levels of progesterone during pregnancy may act via induction of the transcriptional repressor, ZEB1, to repress contraction-associated genes in the quiescent uterus. Decreased expression of the miR-200 family by high levels of ZEB1 would relieve suppression of ZEB2 (as well as ZEB1 itself), resulting in further repressive action on their downstream targets, helping to further maintain uterine quiescence by repressing contractile gene expression.

Near term, the decrease in circulating P_4 and/or decrease in PR function associated with labor results in downregulation of ZEB1 expression, and, in turn, an upregulation of the miR-200 family, further suppressing ZEB1 and ZEB2. This, in turn, results in derepression of ZEB1 and ZEB2 target genes, resulting in increased uterine contractility and labor by inducing contractile gene expression,

Since contraction-associated genes have not previously been reported to be targets of ZEB1 and ZEB2, we next conducted studies aimed at exploring the connection (see Section 6).

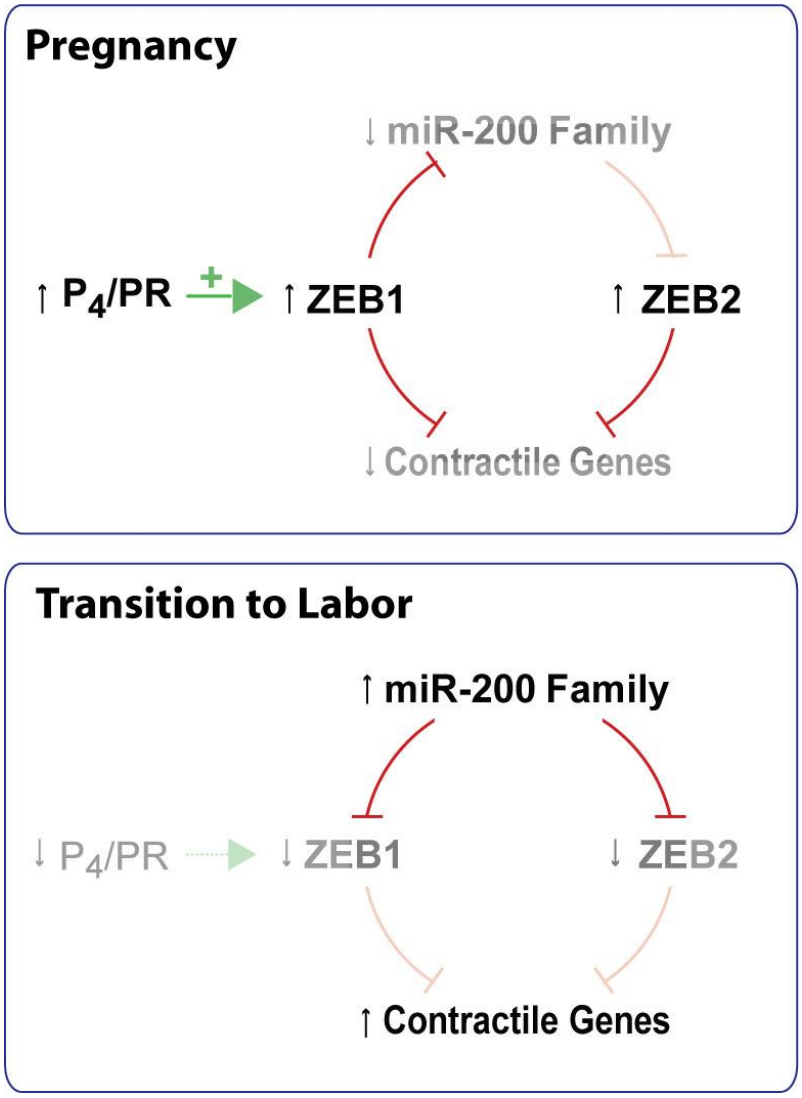

Figure 2-5.6. Hypothesized Model for Regulation of the miR-200 Family and Targets, ZEB1 and ZEB2, in Gestation and Labor. During pregnancy, P_4/PR increase expression of ZEB1, which acts to suppress the miR-200 family, as well as contraction-associated genes. Decreased expression of the miR-200 family relieves suppression of ZEB2 (as well as ZEB1), resulting in further downregulation of contractile genes. Near term, a decrease in circulating P_4 and/or a decrease in PR function results in downregulation of ZEB1 expression, and, in turn, an upregulation of the miR-200 family, further suppressing ZEB1 and ZEB2. This removes the brakes from contractile gene expression, resulting in increased uterine contractility and labor.

Materials and Methods

Mice and Murine Tissue Collection. Eight-week-old, timed-pregnant ICR/CD1 females were purchased from Harlan Laboratories were mated and tissues harvested as described in Section 1.

Progesterone Treatment Studies. The timed-pregnant mice were injected subcutaneously daily with progesterone (1μg P_4 in 0.5 mL sesame oil), or with sterile oil (0.5 mL), in the flank region, from 15.5 dpc through 18.5 dpc. For these experiments, vehicle-injected mice were sacrificed in labor (upon the birth of one pup); time-matched P_4 treated animals were sacrificed directly afterwards. None of the P_4 treated animals progressed to labor at 19.0 dpc.

qRT-PCR Analysis of hsa-miR-200b/429 and mmu-miR-200b/429. Reverse transcription and TaqMan qPCR (Applied Biosystems) were performed as described in Section 1 with the following primers and probes: Applied Biosystems hsa-miR-200b Assay ID# 002251; Applied Biosystems hsa-miR-429 Assay ID# 001024; Applied Biosystems mmu-miR-200b Assay ID# 002251; Applied Biosystems mmu-miR-429 Assay ID# 001077, and Applied Biosystems U6 snRNA Assay ID # 001973.

qRT-PCR Analysis of Human and Murine ZEB1 & ZEB2. RNA was deoxyribonuclease treated (Invitrogen), Superscript III reverse transcribed (Invitrogen), and SYBR Green PCR (Applied Biosystems) was performed as described in Section 2. Expression of murine and human ZEB1 and ZEB2 was determined using forward and reverse primers detailed in Table 2-2.2. Murine GAPDH was used as an internal control for animal studies. For studies in human cells, h36B4 was used as an internal control (Table 2-2.2).

Immunoblot Analysis. Immunoblots for ZEB1 protein were conducted using nuclear extracts of flash frozen myometrial tissues from progesterone or vehicle treated mice, as detailed in Section 2.

Cell Culture. Human embryonic kidney (HEK-293) cells were maintained in DMEM (Gibco) supplemented with 10% FBS. Human breast cancer T47D cells were maintained in RPMI medium with 10% fetal bovine serum (FBS) and 100 µM insulin.

Effects of Progesterone on ZEB1 and ZEB2 Expression in Cultured T47D Breast Cancer Cells. PR positive T47D human breast cancer cells were checked for viability by Trypan blue staining, counted, and seeded at

3×10^5 cells/well in 6-well plates for PR stimulation assays. Cells were cultured in phenol red-free medium supplemented with charcoal-stripped FBS for 24 h before treatment with dimethyl sulfoxide (DMSO) or P_4 (10^{-7}M) for 12h or 24 h in medium without phenol red or FBS. RNA from cells was then harvested for further analysis by qRT-PCR using the Qiagen RNeasy Minikit, according to the manufacturer's instructions (Qiagen cat# 74104).

Analysis of P_4/PR Regulation of *ZEB1* Promoter Activity. For investigation of effects of P_4/PR on *ZEB-1* promoter activity, 978 bp of 5'-flanking region of the *hZEB1* gene (-978 bp to +7bp) was amplified from a human genomic DNA and cloned into pGL4 plasmid to produce a *ZEB1-Luciferase* reporter construct. To analyze effects of P_4/PR on *hZEB1* promoter activity, HEK293 cells were seeded in 24 well plates and transiently transfected using Fugene 6 transfection reagent (Roche) with the *ZEB1-Luciferase* reporter construct (100 ng), Renilla luciferase plasmid (20 ng, Promega), and wild-type *CMV-PR-B* expression vector (100 ng, kindly provided by Donald McDonnell, Duke University) or an expression vector containing mutant PR-B (mutPR-B_{DBD}) with three point mutations in the DNA-binding domain (G585E-S586G-V589A) that abrogate PR-B DNA binding activity (Quiles et al., 2009). One day after

transfection, cells were treated with DMSO (V) or P_4 (100 nM) for 24 h in medium without phenol red or FBS. Cells from each treatment group were then harvested in 100 μl of 1X Passive lysis buffer (Promega). Firefly luciferase and Renilla luciferase activities were assayed using Dual-Luciferase assay system (Promega). To correct for transfection efficiencies, relative luciferase activity was calculated by normalizing Firefly luciferase activity to Renilla luciferase activity obtained from the same sample. pCDNA3 empty vector was also used as a control.

Adenoviral Transduction of ZEB1. Primary mouse myometrial cells, isolated as described in Section 2, were plated in 30 mm dishes at 500,000 cells per well. Twenty-four hours later, recombinant adenoviruses overexpressing ZEB1 or β-galactosidase were added in a minimal volume of medium (1 ml DMEM:F12/well) at a multiplicity of infection (MOI) of 500 pfu/cell. After overnight infection, the cells were washed once with PBS, fed with complete medium and harvested 48-96 h later. Cells overexpressing β-galactosidase were used to assess transduction efficiency (Fig. 2-6.3A) and as a negative control for non-specific effects of adenoviral infection.

CHAPTER 2- SECTION 6
Regulation of Contraction-Associated Genes and Myometrial Contractility by miR-200s and ZEBs

Experimental Design

The transcription factors, ZEB1 and ZEB2, function by directly binding to E-box (5'-CACCTG) sequences in the promoter regions of target genes and recruiting corepressors, such as CtBP, to repress gene transcription (Postigo and Dean, 1999). Because of their widely reported role as transcriptional repressors in a variety of systems and cell types, and their relatively high expression levels in the myometrium until late gestation when they dramatically decline, we hypothesized that ZEB1 and ZEB2 may act to inhibit the expression of genes important in the initiation of parturition.

The uterine myocyte contractile phenotype has been associated with an increase in the differentiated state of the myocyte (Shynlova et al., 2009). Interestingly, ZEB1 is known to act as a negative regulator of muscle differentiation (Postigo and Dean, 1999). This is thought to occur, in part, through its action on cell-cell adhesion molecules, such as adherens junctions, desmosomes, and gap junctions (Vandewalle et al., 2005). Importantly, gap junctions have been shown to play an important role in parturition (Chow and Lye, 1994, Doring et al., 2006, Orsino et al.,

1996). Because of these known associations, it was of interest to investigate whether ZEB1 and ZEB2 have the capacity to repress important contraction-associated genes, and thereby serve to maintain uterine quiescence until term.

Because of their documented importance in parturition, we compared the temporal expression of COX-2 (Tsuboi et al., 2000), CXN-43 (Doring et al., 2006), 20α-HSD, and OXTR in mouse uterus from 15.5 dpc through labor (Figure 2-5.1) to that of ZEB1 and ZEB2. We observed that COX-2 mRNA levels remained low in the mouse uterus throughout most of gestation and then increased precipitously during labor. On the other hand, 20α-HSD increased to peak levels at 17.5 dpc and declined markedly, thereafter (Figure 2-5.1). By contrast, both CXN-43 and OXTR mRNA remained relatively low through 17.5 dpc and increased markedly at 18.5 dpc and in labor and were reciprocally expressed with ZEB1 and ZEB2 mRNA and protein levels, which begin to decline at 17.5 dpc, reaching relatively low levels at 18.5 dpc and during labor. This together with the finding that CXN-43 and OXTR colocalize with ZEBs to the myometrium (Figure 2-5.2), led us to postulate that CXN-43 and OXTR may be targets of ZEB regulation.

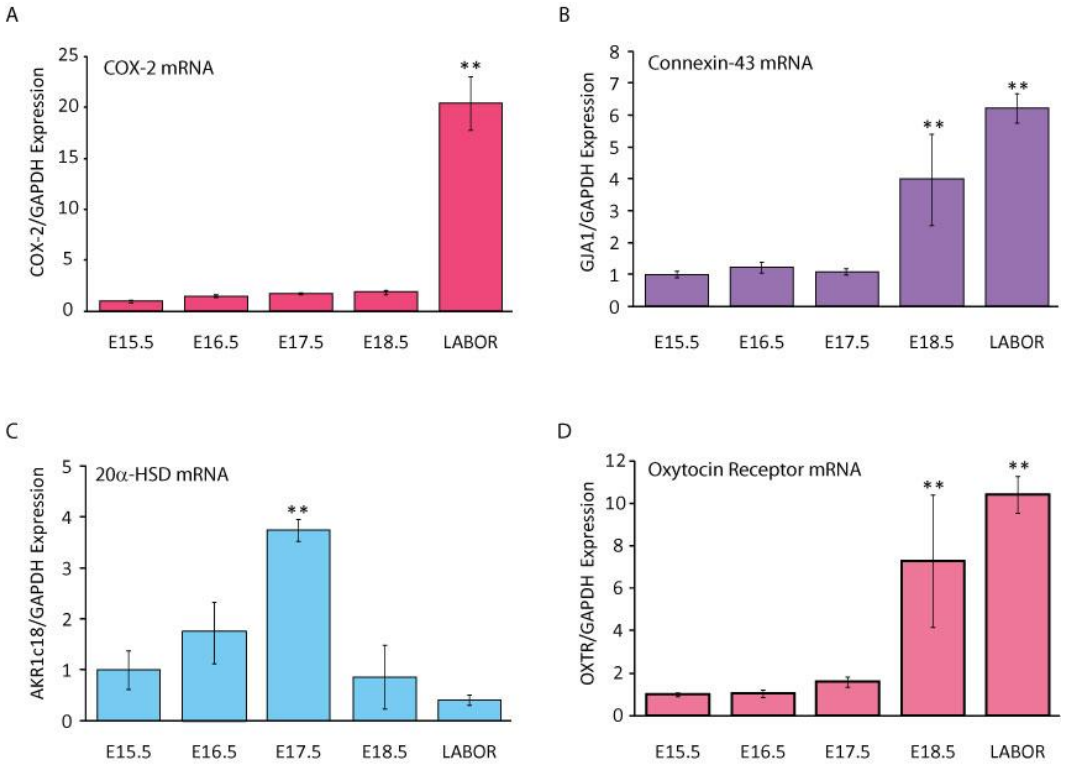

Figure 2-6.1. Of the regulated contraction-associated genes in the murine myometrium**, CXN-43 and OXTR share a temporal profile consistent with their negative regulation by ZEB1 and ZEB2.** (A) COX-2 mRNA levels remained low throughout pregnancy and are significantly upregulated only in labor. (B) Connexin-43 (CXN-43/GJA1) was significantly upregulated beginning at 18.5 dpc. (C) 20α-HSD/AKR1c18 mRNA levels were significantly upregulated at 17.5 dpc, but declined thereafter. (D) Like, CXN-43, OXTR mRNA levels were significantly upregulated beginning at 18.5 dpc. mRNA expression of each gene was determined by qRT-PCR, normalized to GAPDH, and expressed as fold-increase over 15.5 dpc. Mean ± SEM values are shown. One-way ANOVA, COX-2: $F(4,20)= 28.83$, $p<.0001$; CXN-43: $F(4,20)=12.93$, $p<.0001$; 20α-HSD/AKR1c18: $F(4,20)= 7.8$, $p=0.0006$; OXTR: $F(4,20)=11.03$, $p<.0001$. Multiple comparison test compared to 15.5 dpc: **p<0.01, n = 5-10 mice per group.

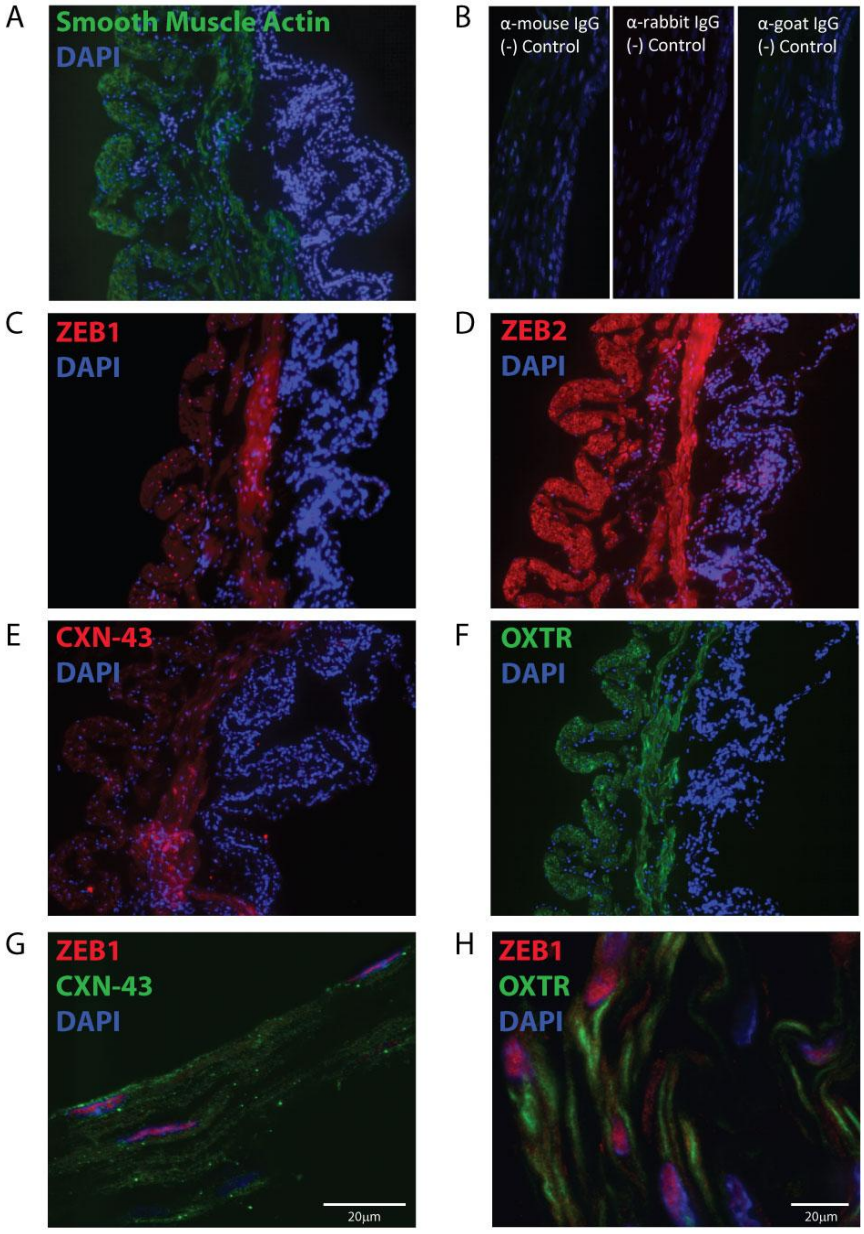

Figure 2-6.2. ZEB1 and ZEB2 are colocalized with CXN-43 and OXTR in the myometrium of the murine uterus during pregnancy. Sections of pregnant murine uterus were stained for (A) smooth muscle actin (green) to localize the myometrium and DAPI (blue) to localize the nuclei of cells. (B) Secondary antibody alone demonstrates extremely low background reactivity. (C) Immunohistochemistry for ZEB1 (red) and (D) ZEB2 (red) reveal their primary localization to the myometrium, along with (E) CXN-43 (red) and (F) OXTR (green). (G) Double staining of ZEB-1 and CXN-43 or (H) ZEB-1 and OXTR demonstrates expression of these proteins within the same myocytes.

Results: Modulated by the miR-200s, ZEB1 and ZEB2 Repress Contractile Genes and Reduce Contractility of Myometrial Cells

To examine the effects of ZEB1 and ZEB2 overexpression on CXN-43 and OXTR mRNA levels, hTERT-HM myometrial cells were infected with recombinant adenoviruses expressing ZEB1 and ZEB2 or expressing β-Gal, as control. Transduction of the myometrial cells with recombinant adenoviruses expressing ZEB1, ZEB2 or β-Gal, as control (Figure 2-6.3), resulted in a significant suppression of CXN-43 and OXTR mRNA levels after 48 and 72 h (Figure 2-6.4). This demonstrates negative regulation of these two contraction-associated genes by the ZEB family of transcription factors.

Because of the pronounced inhibitory effect of ZEB1 and ZEB2 on expression of CXN-43 and OXTR, we examined the effects of ZEB1 and ZEB2 overexpression on contractility of uterine myocytes. To carry out these studies, we utilized collagen gel contraction assays (Rhee and Grinnell, 2007, Dallot et al., 2003, Fitzgibbon et al., 2009), in which hTERT-HM cells, transduced with adenoviruses overexpressing ZEB1, ZEB2, or β-gal (control), were embedded into 3D collagen gel matrices (Figure 2-6.A) so that myocytes could contract within the matrix in response to oxytocin treatment. Oxytocin, a key hormone that enhances uterine contractility at term (Blanks and Thornton, 2003), significantly

induced contraction of collagen gel matrices embedded with untransduced and β-gal-transduced hTERT-HM cells (Figure 2-6.5B). This effect of oxytocin was significantly abated in the hTERT-HM cells transduced with ZEB1 and ZEB2 expression vectors, demonstrating a direct effect of ZEB1 and ZEB2 to inhibit myometrial contractility *in vitro* (Figure 2-6.5B).

To further elucidate the mechanism by which ZEB1 and ZEB2 downregulate expression of CXN-43 and OXTR, we conducted chromatin immunoprecipitation followed by qPCR analysis to determine whether ZEB1 and ZEB2 bind the promoters of CXN-43, OXTR, and the miR-200b-a-429 cluster *in vivo*. Analysis revealed a significant binding of both ZEB1 and ZEB2 to the promoters of each target. Furthermore, binding of ZEB1 and ZEB2 was consistently decreased between 15.5 dpc and labor (Figure 2-6.6). These data provide direct evidence that ZEB1 and ZEB2 interact with the promoters of CXN-43 and OXTR to repress their expression until term.

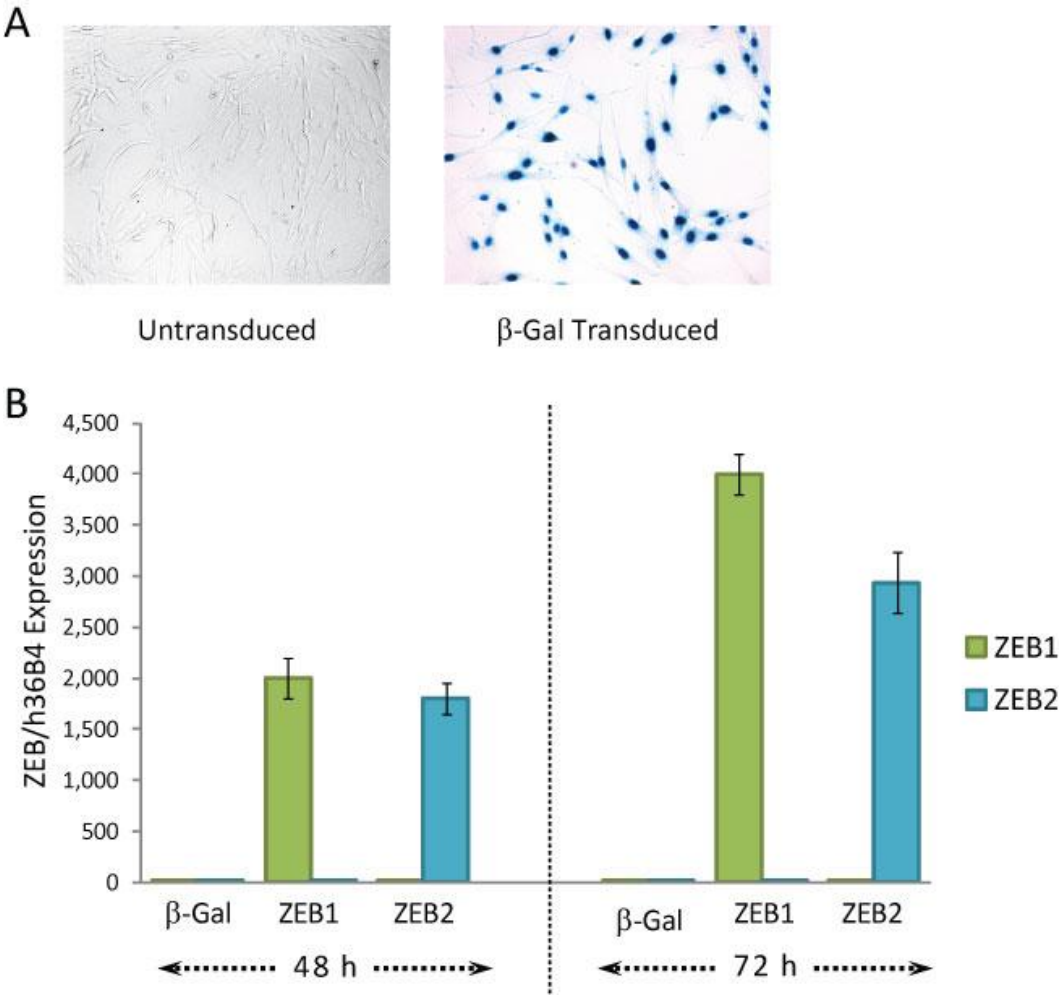

Figure 2-6.3. hTERT-HM cells are efficiently transduced by recombinant adenoviruses expressing ZEB1 or ZEB2. (A) Representative images of hTERT-HM cells transduced with β-Gal-expressing control virus, as compared to untransduced cells. Untransduced and β-Gal-transduced samples were stained for 1 hour for β-galactosidase expresssion. (B) qRT-PCR to assess overexpression of ZEB1 or ZEB2 in cells transduced with either ZEB1, ZEB2 or β-Gal-expressing recombinant adenoviruses. Only cells transduced with ZEB1 or ZEB2 showed robust overexpression of these transcription factors. Neither gene was upregulated in β-Gal controls.

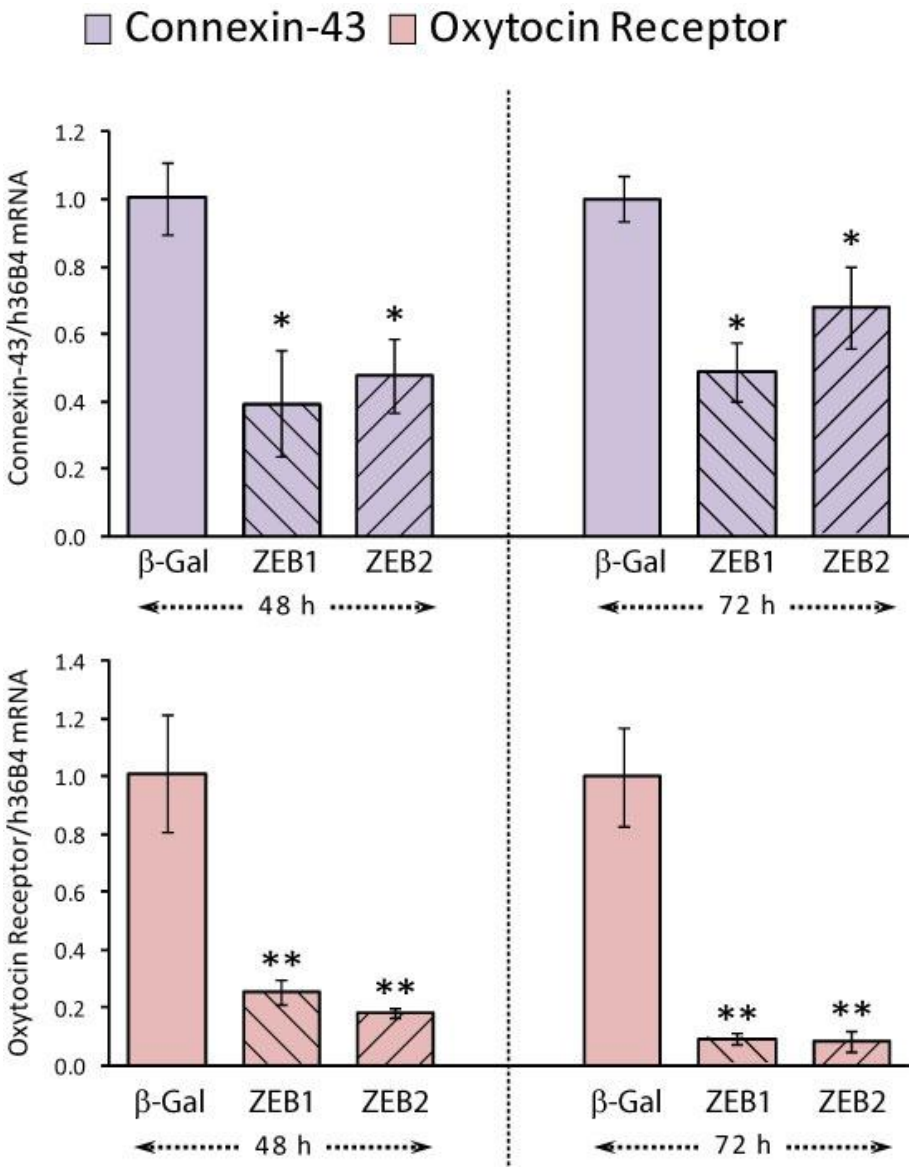

Figure 2-6.4. Overexpression analyses reveal a role for ZEB1 and ZEB2 in contraction-associated gene regulation. Human myometrial cells transduced with either ZEB1 or ZEB2 expressing adenoviruses showed a significant reduction in endogenous CXN-43 and OXTR expression 48 and 72 hours post-transduction. The levels of each transcript were determined by qRT-PCR, normalized to GAPDH, and expressed as fold change over β-gal transduced controls. Mean ± SD values are shown. Student's t-test, *p<0.05, **p<0.01. Data are inclusive of three replicate experiments.

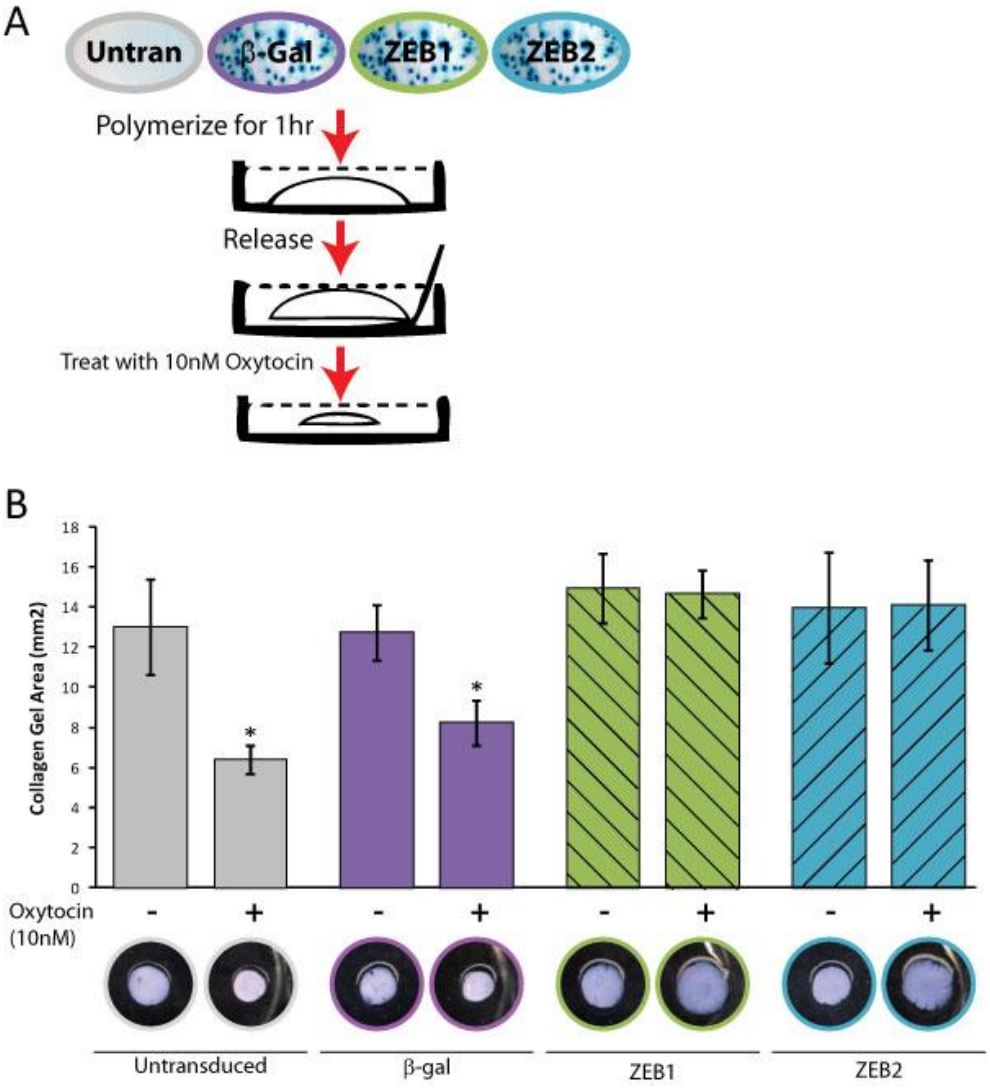

Figure 2-6.5. ZEB1 and ZEB2 suppress human myometrial cell contractility. (A) Diagram of experimental overview for gel contractility experiment. Untransduced cells or cells transduced with β-Gal, ZEB1, or ZEB2 for 48 hours were embedded into collagen gels and allowed to polymerize for 1h. Gels were then released from the dish, to allow free contraction in response to 10 nM oxytocin. (B) Human myometrial cells transduced with either ZEB1 or ZEB2 expressing adenoviruses were embedded into collagen gel matrices 48 hours following transduction and treated with 10 nM oxytocin to stimulate contraction. Both untransduced and β-gal transduced matrices contracted significantly (*p <0.05) after 24 hours of oxytocin treatment. However, oxytocin-induced contractility was lost in cells overexpressing ZEB1 or ZEB2. Contraction was assessed by measurement and calculation of mean gel area (mm^2) ± SD. A representative human-myometrial-cell-embedded collagen gel is shown below the data for each group. Data plotted are inclusive of three replicate experiments.

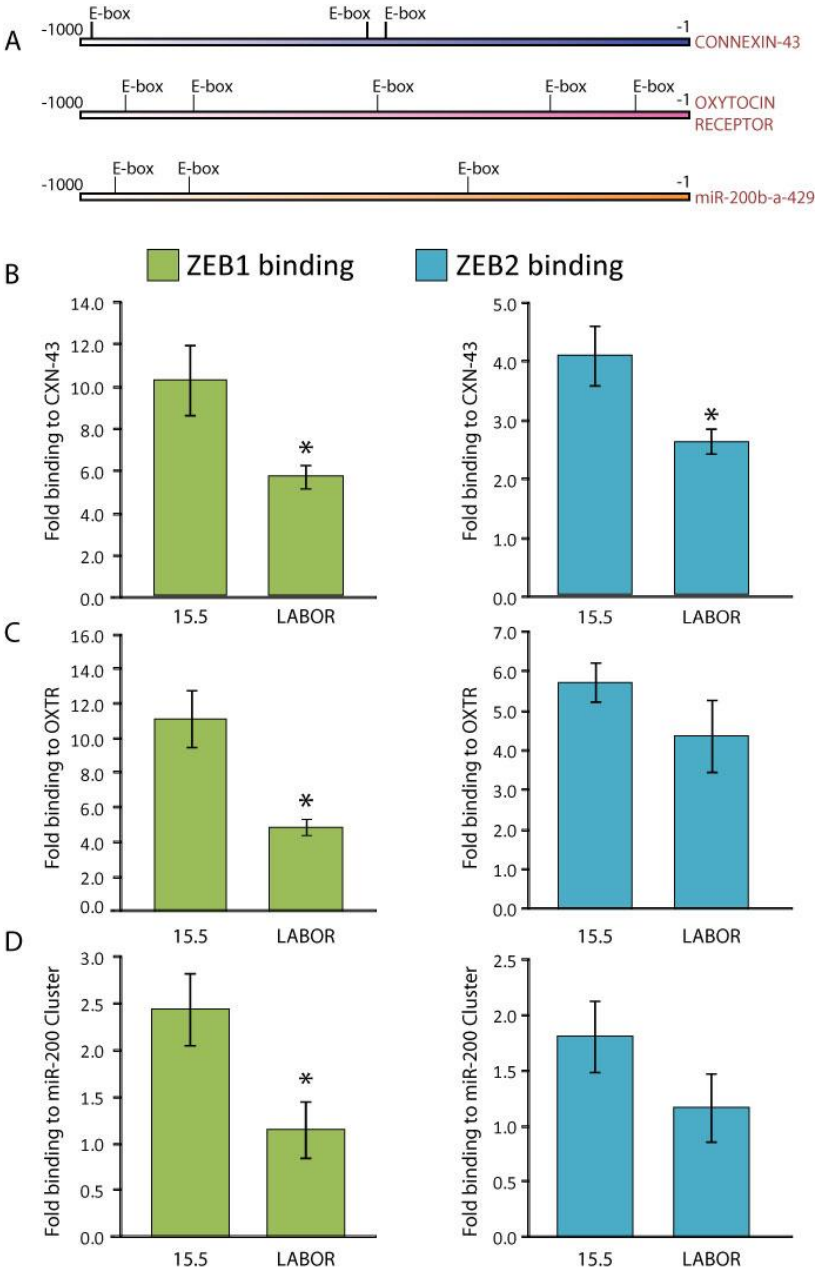

Figure 2-6.6. ZEB1 and ZEB2 bind to the promoters of CXN-43, OXTR, and the miR-200b-a-429 cluster. (A) Diagram depicting the first 1 kb upstream of the gene promoter for each ZEB1 and ZEB2 target, highlighting E-box sequences within this region. Chromatin immunoprecipitation followed by qPCR analysis was used to determine that ZEB1 and ZEB2 bind the promoters of **(B)** CXN-43, **(C)** OXTR, and **(D)** the miR-200b-a-429 cluster. Data shown are binding, normalized to input, and expressed as fold increase over IgG controls. Data are the means ± SEM of 10 mice per time point from two replicate experiments. Student's t-test, *p<0.05.

Discussion

Together with the data presented in Section 5, the studies presented herein implicate ZEB1 as a progesterone regulated gene, which, along with ZEB2, acts as an effector of myometrial contractility. ZEB1 and ZEB2 are repressed at term by the dual actions of progesterone withdrawal and increased expression of the miR-200 family, which feeds back to further repress these factors.

Interestingly, ZEB1 and ZEB2 are known to bind paired E-box sites (Bracken et al., 2008). Such sites are found in all of the ZEB1 and ZEB2 targets implicated here, with one paired site in each of the promoters of CXN-43 and the miR-200b-a-429 cluster, and two paired E-box sites in the OXTR promoter (Figure 2-6.6). The additional paired E-box site in the OXTR may contribute to the increased sensitivity of this gene to repression by ZEB1 and ZEB2 overexpressing adenoviruses (Figure 2-6.4).

It is interesting that ZEB1 and ZEB2 maintain uterine quiescence by negatively regulating two independent pathways by which myometrial cells are transformed into contractile cells at term. CXN-43 is a protein that forms gap junctions between myocytes to allow for the free passage of ions between cells, resulting in coordinated contractility. The mechanism

whereby OXTR enhances uterine contractility is quite different, in that OXTR acts via a G_q-coupled signaling pathway to increase intracellular calcium and induce smooth muscle contraction. Near term, the decline in P_4 and/or PR function causes a reduction in expression of ZEB1 and ZEB2 and a consequent increase in expression of the miR-200 family, which further suppresses ZEB expression. This decline in ZEB expression causes a profound increase in myometrial contractility. Future studies will be needed to examine the impact of ZEB1 and ZEB2 overexpression on the timing of parturition in mice.

Materials and Methods

Mice and Murine Tissue Collection. Eight-week-old, timed-pregnant ICR/CD1 females were purchased from Harlan Laboratories were mated and tissues harvested as described in Section 1. For immuno-histochemical (IHC) staining of the uterus, pregnant mice at 15.5 and 18.5 dpc were deeply anesthetized with an injection of a ketamine-xylazine-acepromazine mixture and transcardially perfused with 4% paraformaldehyde in PBS. The uteri were dissected and pups and placental material removed. Small tissue blocks of the uteri were stored in 4% paraformaldehye at 4ºC overnight and then transferred into a 30% sucrose solution (in PBS) at 4ºC. After 2 days, the tissue was immerged in 2-methylbutane and flash frozen in liquid $N_{2.}$ 12 µm thick sections were cut on a cryotome and stored at -20˚C.

ZEB1 and ZEB2 Plasmid Construction. Genomic fragments for ZEB1 and ZEB2 were each released from vectors provided by Dr. Yujiro Higashi (Osaka University, Osaka, Japan) using KpnI (Roche) and XbaI (Roche) restriction enzymes. Fragments were subcloned into a pACCMVpLpA(-)-loxP-SSP shuttle vector. Recombinant adenoviruses were constructed in the laboratory of Robert Gerard (UT Southwestern) by Cre-lox recombination in vitro with cAd5dl7001loxP and transfected into 911 cells

using Lipofectamine2000. Viral clones were propagated in 911 cells; viral supernatants were clarified by centrifugation and titered by plaque assay. Aliquots of virus were stored frozen at -80C until use.

Adenoviral Infection and ZEB1 and ZEB2 Overexpression. hTERT-HM cells were plated in 30 mm dishes at 500,000 cells per well. Twenty-four hours later, recombinant adenoviruses overexpressing ZEB1, ZEB2, or β-galactosidase were added in a minimal volume of medium (1 ml DMEM:F12/well) at a multiplicity of infection (MOI) of 85-500 pfu/cell. After overnight infection, the cells were washed once with PBS, fed with complete medium and harvested 48-9 h later. Cells overexpressing β-galactosidase were used to assess transduction efficiency (Fig. 2-6.3A) and as a negative control for non-specific effects of adenoviral infection.

qRT-PCR Analysis of Human and Murine Gene Expression. RNA was deoxyribonuclease treated (Invitrogen), Superscript III reverse transcribed (Invitrogen), and SYBR Green PCR (Applied Biosystems) performed as described in Section 2. Expression of murine and human genes was determined using forward and reverse primers detailed in Table 2-2.2. Murine GAPDH was used as an internal control for animal studies. For

studies in human cells, h36B4 was used as an internal control (Table 2-2.2).

Immunohistochemistry. Cryosections were postfixed with formalin (3.7% in >PBS) for 10 minutes and blocked with normal goat serum or normal donkey serum for 30 min. Incubation with the primary antibodies was performed over night at 4°C. The following antibodies were used: mouse-α-smooth muscle actin (Sigma, 1:1000), rabbit-α-ZEB1 (Santa Cruz, 1:100), rabbit-α-ZEB2 (Santa Cruz, 1:100), rabbit-α-connexin43 (Invitrogen, 1:200), goat-α-connexin43 (Santa Cruz, 1:50), and goat-α-oxytocin receptor (Santa Cruz, 1:1000). Subsequently, the sections were incubated with the appropriate, fluorphore-labeled secondary antibodies (goat-α-mouse-DyLight488, goat-α-rabbit-Cy3, donkey-α-rabbit-DyLight-549 and donkey-α-goat-DyLight488, all 1:750 in PBS, all Jackson ImmunoResearch) at RT for 1 h. Nuclei were counterstained with 4,6-diamino-2-phenylindole (DAPI, Sigma, 1:100,000 in PBS) for 5 min at RT and the sections were mounted with fluorescence mounting medium (Dako). For the oxytocin receptor/ZEB1 double labeling the sections were first incubated in a mixture of both primary antibodies, followed by incubation with a mixture of both primary antibodies. Images were

acquired with a confocal microscope (Leica TCS SP5) and z-projections of z-stacks were generated with ImageJ software (NIH).

Collagen Matrix Contractility Assay. hTERT-HM cells transduced with adenoviral vectors overexpressing ZEB1, ZEB2, or β-galactosidase (control), as above, were plated in collagen gels. Briefly, subconfluent cells with or without prior transduction with recombinant adenoviruses were harvested with trypsin, centrifuged at 1000 ×*g* for 5 min, and resuspended in serum-free DMEM:F12. The number of cells was ascertained and the viability of cells was checked by trypan blue exclusion using a Countess Automated Cell Counter (Invitrogen). Type-I rat tail collagen solution (BD Biosciences, cat# 356236) was adjusted to pH 7.2 with 1 N NaOH. The final concentration of collagen was 1.0 mg/ml. The appropriate number of hTERT-HM cells was then added to the neutralized collagen solution to achieve 2 x 10^5 cells/gel, mixed, and incubated on ice for 5 min. Collagen gel-cell suspensions were pipetted into untreated 12-well culture dishes that had been pre-scored with a circle (0.5 mm radius) using a plate scorer (Four Seasons Decorations, Dallas, TX), and incubated for 1 h at 37°C to allow gelling. One milliliter of fresh DMEM, either unsupplemented (control) or supplemented with 10 nM oxytocin, was added over the cell-collagen matrix. The gel matrices were then

gently detached from the sides of the scored circle and lifted off the bottom of the well. The areas of the gels were measured periodically for up to 48 h. Maximum effects on gel contraction were obtained within 48 h of culture. Images of the floating gels were captured and digitized using a flatbed scanner (Hewlett Packard). The area of each gel was measured using Adobe Illustrator CS2 and the final area (mm^2) of each gel was compared.

Chromatin Immunoprecipitation (ChIP)

Uterine tissues were harvested from eight-week-old, timed-pregnant ICR/CD1 females at 15.5 dpc and 18.5). The uteri were cleared of all embryonic material and maternal decidua, and further enriched for myometrium by sterile scraping and blotting with a paper towel. The remaining myometrial tissues were homogenized in cold 1x PBS, protease inhibitor cocktail (Roche), and 10 mM PMSF. Homogenized samples were incubated with 1% formaldehyde, protease inhibitor cocktail (Roche), and 10mM PMSF for 15 min at room temperature to cross-link proteins and DNA. Samples were then washed twice in cold 1x PBS, protease inhibitor cocktail (Roche), and 10 mM PMSF, and flash frozen. Chromatin immunoprecipitation was conducted using Chromatin Immunoprecipitation (ChIP) Assay Kit (Milipore, cat# 17-295). Samples were thawed by the

addition of 1000 µl lysis buffer (Milipore cat# 20-163. [1% SDS, 10 mM EDTA, 50 mM Tris, pH 8.1]). The lysates were sonicated on ice 3 times at 40% for 10 seconds to produce sheared, soluble chromatin. The soluble chromatin was precleared with Protein A Agarose/Salmon Sperm DNA (50% Slurry), (Milipore cat# 16-157C. [1.5 mL packed beads with 600 mg sonicated salmon sperm DNA, 1.5 mg BSA and ~4.5 mg recombinant Protein A, suspended in TE buffer, pH 8.0, containing 0.05% sodium azide in liquid suspension]) (75 µl) at 4 C for 30 min with rotation. The samples were microfuged at 14,000 rpm to pellet the beads, and the supernatant containing the sheared chromatin was placed in new tubes. DNA concentrations were determined by spectrophotometer and equivalent amounts of precleared chromatin were incubated either with antibodies for ZEB1 (Santa Cruz, H-102, SC-25388) or ZEB2 (Santa Cruz, H-260, SC-48789), at 4 C overnight. An aliquot incubated with nonimmune IgG was used as a control. Protein A Agarose/Salmon Sperm DNA (50% slurry), (Milipore cat# 16-157C) (60 µl) were added to each tube, the mixtures incubated for 1 h at 4 C, and the immune complexes collected by centrifugation. The beads containing the immunoprecipitated complexes were washed sequentially for 5 min in Low Salt Immune Complex Wash Buffer (Milipore cat# 20-154. [0.1% SDS, 1% Triton X-100, 2 mM EDTA, 20 mM Tris-HCl, pH 8.1, 150 mM NaCl]), High Salt Immune Complex

Wash Buffer (Milipore cat# 20-155. [0.1% SDS, 1% Triton X-100, 2 mM EDTA, 20 mM Tris-HCl, pH 8.1, 500 mM NaCl]), LiCl Immune Complex Wash Buffer, (Milipore cat# 20-156. [0.25 M LiCl, 1% IGEPAL-CA630, 1% deoxycholic acid (sodium salt), 1 mM EDTA, 10 mM Tris, pH 8.1]), and TE Buffer, (Milipore cat# 20-157. [10 mM Tris-HCl, 1 mM EDTA, pH 8.0]). The beads were eluted with 250 µl freshly prepared elution buffer (1% SDS, 0.1 mM $NaHCO_3$, and 20 µg salmon sperm DNA, (Milipore, cat# 16-157)) at room temperature. This was repeated once, and eluates were combined. Cross-linking of the immunoprecipitated chromatin complexes and input controls (10% of the total soluble chromatin) was reversed by heating the samples at 65 C for 4 h. Proteinase K (15 µg; Invitrogen) was added to each sample in buffer [50 mM Tris-HCl (pH 8.5), 1% SDS, and 10 mM EDTA] and incubated for 1 h at 45 C. The DNA was purified by phenol-chloroform extraction and precipitated in ethanol overnight at –20 C. Samples and input controls were diluted in 10–400 µl RNAse/DNAse-free water prior to qPCR. Quantitative PCR was employed using at least two primer sets per gene to confirm binding to the *CXN-43*, *OXTR*, and *miR-200b-a-429 cluster* promoters:

Oxytocin Receptor:

1st -F	CACGGTTCTCCTGGTTTGTT
1st–R	CGGCCTTGAGGCTCTTTAA
2nd-F	GACCCCAGGAAGATGTACCC
2nd -R	AGCCTCTCCCCACAGAGAAC

Connexin-43

1st-F	TCTCGTCAGCACATTGAAACT
1st -R	AGGGGAGGGAGGAAGAAAAG
2nd -F	TCCACGGGTCTGGTTGTG
2nd -R	TGCCCAAGGTGTGTGAAG

miR-200b-a-429 Cluster:

1st -F	TGACACACGCCTTCGTTG
1st -R	AGTCTCCCATACAGAGCCAAG
2nd -F	CAGCTCTTTCGGGCTGTC
2nd -R	AGGCCCAGAGGAAGGACTTA

CHAPTER 3
Conclusion

Our understanding of the mechanisms leading to the onset of parturition has increased considerably in recent years (Mendelson, 2009). Based on investigations from our laboratory and others, we postulate that the timing of parturition is mediated by integrated signaling pathways from both the mother and maturing fetus (Condon et al., 2004). These culminate in an inflammatory response within the uterus and cervix, which leads to a reduction in PR function (Brown et al., 2004, Kalkhoven et al., 1996, Condon et al., 2003), exacerbated inflammatory signaling, cervical ripening, and the activation of contraction-associated genes within the myometrium.

Despite our growing understanding of the signals and pathways leading to the initiation of labor, much remains to be discovered regarding the mechanisms whereby the myometrium is transformed from a refractory, near-quiescent state to a highly contractile unit, capable of responding to a variety of signals from both the fetus and the mother. The present research sheds new light on this extremely important transitional period within the maternal uterus. Our findings, which elucidate a novel regulatory pathway involving the miR-200 family and their targets, ZEB1 and ZEB2, provide new insight into the mechanisms by which P_4/PR

maintains uterine quiescence throughout most of pregnancy and that mediate the myometrial transformation leading to parturition.

MicroRNAs have been shown in a variety of systems (inflammation, reproduction, muscle development) to coordinate and fine-tune gene regulation, effectively synchronizing complex physiological events. While miRNAs have been implicated in several female reproductive processes, such as implantation (Chakrabarty et al., 2007, Hu et al., 2008), ovarian function (Lei et al., 2010, Ro et al., 2007), and reproductive pathology (Boren et al., 2008, Marsh et al., 2008, Pan et al., 2007, Pineles et al., 2007), their roles in promoting receptivity of the uterine myometrium to contractile signals has never been studied. Because of their near universal homology among vertebrate species, we hypothesized that miRNAs may play an important and conserved role in mammalian parturition.

By using a multiple array-based approach, we were able to uncover gene networks outside the arsenal of genes known to be important in mammalian parturition. Specifically, we found that the miR-200 family of miRNAs was upregulated in the murine myometrium beginning at 17.5 dpc and that two of their targets, ZEB1 and ZEB2, identified through bioinformatic analysis and gene expression microarrays, were coordinately suppressed. The temporal regulation of miR-200b/429 and ZEB1 and ZEB2 beginning at 17.5 dpc is of particular interest, as this

marks an important time of transition in the maternal uterus, during which there is a switch from quiescence and resistance to inflammatory signals, to increased receptivity to stimuli that trigger uterine contractility (Shynlova et al., 2009).

Alterations in P_4/PR function have been suggested to play an important role in myometrial conversion to a contractile phenotype during pregnancy (Shynlova et al., 2009). For example, at 20.5 dpc in the rat (which corresponds to 17.5 dpc in the mouse) a “synthetic to contractile switch” occurs, in which myometrial proliferation declines, while myocyte attachment to basement membranes and reorganization of myometrial cells increases (Shynlova et al., 2009). This is associated with a marked increase in basement membrane matrix synthesis and increased expression of genes encoding contraction-associated proteins. Notably, P_4 withdrawal appears to be a prime player in the initiation of this ’switch,’ as these same phenotypic changes in the myometrium are induced upon RU486 injection and delayed by exogenous P_4 treatment (Shynlova et al., 2009). The temporal upregulation of the miR-200 family and downregulation of ZEB1 and ZEB2 expression in the pregnant mouse uterus at 17.5 dpc, which just precedes the time of induction of the contraction-associated genes, *CXN-43* and *OXTR,* marks a critical time for transition to a contractile myometrium.

Our findings suggest that elevated levels of circulating P_4 throughout most of pregnancy directly promote expression of *ZEB1* in the myometrium via binding of PR to the *ZEB1* promoter. Consequently, in pregnant mice after 17.5 dpc when P_4 levels and PR function decline (Virgo and Bellward, 1974), ZEB1 mRNA and protein levels in the uterus are significantly reduced. Because ZEB1 directly binds and represses the miR-200b/429 promoter (Bracken et al., 2008, Burk et al., 2008), expression of the miR-200 family is reciprocally increased. Interestingly, P_4/PR does not directly regulate ZEB2 in the mouse myometrium or in cultured human cells. We suggest that the observed decline in ZEB2 during late gestation and in response to RU486 treatment is due to the rise in miR-200 family expression, which in turn represses both ZEB1 and ZEB2 (Figure 2-5.6). This negative feedback loop, which is supported by our data in pregnant myometrium, cultured myometrial cells, and by published findings in other cell types (Bracken et al., 2008, Burk et al., 2008), may explain the kinetics of miR-200b/429, ZEB1, and ZEB2 expression throughout gestation and in preterm labor.

In addition to defining the regulation of miR-200b/429 and its targets, ZEB1 and ZEB2, we also wished to discern the functional role(s) of these players in the myometrium toward term. Through overexpression studies of ZEB1 and ZEB2 in cultured human myometrial cells, we have

shown that ZEB1 and ZEB2 downregulate the expression of *CXN-43* and *OXTR*, and that ZEB overexpression inhibits oxytocin-mediated contraction of myometrial cells embedded in a collagen matrix. A role for CXN-43 and OXTR in myometrial contractility has long been appreciated, as expression of both these genes enhances receptivity of the uterus to the contractile signals of labor. As mentioned, CXN-43 is responsible for the formation of gap junctions in the myometrium, which have been shown to mediate intercellular coupling in order to coordinate the synchronous myometrial contractions necessary for successful labor (Balducci et al., 1993, Chow and Lye, 1994). In addition, mice with a smooth muscle-specific deletion of the *CXN-43* gene manifest a significant delay in the timing of parturition (Doring et al., 2006).

The action of oxytocin as an uterotonic agent is widely accepted. It is known that exogenous oxytocin can increase myometrial contractility and induce labor in mice and humans (Blanks and Thornton, 2003). Conversely, antagonists of the OXTR are effective in maintaining uterine quiescence in humans (Goodwin et al., 1994) and rodents (Antonijevic et al., 1995). However, the role of oxytocin and the OXTR in normal parturition is uncertain, since *oxytocin* gene knockout mice undergo parturition and give birth to live pups (Young et al., 1996, Nishimori et al., 1996), and mice deficient in the OXTR manifest normal timing and

duration of parturition (Takayanagi et al., 2005). These unexpected phenotypes may be due to a functional redundancy of the oxytocin/OXTR signaling system and/or to compensatory upregulation of other uterotonic systems, such as COX-2/prostaglandins.

Collectively, our findings suggest that ZEB1 is a key PR target gene in the myometrium that inhibits expression of contractile genes and the miR-200 family throughout most of pregnancy (Figure 2-5.6). Near term, signals from fetus and mother, including developmental induction of fetal SP-A, mechanical stretch of the maternal uterus due to fetal growth, and secretion of cortisol from the maturing fetal adrenal, cause an increased uterine inflammatory response, leading to a decline in local P_4 and/or PR function and the activation of contractile genes. The decline in PR function near term causes a downregulation of *ZEB1* gene expression, which in turn, results in derepression and upregulation of miR-200b/429 expression. The resulting elevated levels of these miRNAs can then feedback and repress both ZEB1 and ZEB2 (Figure 2-5.6). This negative feedback loop, which is supported by the present findings in pregnant mouse and human myometrium and in cultured human myometrial cells, as well as published reports by others (Bracken et al., 2008, Burk et al., 2008), results in further induction of contractile gene expression and labor. Taken together, our findings implicate a novel pathway in the regulation of

uterine contractility during pregnancy and parturition that is conserved from mice to humans, and may ultimately open new avenues for development of effective therapeutics for prevention of preterm labor.

Future Directions

Future experiments will be needed to confirm the relative impact of both miR-200s and ZEB1 and ZEB2 on the timing of labor and the physiology of parturition *in vivo*. For these studies, we plan to generate transgenic mice inducibly overexpressing ZEB1 or ZEB2 within the myometrium and determine effects on the length of gestation. Based on the findings of the current study, we believe that ZEB1 and ZEB2 are important players in the maintenance of uterine quiescence throughout most of pregnancy. We, therefore, hypothesize that mice overexpressing ZEB1 and/or ZEB2 will manifest longer gestation periods (>19.5 dpc) as compared to C57Bl/6 controls. Conversely, because members of the miR-200 family antagonize the action of ZEBs as term approaches, we hypothesize that mice inducibly overexpressing the miR-200b-a-429 cluster within the myometrium would manifest shorter gestational periods (<19.5 dpc) as compared to wild-type controls. Nevertheless, because the miR-200 family and ZEBs undoubtedly have targets in addition to those implicated in the current studies, obtaining a direct readout between a

manipulation of the gene and the physiology of pregnancy and parturition may be difficult. In addition, because ZEB1 and ZEB2 have been associated with the progression of cancer cells to a metastatic phenotype (Bracken et al., 2008, Gibbons et al., 2009, Burk et al., 2008) and in immune system development (Wang et al., 2009, Williams et al., 1991), mice overexpressing these transcription factors should be carefully monitored for the development of disease.

As an alternative to studies of transgenic mice, another approach could be to treat mice with miRNA sponges to the miR-200 family and assess changes in parturition timing. MicroRNA sponges are expressed sequences corresponding to the target sequences of specific mRNAs that function by competing for binding to endogenous targets of a specific microRNA or miRNA family (Ebert et al., 2007). miRNA sponges may be of particular use in investigating the functional effects of the entire miR-200 family, because unlike antagomiRs that block the effects of a specific miRNA, miRNA sponges can antagonize effects of all miRNAs sharing a common seed sequence. On the other hand, treatment of pregnant mice with miRNA sponges- whether by intravenous or intrauterine injection- may prove technically challenging due to the increased surface area of the pregnant myometrium and the reported inability of miRNA sponges to cross the endothelial barrier (Whitehead et al., 2009). Nevertheless,

successful delay of labor by treatment with miRNA sponges would be of particular importance, since this could suggest their efficacy as potential therapeutic agents for the treatment of preterm labor in high-risk human patients.

In addition to exploring the relevance of the miR-200 family and their targets, ZEB1 and ZEB2, *in vivo*, much remains to be understood as to how each of these players is regulated during late gestation and in labor. Recent investigations have implicated an induction of miR-429 within the uterus of ovariectomized mice in response to exogenous estrogen (Nothnick and Healy, 2010). This is of potential interest, since circulating estrogen levels increase toward the end of gestation and have been proposed to antagonize the actions of progesterone to maintain uterine quiescence. While effects of estrogen treatment on other members of the miR-200 family were not investigated, these findings underscore the possible role of estrogen in antagonizing progesterone action by enhancing expression of miR-200 family members and suppressing ZEB1/2 expression near term.

While the miR-200/ZEB axis appears to play a key role in myometrial contractility, the miR-200 family is predicted to regulate many other gene targets. For example, miR-200b/429 are predicted by Target Scan to bind and downregulate CtBP. Exploration of this, as yet,

unvalidated target would be of great interest because CtBP is known to serve as a corepressor with ZEB1 to mediate transcriptional repression (Postigo and Dean, 1999). Thus, not only would miR-200s target ZEB1/2, but they would also target a major corepressor, further inhibiting ZEB repressive activity. Additionally, future studies could explore other gene targets repressed by the miR-200 family through gene expression microarrays in cultured myometrial cells using the recombinant adenovirus overexpressing the miR-200b-a-429 cluster generated in the present research.

Along these same lines, the role of ZEB1 and ZEB2 in the maintenance of gestation has yet to be fully explored. Investigations of additional gene targets of ZEB1 and ZEB2 in the myometrium may provide novel insight into the transcriptional mechanisms that mediate myometrial contractility at term. For example, in addition to gap junction proteins, ZEB1 and ZEB2 are known to regulate proteins forming tight and adherens junctions (Vandewalle et al., 2005), as well as proteins forming basement membranes, such as laminins (Spaderna et al., 2006). By targeting these structural molecules in the uterus, ZEBs may contribute to the switch from a synthetic to a contractile phenotype of the myometrium near term (Shynlova et al., 2009). Interestingly, mice with a targeted deletion in laminin fail to initiate parturition altogether (Indrani Bagchi,

personal correspondence). Chromatin immunoprecipitation of specific gene targets, as well as genome-wide analysis of ZEB1 and ZEB2 binding to the genome of myometrial cells from midpregnant uterus using ChIP-seq, may also reveal novel pathways that contribute to uterine contractility.

Based on the current studies, we believe the action of the miR-200 family and targets, ZEB1 and ZEB2, to be downstream of the signals that initiate labor. In this way, downregulation of ZEB1 and ZEB2 by miR-200b/429 at term serves to sensitize the myometrium to contractile signals, via the upregulation of CXN-43 and OXTR. Therefore, it would be of interest to test our hypothesis, by investigating whether expression of miR-200b/429 or ZEB1 and ZEB2 are altered in mouse models of preterm (*e.g.* intraamniotic SP-A injection) or post-term (*SP-A*/*SP-D*-deficient or *SRC-1*/*SRC-2*-deficient mice) labor.

Lastly, because miRNAs have been shown to pass through gap junctions made up of CXN-43 (Valiunas et al., 2005) proteins, it would be interesting to explore the possibility that the upregulation of CXN-43 and gap junctions at term in response to ZEB downregulation serve to further facilitate suppression of ZEBs by allowing passage of miR-200s between myocytes. One might be able to initially test this possibility by treating human myometrial cells with fluorescently labeled miRmimics via micro-injection of single cells, and observing adjacent cells for the potential

intercellular transport of miR-200s (Valiunas et al., 2005). Alternatively, myocytes pretreated with fluorescently labeled miRmimics can be co-cultured with un-treated cells and monitored for the translocation of miRNAs to the untreated cells (Wolvetang et al., 2007).

Ultimately, by regulating many gene targets, both the miR-200 family and ZEB transcription factors may play a master regulatory role in directing gene expression during the switch from the quiescent to the contractile myometrium.

Acknowledgments

We thank Dr. Y. Higashi (Osaka University, Osaka, Japan) for murine ZEB1 and ZEB2 expression plasmids, Dr. A. Pertsemlidis for array analysis, Dr. W. Renthal and Dr. P. Kumar for expertise with ChIP, J. Shelton for help with ISH, G. Goodall for provision of a human miR-200b-a-429 cluster plasmid, J. Prange-Kiel and A. Click for help with IHC, and Dr. F. Grinnell and Dr. C. Ho for instruction in collagen matrix assays (UT Southwestern Medical Center). Work in the laboratory of C.R.M. was supported by the National Institutes of Health (5-P01-HD11149) and the March of Dimes Birth Defects Foundation (#21-FY07-601).

APPENDIX: Year One of Graduate Training

Iwona Stroynowski Laboratory

Brain-Expressed Isoforms of the Nonclassical Class I MHC Antigen Encode Qdm Peptide

Abstract

Although the human non-classical class Ib major histocompatibility complex (*Mhc*) locus, *HLA-G*, is known to act as an immune suppressor in immune-privileged sites, little is currently known regarding participation of the rodent class Ib *Mhc* in similar pathways. Here, we investigated the expression properties of the mouse non-classical *Mhc H2-Q5*^{k} gene, previously detected in tumors and tissues associated with pregnancy. We find that *H2-Q5*^{k} is alternatively spliced into multiple novel isoforms in a wide panel of tissues. Unlike other known class I MHC it is most highly transcribed in the brain, where the classical class Ia *Mhc* products are scarce. The truncated isoforms are selectively enriched in sites of immune privilege and are translated into cell surface proteins in neural crest-derived transfected cells. Furthermore, we present data supporting a model whereby Q5^{k} isoforms serve an immune-protective role by donating their Qdm leader peptide to Qa-1, in a pathway homologous to HLA-G leader fragment binding HLA-E and inhibiting CD94/NKG2A-positive cytotoxic cells. Collectively, these studies demonstrate that *H2-Q5*^{k} may play tissue specific roles in regulating immune surveillance.

Novel Isoforms of the Class Ib MHC Antigen Q5 Encode Qdm Peptide and are Enriched in Brain

Qa-1 and its functional human homologue, HLA-E, are evolutionarily conserved, widely expressed nonclassical MHC (class Ib) antigens. Similar to the classical class I MHC (class Ia), they associate with small peptides and present them on the cell surface (Jensen et al., 2004, Rodgers and Cook, 2005).

However, unlike classical MHC, Qa-1 and HLA-E are relatively monomorphic (Hermel et al., 2004, Pyo et al., 2006), a fact underscored by the finding that in normal cells they are predominantly bound to one type of a highly hydrophobic peptide ligand, derived from the signal sequences of MHC class I molecules (Aldrich et al., 1994, DeCloux et al., 1997, Kurepa et al., 1998, Kambayashi et al., 2004, Oliveira et al., 2010, Miller et al., 2003). In human, the peptide ligand with the highest affinity for HLA-E is derived from HLA-G, a nonclassical class I MHC heavy chain expressed at the maternal-fetal interface and, to a lesser degree or conditionally, in other immune-privileged sites (eye, brain, prostate, tumors) and thymus (Carosella et al., 2008, Hunt and Langat, 2009). In mice, the dominant Qa-1 peptide ligand is referred to as Qa-1 determinant modifier or Qdm (Aldrich et al., 1994), and, so far, has been shown to originate solely from the signal sequences of class Ia MHC, such as H2-D/L (Aldrich et al., 1994, DeCloux et al., 1997, Kurepa et al., 1998, Kambayashi et al., 2004). The similarities between HLA-E and Qa-1 reflect their conserved functions in the innate/adaptive immune system. Both regulate NK and T cells via a family of invariant CD94/NKG2 receptors (Jensen et al., 2004, Miller et al., 2003). Cells expressing HLA-E or Qa-1/Qdm complexes are typically protected from lysis by CD94/NKG2 cytotoxic cells, while those that lack them are generally killed (Braud et al., 1998, Vance et al., 1998). Thus binding of Qdm-like peptides to their class Ib partners is thought to play an important role in protection of class Ia-deficient cells from cell mediated lysis. In human, the canonical HLA-G peptide donor and, possibly, its alternatively spliced isoforms, are thought to contribute to cell immunoprotection by additional mechanisms (Carosella et al., 2008, Hofmeister and Weiss, 2003).

Since in mice the expression of Qdm-producing class Ia MHC alleles is low in the immune-privileged sites, such as brain, eye and testis (Singer and Maguire, 1990) the question arises whether Qa-1 might rely in these organs on another source for Qdm. We thus sought to investigate if any of the known class Ib MHC participates in this pathway. Here, we describe that the non-classical

expression pattern of Qdm-encoding class Ib *Mhc*, designated in *H2*^{k} haplotypes C3H/HeN and AKR as *H2-Q5*^{k} (Watts et al., 1989, Weiss et al., 1989), includes immune-privileged sites and is associated with transcription of alternatively spliced *HLA-G*-like isoforms. We also examined co-expression of *H2-Q5*^{k} and *H2-T23*, the gene that encodes Qa-1 in mice, in a model tumor line and report that their protein products may indeed interact with each other and participate in cellular interactions.

H2-Q5^{k} was chosen as an attractive candidate for our studies because we have identified it as one of only two mouse *Mhc* class Ib genes encoding a canonical Qdm (AMAPRTLLL) in their first exons (the other being liver-specific *H2-Q10* (Mellor et al., 1984)). In addition, previous studies suggested that *H2-Q5*^{k}, like *HLA-G*, is overexpressed in tumors and found in pregnancy tissues (Seo et al., 1992, Noguchi et al., 2004, Schwemmle et al., 1991, Reyes-Engel et al., 1993). It encodes a typical transmembrane class I heavy chain, with amino acid sequences compatible with antigen presentation functions (Watts et al. 1989; Weiss et al. 1989).

In order to characterize the sites where Q5^{k} may function as an important Qdm source for Qa-1, we performed a tissue-wide expression study of class I *Mhc* genes in *k* haplotype mice C3H/HeN and AKR, using semi-quantitative RT-PCR analysis with gene-spanning primers as described in Fig. 1. Representative data from multiple mice of both sexes (aged 7- 30 weeks) demonstrate that *H2-Q5*^{k} mRNA species can be detected in all tissues tested. An inverse distribution pattern between *H2-Q5*^{k} (Fig.1 b, c) and the classical *H2-K*^{k}*/D*^{k} (data not shown) was reproducibly observed in brain, where the class Ia transcripts were always very scarce, and *H2-Q5*^{k} was most abundant. These analyses revealed also that *H2-Q5*^{k} is alternatively spliced and gives rise to the canonical construct, as well as two novel isoforms, whose exon-intron organization was determined by cDNA cloning and sequencing. The AKR isoforms are diagrammed in Fig. 1a. The longest, canonical *H2-Q5*^{k} contains six exons encoding: a leader peptide (L), the α_1 domain, the α_2 domain, the α_3 domain, a transmembrane domain (TM), and a

short cytoplasmic tail (CYT). The middle-sized isoform, α_1-α_3-TM, bypasses the exon 3 encoding MHC α_2 domain, while the shortest isoform, α_1-TM, splices out both, the MHC α_2 and α_3 domain coding regions. Most interestingly, densitometry analysis of *H2-Q5*^{k} isoform expression showed a reproducible predominance of the *H2-Q5*^{k} α_1-α_3-TM isoform in brain (Fig. 1b). Enhanced levels of shorter isoforms, relative to the canonical *H2-Q5*^{k}, were also observed in the testis, eye and heart.

Next, in order to evaluate the potential of Q5^k to function as a binding partner for Qa-1, we performed tissue-wide expression analysis of *H2-T23*. As expected from previous studies (Transy et al., 1987), the canonical *H2-T23* transcripts are found ubiquitously, suggesting that Qa-1 could bind Q5^k-derived peptides in any of the examined tissues, including brain (Fig. 1c).

To identify whether the enrichment of *H2-Q5*^{k} transcripts seen in brain was specific to defined subregions of this organ, we employed semi-quantitative, as well as quantitative real-time, RT-PCR on total RNA isolated from olfactory bulb, striatum, thalamus, hippocampus, cortex and cerebellum from adult C3H/HeN and C57BL/6 mice (Fig. 2). Transcriptional activity of the *H2-Q5*^{k} gene amplified with gene-spanning (F: 5'-GGCACCGGATCCCAGATGT-3', R: 5'-CACCTGAACACATCGTCTGTCACTC-3') and gene-specific, real-time RT-PCR internal primers (F: 5'-GGCACCGGATCCCAGATGTG-3', R: 5'-TCGGGGCTCCCCGAAGTT-3') was similar in all brain substructures (Fig. 2 and data not shown). Surprisingly**,** we detected *H2-Q5*^{k}-like transcripts in C57BL/6 brain as well, though the *Q5*^{k} homolog has not yet been reported in this mouse strain. Amplification and DNA sequencing of *Q5*^{k}-like transcripts from C57BL/6 melanoma B78H1, and from the testis of adult C57BL/6 mice confirmed this finding (Fig. 2 and data not shown). Importantly, only two isoforms were detected in the C57BL/6 cells: α_1-α_3-TM and α_1-TM. Both were identical to their *H2*^{k} haplotype homologs isolated from AKR lymphoma BW5147 cells in the sequenced regions and differed substantially from all the known C57BL/6 class I *Mhc* sequences, including the highly divergent *Mhc* class Ib, designated in the

literature as *H2-Q5*^{b} (Robinson et al., 1988). Absence of the α_2 coding region in the *H2-Q5*^{k}-like transcripts may indicate deletion of exon 3 in the C57BL/6 homologous gene, or presence of a translational stop codon within the α_2 coding segment, which could induce nonsense mediated transcript degradation of the canonical isoform as reported for other class Ib *Mhc* (Guidry and Stroynowski, 2005). Cloning, sequencing and further studies of this novel C57BL/6 class Ib gene or pseudogene, are required to address these interpretations.

We next wished to address whether *H2-Q5*^{k} encodes proteins that may be expressed on the cell surface and therefore be accessible to class I MHC-specific receptors on innate and adaptive immune effectors. To determine if α_1-α_3-TM and/or α_1-TM protein products of alternatively spliced *H2-Q5*^{k} transcripts are expressed on the cell surface, we engineered an N-terminal FLAG epitope tag between the *H2-Q5*^{k} exon 1-encoded, co-translationally cleaved leader sequence and the exon 2-encoded α_1 domain, according to a strategy reported in Fulton, et al (Fulton et al., 1995). Due to technical difficulties, we were unable to generate a FLAG-tagged canonical *H2-Q5*^{k} construct. The constructs with two truncated isoforms were then stably transfected (with or without the transporter associated with antigen processing 2 [*Tap2*] gene) into the neural crest-derived B78H1 melanoma, a cell line that does not transcribe any endogenous class I *Mhc* (with the exception noted above of small amounts of the alternatively spiced transcripts of *H2-Q5*^{b}) or *Tap2* and only low levels of other chaperones important for class I MHC assembly, but constitutively expresses the β_2-microglobulin (β_2m) light chain ((Chiang et al., 2003) and Fig. 3 legend). Stable transfectants were assayed for cell surface expression of the FLAG epitope by flow cytometry. Both Q5^{k} α_1-α_3-TM and Q5^{k} α_1-TM proteins were detected on TAP-positive and TAP-negative transfectants (Fig. 3). Both failed to associate with β_2m as judged by lack of reactivity with a β_2m-specific antibody. Similarly, we failed to detect any cell surface β_2m on TAP-positive or negative stable transfectants expressing transcripts of the canonical (FLAG-deficient) *H2-Q5*^{k} (data not shown and Fig. 4). This suggests that full size Q5^{k} heavy chain is not displayed on the surface of the

model tumor or may be β_2m-independent as reported for some other class I MHC (Allen et al., 1986, Gonen-Gross and Mandelboim, 2007).

We further wished to assess whether the $Q5^k$ protein variants can serve as sources of Qdm for Qa-1. As previously mentioned $Q5^k$ is one of only two known class Ib MHC in which we were able to identify the Qdm AMAPRTLLL motif in the leader peptide using BLAST searches of NCBI nucleotide banks (http://blast.ncbi.nlm.nih.gov/). The liver-secreted, β_2m-associated Q10 (also discussed here) is the other. To address if Qdm can be generated from the $Q5^k$ or Q10 signal sequences and displayed in association with Qa-1 on the cell surface, we expressed $Q5^k$ or, as an internal control, Q10, in an *H2-T23*-transfected B78H1 clone (with and without TAP) and assayed for Qdm-associated Qa-1 by flow cytometry with anti-β_2m antibodies. This assay takes advantage of several properties of heavy chain class Ia and Ib MHC-negative, β_2m-positive B78H1 cells, Qa-1, $Q5^k$ and Q10. As we demonstrate in the present study (Fig. 4 and (Guidry 2008)), neither canonical $Q5^k$ nor its truncated protein variants bind β_2m at the cell surface. While the Q10 molecule can associate with β_2m, it lacks the TM domain, is soluble and cannot contribute to cell surface pools of β_2m-associating class I MHC (Devlin et al., 1985). Due to the general absence of endogenous class I transcripts in the B78H1 cell line (Chiang et al., 2003) both the H2-D^b-derived Qdm is not produced, and the Qa-1 heavy chain transcription is deficient. Expression of stable Qa-1/β_2m complexes on the cell surface requires binding of Qdm (Robinson et al., 1998, Guidry, 2008). Thus, we predicted that after the *H2-T23* gene (driven by a strong promoter) is transfected into the B78H1 cells, the Qa-1 protein would be detectable as the only β_2m-associated class I MHC on the cell surface, provided that it is stabilized by the high affinity Qdm or Qdm-like peptides. Scarcity of the endogenous Qdm in the *H2-T23* transfected B78H1 cells leads to a very low expression of Qa-1/β_2m, even when the cells are treated with interferon-γ (IFNγ) to enhance the antigen processing pathway (Fig. 4 and (Guidry 2008)). When the *H2-23* positive B78H1 cells are super-transfected with *H2-$Q5^k$* or *H2-Q10* expressing constructs, any

cell surface expression of β_2m above the background will be contributed by the association of the Qa-1 with $Q5^k$ or Q10-derived Qdm. These predictions have been confirmed by experiments showing that the Qa-1/β_2m complex is enhanced on B78H1 melanoma cells in the presence of Q10 in a TAP-dependent manner (Fig. 4a and (Guidry 2008)). As additional controls, we attempted to prepare a Q10 mutant with a defective leader peptide, but since this proved technically unsuccessful, we constructed, and analyzed a mutant gene *H2-Q10 α_3 (2nd ATG)*, from which we removed the first N-terminal methionine codon, thus replacing Qdm with a non-binding, truncated variant MAPRTLLL (Fig. 4 legend). As expected, this mutant class I MHC did not enhance cell surface levels of Qa-1/β_2m, while its immediate parent, *H2-Q10 a_3 (1st ATG)*, encoding intact Qdm, did so to the same level as the wild type *H2-Q10*, in a TAP-dependent fashion (Fig. 4 and data not shown, (Guidry, 2008)).

In Fig. 4b we demonstrate that the presence of canonical *H2-$Q5^k$* or the brain-abundant α_1-α_3-TM isoforms in the *H2-T23* transfected B78H1 cells also elevates expression of Qa-1/β_2m complexes with respect to cells expressing Qa-1 alone. The α_1-TM isoform was not examined for technical reasons. Importantly, this effect can be reproducibly observed in TAP-positive as well as TAP-negative cells, suggesting that the examined $Q5^k$ proteins can contribute Qdm to Qa-1 via a TAP-independent pathway. Thus, Qdm processing/loading into Qa-1 may bypass TAP-dependent retrograde transfer (Bai et al., 2000) and occur differently for $Q5^k$ and Q10/H2-D/L. Interestingly, we note that the amino acid residue preceding Qdm in the $Q5^k$ leader is W (tryptophan), while in H2-D^b and Q10 it is G (glycine). This “context” variation may potentially allow ER-based proteases to process Qdm from the $Q5^k$ leaders in the ER, by a mechanism that differs from the cytoplasmic Qdm release from H2-D^b leaders and necessitates proteasome/cytoplasmic peptidase trimming. The TAP-independent pathway may be of functional significance in brain cells, where expression of TAP is deficient (Neumann et al., 1997).

In summary, we report here that the nonclassical class I *Mhc*, *H2-Q5*^{k}, has a wider tissue and strain distribution than previously thought (Seo et al., 1992, Noguchi et al., 2004, Schwemmle et al., 1991, Reyes-Engel et al., 1993). Extending earlier surveys to more tissues and using more sensitive RT-PCR approaches and different primers, we observed that canonical *H2-Q5*^{k} as well as two novel, prominently transcribed isoforms predominate in immune-privileged sites, particularly in brain, where classical class Ia are scarce, and alternative splicing of transcripts is generally enhanced (Lipscombe, 2005). We thus speculate that various *H2-Q5*^{k} gene products may participate in this organ in specialized non-immune and/or immune interactions. This possibility is in line with recent findings implicating class I MHC in modulation of neuronal plasticity (Shatz, 2009) and/or regulation of CTL/NK responses during viral infections or autoimmune diseases in the brain (Wiendl et al., 2002, Megret et al., 2007, Huang et al., 2009, Segal, 2007). In addition, the presence of functional Qdm in the Q5^{k} leader sequence and its intracellular association with Qa-1 may predispose it to bind CD94/NKG2A receptors and inhibit cytotoxic cells that breach the blood/brain barrier during various pathological processes. Expression of the novel isoforms on the cell surface of model cells points to possible interactions with other types of known or unknown MHC-reactive receptors, such as, for example, class I-promiscuous, brain expressed paired immunoglobulin like receptor-B (PIR-B) (Syken et al., 2006). The widespread expression of *H2-Q5*^{k} in tumors may underscore its function as an immune suppressor, similar in some aspects to HLA-G in its leader signal properties, generation of alternatively spliced isoforms, and expression pattern favoring immune privileged sites.

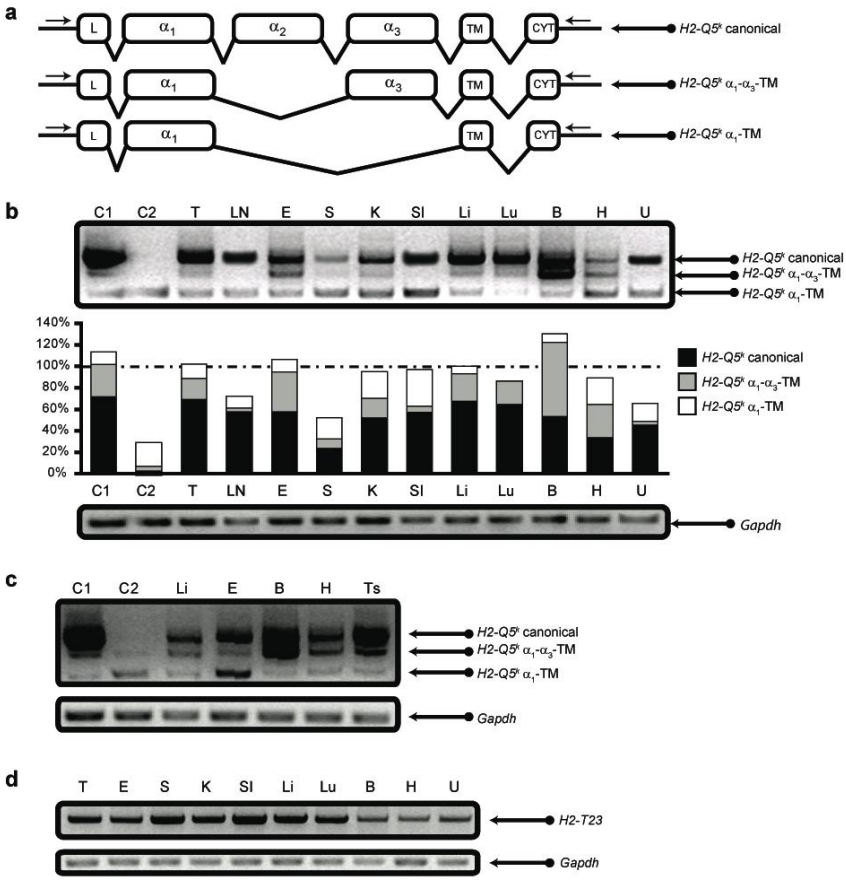

Fig. 1 Expression of alternatively spliced *H2-Q5*^{k} transcripts in *H2*^{k} tissues is most pronounced in the brain. **a** Diagram of the three novel *H2-Q5*^{k} isoforms confirmed by DNA cloning and sequencing of RT-PCR products. L: leader peptide coding exon 1; α_1-α_3: three extracellular (MHC α_1, α_2, α_3) domain coding exons 1-3; TM: transmembrane domain coding exon 5; CYT: cytoplasmic tail coding exon 6. The small arrows designate positions of gene spanning primers used for RT-PCR amplification of differentially spliced isoforms (Forward: 5'-GGCACCGGATCCCAGATGT-3', Reverse: 5'-CACCTGAA-CACATCGTCTGTCACTC-3'). Canonical *H2-Q5*^{k} and *H2-Q5*^{k} α_1-α_3-TM encode three extra amino acids (GKE) at the 3' end of the α_3 coding exon compared to the transcript sequence predicted by Weiss et al (1989). The cytoplasmic tail of all isoforms is encoded by the 3' portion of exon 5 and a single triplet (encoding G), located downstream of exon 5 and upstream of the reverse gene spanning primer (the exact position of exon 6 within this region is not known). The sequence of *H2-Q5*^{k} longest isoform matches the canonical AKR BW5147 thymoma *H2-Q5*^{k} sequence reported by Seo et al (1992).The sequences of all three isoforms have been submitted to GenBank and are awaiting assignment of a permanent identifier. **b upper panel** Tissue distribution of *H2-Q5*^{k} isoforms in adult female C3H/HeN mice and control cell lines revealed by semiquantitative RT-PCR. Control line C1: BW5147 (AKR *H2*^{k} derived thymoma); control cell line C2: B78H1 (C57BL/6-derived melanoma (see Fig. 2)). All RT-PCR reactions were performed using Platinum® Taq DNA Polymerase High Fidelity (Invitrogen,

Carlsbad, CA) with 32 amplification cycles on 200 ng total cellular RNA, isolated and purified from tissues using Tri Reagent® RT (Molecular Research Center, Inc., Cincinnati, OH) and reverse transcribed using the Omniscript® RT Kit (Qiagen, Valencia, CA). PCR products were run on a 1% agarose gel and visualized with ethidium bromide. All data shown are representative of at least three experiments. *Gapdh* transcript levels are shown to confirm cDNA quality. *Gapdh* primers F: 5'-TGAAGGTCGGTGT-GAACGGATTTG-3', R: 5'-GGCCTTCTCCATGGTGGTGAAGAC-3'.T: Thymus, LN: Lymph Node, E: Eye, S: Spleen, K: Kidney, SI: Small Intestine, Li: Liver, Lu: Lung, B: Brain, H: Heart, U: Uterus, Ts: Testis. **b lower panel** Densitometry analysis of the banding patterns shown in the upper panel b. The cumulative levels of isoforms detected in liver were arbitrarily set as 100%. **c** Semiquantitative RT-PCR on selected tissues of adult male C3H/HeN mice. The RT-PCR conditions were performed as in b. **d** Tissue expression analysis of *H2-T23* by semiquantitative RT-PCR. Primers used to amplify *H2-T23* were F: 5'-GTGAGGATGTTGCTTTTTGCC-3', R: 5'-AGCCCCCCTAGGGATTTTC-3'

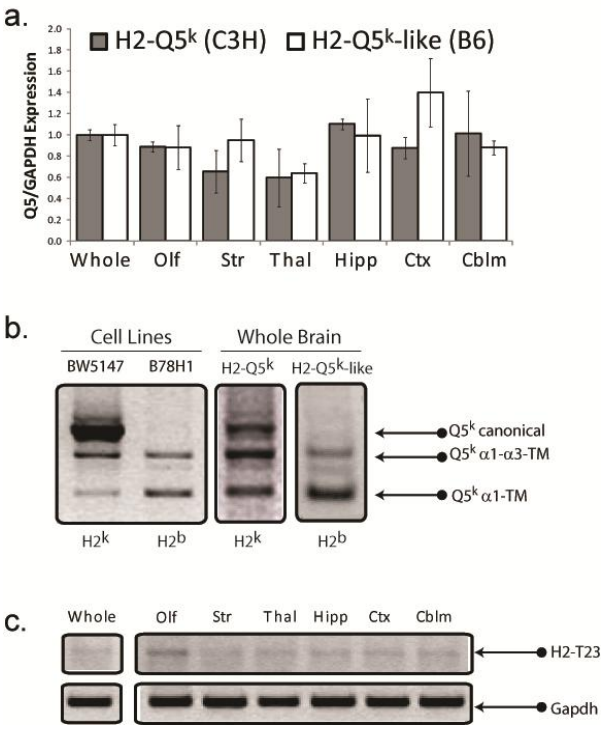

Fig. 2 *H2-Q5*^{k} homologous transcripts encoded by *H2*^{k} and *H2*^{b} mice are expressed throughout the brain. **a** Transcriptional activity of *H2-Q5*^{k} was monitored in different substructures of adult brains of C3H/HeN and C57BL/6 mice by quantitative, real time RT-PCR with primers hybridizing to all three isoforms of *H2-Q5*^{k} (specific to *H2-Q5*^{k} 5' UTR/exon 1 F: 5'-GGCACCGGATCCCAGATGTG-3' and exon 2 R: 5'-TCGGGGCTCCCCGAAGTT-3'). *Gapdh* primers were F: 5'-AGGTCGGTGT-GAACGGATTTG-3', R: 5'-TGTAGACCATGTAGTTGAGGTCA. Quantitative, real-time-PCR of various brain regions shows statistically equivalent expression of *H2-Q5*^{k} mixed isoform sequences in all brain regions ($p > 0.05$, $n = 4$). Real-time PCR was performed on 50 ng RNA isolated as in Fig. 1, deoxyribonuclease treated (Invitrogen), reverse transcribed using the Superscript® III Reverse Transcription Kit (Invitrogen) and amplified using SYBR® Green (Applied Biosystems, Foster City, CA) on an ABI Prism® 7700 Detection System (Applied Biosystems). Relative gene expression was calculated using the ΔΔCt method as described in Bookout et al (Bookout and Mangelsdorf, 2003); data were normalized to GAPDH and expressed as fold increase over whole brain. Mean ± SEM values are shown. Whole: Whole Brain, Olf: Olfactory Bulb, Str: Striatum, Thal: Thalamus, Hipp: Hippocampus, Ctx: Cortex, Cblm: Cerebellum. Semiquantitative RT-PCR performed on the same brain region samples revealed isoform distribution similar to those observed in the whole brain samples (data not shown and see b) **b** Differential expression pattern of *H2-Q5*^{k} isoforms in brains and tumors derived from *H2*^{k} and *H2*^{b} mice. Sequence identity of the middle and lower *H2-Q5*^{k}–like isoforms in B78H1 and C57Bl/6 testis was confirmed by sequencing of the DNA bands excised from agarose gels. **c** *H2-T23 (*encoding Qa-1) is transcribed at similar levels in all tested brain substructures. Conditions, primers and reagents for the RT-PCR in b and c were as described in Fig. 1

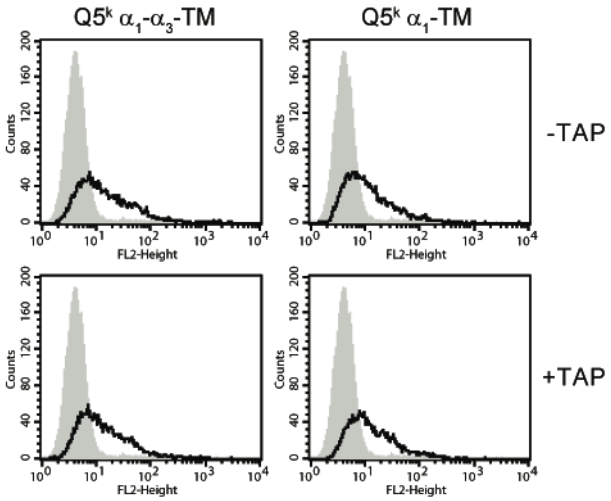

Fig. 3 Alternatively spliced *H2-Q5*^{k} isoforms are expressed on the cell surface of neural-crest-derived melanoma cells in a TAP-independent manner. N-terminally FLAG-tagged (DYKDDDDK) *H2-Q5*^{k} α_1-α_3-TM and *H2-Q5*^{k} α_1-TM (under the CMV promoter in the pCDNA3.1N vector, Invitrogen) were individually co-transfected into the B78H1 cells with and without the *Tap2* gene, as described in Chiang et al. (2003). Stable, antibiotic resistant transfectants were cloned, and the transcriptional activities of *Tap2* and the gene of interest were ascertained by RT-PCR. Q5^{k} expression was monitored in RT-PCR-analyzed clones by flow cytometry (FACScan^{TM} with CellQuest^{TM} Pro software, BD Biosciences, San Jose, CA) using polyclonal rabbit anti-FLAG® antibodies (Sigma-Aldrich, St. Louis, MO). The staining data shown is representative of multiple experiments on at least six different clones for each construct. The histograms filled with grey correspond to staining of vector-transfected B78H1 (background staining); histograms with thick black lines correspond to TAP-positive or negative B78H1 transfected with the indicated construct

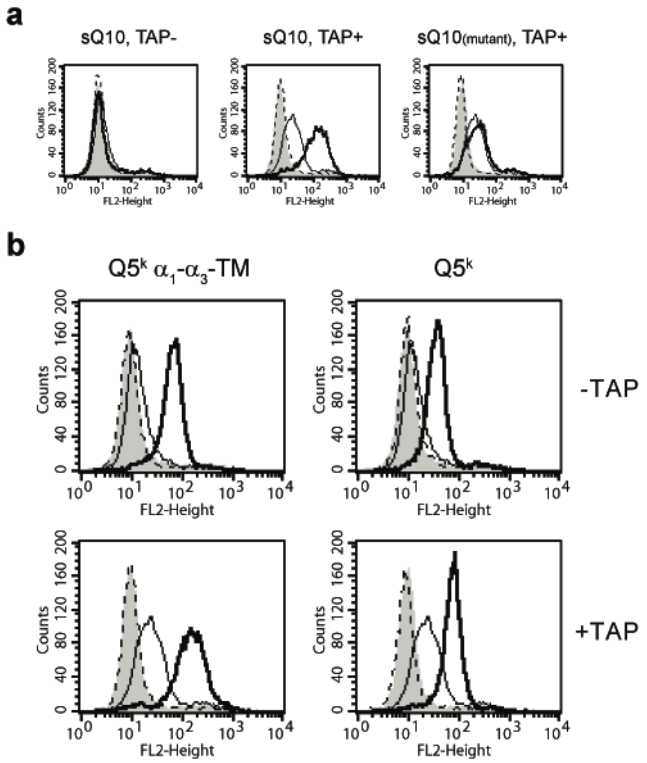

Fig. 4 Expression of canonical and alternatively spliced isoforms of *H2-Q5*^{k} upregulates Qa-1/β_2m complexes on the surface of melanoma cells. **a** Presence of the control, intact Qdm (AMAPRTLLL) in the Q10 leader upregulates Qa-1/β_2m in a TAP-dependent fashion. The cDNAs encoding soluble, canonical sQ10 and N-terminally truncated sQ10 α_3 (with altered Qdm sequence: MAPRTLLL) were inserted into the bicistronic pEFIRES-P vector under a strong EF1α promoter (Hobbs et al., 1998) and were stably transfected into the cloned B78H1 cells, positive or negative for *Tap2* and/or *H2-T23* transcripts (Imani and Soloski, 1991). All transfected cell lines were treated for 48 h with 20 U/mL IFNγ and assayed for surface Qa-1/β_2m expression by flow cytometry using anti-β_2m antibody S19.8. **b** The recombinant *H2-Q5*^{k} cDNAs encoding *H2-Q5*^{k} canonical and *H2-Q5*^{k} α_1-α_3-TM isoforms were constructed, transfected and tested for their ability to upregulate β_2m associated Qa-1 as described above. Results are representative of three independently performed experiments. All constructs were sequenced before transfection. Presence of the class I *Mhc* and *Tap2* transcripts in all clones and lines of B78H1 cells was confirmed by RT-PCR/sequencing. Growth conditions, antibiotic selection, subcloning methods and additional procedural details are described in (Guidry, 2008). Histogram in gray – Qa-1/β_2m on B78H1 cells transfected with empty vector control; thin line – Qa-1 expressing only; dotted line – sQ10 or Q5^{k} expressing isoform only; thick line – Qa-1 and indicated sQ10 or Q5^{k} isoform.

The sequences of class I MHC leader peptides (containing Qdm [underlined], predicted from exon DNA sequence) are as follows:

D^{b}: MG<u>AMAPRTLLL</u>LLAAALAPTQTRA
Q10: MG<u>AMAPRTLLL</u>LLAAALAPTQTQA
$Q5^{k}$: MW<u>AMAPRTLLL</u>LLAAALTLTQTRA

BIBLIOGRAPHY

ABEL, M. H. & HOLLINGSWORTH, M. 1986. Comparison of nifedipine and diltiazem with salbutamol for prevention of preterm delivery in the ovariectomized, oestrogen-treated late pregnant rat. *J Reprod Fertil,* 77**,** 559-68.

AGNEW, G. & TURNER, M. J. 2009. Vaginal prostaglandin gel to induce labour in women with one previous caesarean section. *J Obstet Gynaecol,* 29**,** 209-11.

ALBINSSON, S., SUAREZ, Y., SKOURA, A., OFFERMANNS, S., MIANO, J. M. & SESSA, W. C. 2010. MicroRNAs Are Necessary for Vascular Smooth Muscle Growth, Differentiation, and Function. *Arterioscler Thromb Vasc Biol*.

ALDRICH, C. J., DECLOUX, A., WOODS, A. S., COTTER, R. J., SOLOSKI, M. J. & FORMAN, J. 1994. Identification of a Tap-dependent leader peptide recognized by alloreactive T cells specific for a class Ib antigen. *Cell,* 79**,** 649-58.

ALLEN, H., FRASER, J., FLYER, D., CALVIN, S. & FLAVELL, R. 1986. Beta 2-microglobulin is not required for cell surface expression of the murine class I histocompatibility antigen H-2Db or of a truncated H-2Db. *Proc Natl Acad Sci U S A,* 83**,** 7447-51.

ALLPORT, V. C., PIEBER, D., SLATER, D. M., NEWTON, R., WHITE, J. O. & BENNETT, P. R. 2001. Human labour is associated with nuclear factor-kappaB activity which mediates cyclo-oxygenase-2 expression and is involved with the 'functional progesterone withdrawal'. *Mol Hum Reprod,* 7**,** 581-6.

AMBROS, V. 2004. The functions of animal microRNAs. *Nature,* 431**,** 350-5.

ANTONIJEVIC, I. A., DOUGLAS, A. J., DYE, S., BICKNELL, R. J., LENG, G. & RUSSELL, J. A. 1995. Oxytocin antagonists delay the initiation of parturition and prolong its active phase in rats. *J Endocrinol,* 145**,** 97-103.

BAI, A., ALDRICH, C. J. & FORMAN, J. 2000. Factors controlling the trafficking and processing of a leader-derived peptide presented by Qa-1. *J Immunol,* 165**,** 7025-34.

BALDUCCI, J., RISEK, B., GILULA, N. B., HAND, A., EGAN, J. F. & VINTZILEOS, A. M. 1993. Gap junction formation in human myometrium: a key to preterm labor? *Am J Obstet Gynecol,* 168**,** 1609-15.

BARTEL, D. P. 2009. MicroRNAs: target recognition and regulatory functions. *Cell,* 136**,** 215-33.

BLANKS, A. M. & THORNTON, S. 2003. The role of oxytocin in parturition. *BJOG,* 110 Suppl 20**,** 46-51.

BOOKOUT, A. L. & MANGELSDORF, D. J. 2003. Quantitative real-time PCR protocol for analysis of nuclear receptor signaling pathways. *Nucl Recept Signal,* 1**,** e012.

BOREN, T., XIONG, Y., HAKAM, A., WENHAM, R., APTE, S., WEI, Z., KAMATH, S., CHEN, D. T., DRESSMAN, H. & LANCASTER, J. M. 2008. MicroRNAs and their target messenger RNAs associated with endometrial carcinogenesis. *Gynecol Oncol,* 110**,** 206-15.

BRACKEN, C. P., GREGORY, P. A., KOLESNIKOFF, N., BERT, A. G., WANG, J., SHANNON, M. F. & GOODALL, G. J. 2008. A double-negative feedback loop between ZEB1-SIP1 and the microRNA-200 family regulates epithelial-mesenchymal transition. *Cancer Res,* 68**,** 7846-54.

BRAUD, V. M., ALLAN, D. S., O'CALLAGHAN, C. A., SODERSTROM, K., D'ANDREA, A., OGG, G. S., LAZETIC, S., YOUNG, N. T., BELL, J. I., PHILLIPS, J. H., LANIER, L. L. & MCMICHAEL, A. J. 1998. HLA-E binds to natural killer cell receptors CD94/NKG2A, B and C. *Nature,* 391**,** 795-9.

BROWN, A. G., LEITE, R. S. & STRAUSS, J. F., 3RD 2004. Mechanisms underlying "functional" progesterone withdrawal at parturition. *Ann N Y Acad Sci,* 1034**,** 36-49.

BURK, U., SCHUBERT, J., WELLNER, U., SCHMALHOFER, O., VINCAN, E., SPADERNA, S. & BRABLETZ, T. 2008. A reciprocal repression between ZEB1 and members of the miR-200 family promotes EMT and invasion in cancer cells. *EMBO Rep,* 9**,** 582-9.

CADEPOND, F., ULMANN, A. & BAULIEU, E. E. 1997. RU486 (mifepristone): mechanisms of action and clinical uses. *Annu Rev Med,* 48**,** 129-56.

CAI, X., HAGEDORN, C. H. & CULLEN, B. R. 2004. Human microRNAs are processed from capped, polyadenylated transcripts that can also function as mRNAs. *RNA,* 10**,** 1957-66.

CAROSELLA, E. D., FAVIER, B., ROUAS-FREISS, N., MOREAU, P. & LEMAOULT, J. 2008. Beyond the increasing complexity of the immunomodulatory HLA-G molecule. *Blood,* 111**,** 4862-70.

CHAKRABARTY, A., TRANGUCH, S., DAIKOKU, T., JENSEN, K., FURNEAUX, H. & DEY, S. K. 2007. MicroRNA regulation of cyclooxygenase-2 during embryo implantation. *Proc Natl Acad Sci U S A,* 104**,** 15144-9.

CHALLIS, J. R. G., MATTHEWS, S. G., GIBB, W. & LYE, S. J. 2000. Endocrine and paracrine regulation of birth at term and preterm. *Endocr Rev,* 21**,** 514-50.

CHEROUNY, P. H., PANKUCH, G. A., ROMERO, R., BOTTI, J. J., KUHN, D. C., DEMERS, L. M. & APPELBAUM, P. C. 1993. Neutrophil attractant/activating peptide-1/interleukin-8: association with histologic chorioamnionitis, preterm delivery, and bioactive amniotic fluid leukoattractants. *Am J Obstet Gynecol,* 169**,** 1299-303.

CHIANG, E. Y., HENSON, M. & STROYNOWSKI, I. 2003. Correction of defects responsible for impaired Qa-2 class Ib MHC expression on melanoma cells protects mice from tumor growth. *J Immunol,* 170**,** 4515-23.

CHOW, L. & LYE, S. J. 1994. Expression of the gap junction protein connexin-43 is increased in the human myometrium toward term and with the onset of labor. *Am J Obstet Gynecol,* 170**,** 788-95.

CHRISTOFFERSEN, N. R., SILAHTAROGLU, A., OROM, U. A., KAUPPINEN, S. & LUND, A. H. 2007. miR-200b mediates post-transcriptional repression of ZFHX1B. *RNA,* 13**,** 1172-8.

COMIJN, J., BERX, G., VERMASSEN, P., VERSCHUEREN, K., VAN GRUNSVEN, L., BRUYNEEL, E., MAREEL, M., HUYLEBROECK, D. & VAN ROY, F. 2001. The two-handed E box binding zinc finger protein SIP1 downregulates E-cadherin and induces invasion. *Mol Cell,* 7**,** 1267-78.

CONDON, J., YIN, S., MAYHEW, B., WORD, R. A., WRIGHT, W. E., SHAY, J. W. & RAINEY, W. E. 2002. Telomerase immortalization of human myometrial cells. *Biol Reprod,* 67**,** 506-14.

CONDON, J. C., HARDY, D. B., KOVARIC, K. & MENDELSON, C. R. 2006. Up-regulation of the progesterone receptor (PR)-C isoform in laboring myometrium by activation of nuclear factor-kappaB may contribute to the onset of labor through inhibition of PR function. *Mol Endocrinol,* 20**,** 764-75.

CONDON, J. C., JEYASURIA, P., FAUST, J. M. & MENDELSON, C. R. 2004. Surfactant protein secreted by the maturing mouse fetal lung acts as a hormone that signals the initiation of parturition. *Proc Natl Acad Sci U S A,* 101**,** 4978-83.

CONDON, J. C., JEYASURIA, P., FAUST, J. M., WILSON, J. W. & MENDELSON, C. R. 2003. A decline in the levels of progesterone receptor coactivators in the pregnant uterus at term may antagonize progesterone receptor function and contribute to the initiation of parturition. *Proc Natl Acad Sci U S A,* 100**,** 9518-23.

COX, S. M., CASEY, M. L. & MACDONALD, P. C. 1997. Accumulation of interleukin-1beta and interleukin-6 in amniotic fluid: a sequela of labour at term and preterm. *Hum Reprod Update,* 3**,** 517-27.

CREIGHTON, C. J., BENHAM, A. L., ZHU, H., KHAN, M. F., REID, J. G., NAGARAJA, A. K., FOUNTAIN, M. D., DZIADEK, O., HAN, D., MA, L., KIM, J., HAWKINS, S. M., ANDERSON, M. L., MATZUK, M. M. & GUNARATNE, P. H. 2010. Discovery of novel microRNAs in female reproductive tract using next generation sequencing. *PLoS One,* 5**,** e9637.

CSAPO, A. 1969. The luteo-placental shift, the guardian of pre-natal life. *Postgrad Med J,* 45**,** 57-64.

CSAPO, A. I., PULKKINEN, M. O. & WIEST, W. G. 1973. Effects of luteectomy and progesterone replacement therapy in early pregnant patients. *Am J Obstet Gynecol,* 115**,** 759-65.

DALLOT, E., POUCHELET, M., GOUHIER, N., CABROL, D., FERRE, F. & BREUILLER-FOUCHE, M. 2003. Contraction of cultured human uterine smooth muscle cells after stimulation with endothelin-1. *Biol Reprod,* 68**,** 937-42.

DARLING, D. S., STEARMAN, R. P., QI, Y., QIU, M. S. & FELLER, J. P. 2003. Expression of Zfhep/deltaEF1 protein in palate, neural progenitors, and differentiated neurons. *Gene Expr Patterns,* 3**,** 709-17.

DE, M. & WOOD, G. W. 1990. Influence of oestrogen and progesterone on macrophage distribution in the mouse uterus. *J Endocrinol,* 126**,** 417-24.

DECLOUX, A., WOODS, A. S., COTTER, R. J., SOLOSKI, M. J. & FORMAN, J. 1997. Dominance of a single peptide bound to the class I(B) molecule, Qa-1b. *J Immunol,* 158**,** 2183-91.

DEVLIN, J. J., LEW, A. M., FLAVELL, R. A. & COLIGAN, J. E. 1985. Secretion of a soluble class I molecule encoded by the Q10 gene of the C57BL/10 mouse. *Embo J,* 4**,** 369-74.

DORING, B., SHYNLOVA, O., TSUI, P., ECKARDT, D., JANSSEN-BIENHOLD, U., HOFMANN, F., FEIL, S., FEIL, R., LYE, S. J. & WILLECKE, K. 2006. Ablation of connexin43 in uterine smooth muscle cells of the mouse causes delayed parturition. *J Cell Sci,* 119**,** 1715-22.

DOUGLAS, A. J., LENG, G. & RUSSELL, J. A. 2002. The importance of oxytocin mechanisms in the control of mouse parturition. *Reproduction,* 123**,** 543-52.

DUDLEY, D. J., BRANCH, D. W., EDWIN, S. S. & MITCHELL, M. D. 1996. Induction of preterm birth in mice by RU486. *Biol Reprod,* 55**,** 992-5.

EGER, A., AIGNER, K., SONDEREGGER, S., DAMPIER, B., OEHLER, S., SCHREIBER, M., BERX, G., CANO, A., BEUG, H. & FOISNER, R. 2005. DeltaEF1 is a transcriptional repressor of E-cadherin and regulates epithelial plasticity in breast cancer cells. *Oncogene,* 24**,** 2375-85.

ELLIOTT, C. L., ALLPORT, V. C., LOUDON, J. A., WU, G. D. & BENNETT, P. R. 2001. Nuclear factor-kappa B is essential for up-regulation of

interleukin-8 expression in human amnion and cervical epithelial cells. *Mol Hum Reprod,* 7**,** 787-90.

FIDEL, P. I., JR., ROMERO, R., MAYMON, E. & HERTELENDY, F. 1998. Bacteria-induced or bacterial product-induced preterm parturition in mice and rabbits is preceded by a significant fall in serum progesterone concentrations. *J Matern Fetal Med,* 7**,** 222-6.

FITZGIBBON, J., MORRISON, J. J., SMITH, T. J. & O'BRIEN, M. 2009. Modulation of human uterine smooth muscle cell collagen contractility by thrombin, Y-27632, TNF alpha and indomethacin. *Reprod Biol Endocrinol,* 7**,** 2.

FLORIO, P., COBELLIS, L., WOODMAN, J., SEVERI, F. M., LINTON, E. A. & PETRAGLIA, F. 2002. Levels of maternal plasma corticotropin-releasing factor and urocortin during labor. *J Soc Gynecol Investig,* 9**,** 233-7.

FRIEDMAN, R. C., FARH, K. K., BURGE, C. B. & BARTEL, D. P. 2009. Most mammalian mRNAs are conserved targets of microRNAs. *Genome Res,* 19**,** 92-105.

FUCHS, A. R. 1995. Plasma, membrane receptors regulating myometrial contractility and their hormonal modulation. *Semin Perinatol,* 19**,** 15-30.

FUCHS, A. R., FIELDS, M. J., FREIDMAN, S., SHEMESH, M. & IVELL, R. 1995. Oxytocin and the timing of parturition. Influence of oxytocin receptor gene expression, oxytocin secretion, and oxytocin-induced prostaglandin F2 alpha and E2 release. *Adv Exp Med Biol,* 395**,** 405-20.

FUCHS, A. R., FUCHS, F., HUSSLEIN, P. & SOLOFF, M. S. 1984. Oxytocin receptors in the human uterus during pregnancy and parturition. *Am J Obstet Gynecol,* 150**,** 734-41.

FULTON, J. E., THACKER, E. L., BACON, L. D. & HUNT, H. D. 1995. Functional analysis of avian class I (BFIV) glycoproteins by epitope tagging and mutagenesis in vitro. *Eur J Immunol,* 25**,** 2069-76.

GEE, G. V., KOESTLER, D. C., CHRISTENSEN, B. C., SUGARBAKER, D. J., UGOLINI, D., IVALDI, G. P., RESNICK, M. B., HOUSEMAN, E. A., KELSEY, K. T. & MARSIT, C. J. Downregulated MicroRNAs in the differential diagnosis of malignant pleural mesothelioma. *Int J Cancer*.

GIBBONS, D. L., LIN, W., CREIGHTON, C. J., RIZVI, Z. H., GREGORY, P. A., GOODALL, G. J., THILAGANATHAN, N., DU, L., ZHANG, Y., PERTSEMLIDIS, A. & KURIE, J. M. 2009. Contextual extracellular cues promote tumor cell EMT and metastasis by regulating miR-200 family expression. *Genes Dev,* 23**,** 2140-51.

GONEN-GROSS, T. & MANDELBOIM, O. 2007. HLA-G complexes are observed on the cell surface. *Hum Immunol,* 68**,** 227-32.

GOODWIN, T. M., PAUL, R., SILVER, H., SPELLACY, W., PARSONS, M., CHEZ, R., HAYASHI, R., VALENZUELA, G., CREASY, G. W. & MERRIMAN, R. 1994. The effect of the oxytocin antagonist atosiban on preterm uterine activity in the human. *Am J Obstet Gynecol,* 170**,** 474-8.

GREGORY, P. A., BERT, A. G., PATERSON, E. L., BARRY, S. C., TSYKIN, A., FARSHID, G., VADAS, M. A., KHEW-GOODALL, Y. & GOODALL, G. J. 2008. The miR-200 family and miR-205 regulate epithelial to mesenchymal transition by targeting ZEB1 and SIP1. *Nat Cell Biol,* 10**,** 593-601.

GRIMSON, A., FARH, K. K., JOHNSTON, W. K., GARRETT-ENGELE, P., LIM, L. P. & BARTEL, D. P. 2007. MicroRNA targeting specificity in mammals: determinants beyond seed pairing. *Mol Cell,* 27**,** 91-105.

GUIDRY, P. A. 2008. *Tissue-Specific Transplantation Antigens: Structurally Unique Isoforms of MHC-Related Proteins in Immunologically Tolerant Milieus.* Ph.D., UT Southwestern.

GUIDRY, P. A. & STROYNOWSKI, I. 2005. The murine family of gut-restricted class Ib MHC includes alternatively spliced isoforms of the proposed HLA-G homolog, "blastocyst MHC". *J Immunol,* 175**,** 5248-59.

HADDAD, Y., CHOI, W. & MCCONKEY, D. J. 2009. Delta-crystallin enhancer binding factor 1 controls the epithelial to mesenchymal transition phenotype and resistance to the epidermal growth factor receptor inhibitor erlotinib in human head and neck squamous cell carcinoma lines. *Clin Cancer Res,* 15**,** 532-42.

HARDY, D. B., JANOWSKI, B. A., COREY, D. R. & MENDELSON, C. R. 2006. Progesterone receptor plays a major antiinflammatory role in human myometrial cells by antagonism of nuclear factor-kappaB activation of cyclooxygenase 2 expression. *Mol Endocrinol,* 20**,** 2724-33.

HASHIMOTO, H., ETO, T., ENDO, K., ITAI, G., KAMISAKO, T., SUEMIZU, H. & ITO, M. 2010. Comparative study of doses of exogenous progesterone administration needed to delay parturition in Jcl:MCH(ICR) mice. *Exp Anim,* 59**,** 521-4.

HASSAN, S. S., ROMERO, R., PINELES, B., TARCA, A. L., MONTENEGRO, D., EREZ, O., MITTAL, P., KUSANOVIC, J. P., MAZAKI-TOVI, S., ESPINOZA, J., NHAN-CHANG, C. L., DRAGHICI, S. & KIM, C. J. 2010. MicroRNA expression profiling of the human uterine cervix after term labor and delivery. *Am J Obstet Gynecol,* 202**,** 80 e1-8.

HERMEL, E., HART, A. J., GUNDUZ, I., ACTON, H., KIM, C., WURTH, M., UDDIN, S., SMITH, C., FISCHER LINDAHL, K. & ALDRICH, C. J. 2004. Polymorphism and conservation of the genes encoding Qa1 molecules. *Immunogenetics,* 56**,** 639-49.

HOBBS, S., JITRAPAKDEE, S. & WALLACE, J. C. 1998. Development of a bicistronic vector driven by the human polypeptide chain elongation factor 1alpha promoter for creation of stable mammalian cell lines that express very high levels of recombinant proteins. *Biochem Biophys Res Commun,* 252**,** 368-72.

HOFMEISTER, V. & WEISS, E. H. 2003. HLA-G modulates immune responses by diverse receptor interactions. *Semin Cancer Biol,* 13**,** 317-23.

HONG, X., LUENSE, L. J., MCGINNIS, L. K., NOTHNICK, W. B. & CHRISTENSON, L. K. 2008. Dicer1 is essential for female fertility and normal development of the female reproductive system. *Endocrinology,* 149**,** 6207-12.

HU, S. J., REN, G., LIU, J. L., ZHAO, Z. A., YU, Y. S., SU, R. W., MA, X. H., NI, H., LEI, W. & YANG, Z. M. 2008. MicroRNA expression and regulation in mouse uterus during embryo implantation. *J Biol Chem,* 283**,** 23473-84.

HUANG, Y. H., ZOZULYA, A. L., WEIDENFELLER, C., METZ, I., BUCK, D., TOYKA, K. V., BRUCK, W. & WIENDL, H. 2009. Specific central nervous system recruitment of HLA-G(+) regulatory T cells in multiple sclerosis. *Ann Neurol,* 66**,** 171-83.

HUNT, J. S. & LANGAT, D. L. 2009. HLA-G: a human pregnancy-related immunomodulator. *Curr Opin Pharmacol,* 9**,** 462-9.

HURT, E. M., SAYKALLY, J. N., ANOSE, B. M., KALLI, K. R. & SANDERS, M. M. 2008. Expression of the ZEB1 (deltaEF1) transcription factor in human: additional insights. *Mol Cell Biochem,* 318**,** 89-99.

HURTEAU, G. J., CARLSON, J. A., SPIVACK, S. D. & BROCK, G. J. 2007. Overexpression of the microRNA hsa-miR-200c leads to reduced expression of transcription factor 8 and increased expression of E-cadherin. *Cancer Res,* 67**,** 7972-6.

HUTVAGNER, G. & ZAMORE, P. D. 2002. A microRNA in a multiple-turnover RNAi enzyme complex. *Science,* 297**,** 2056-60.

IMAMURA, T., LUEDKE, C. E., VOGT, S. K. & MUGLIA, L. J. 2000. Oxytocin modulates the onset of murine parturition by competing ovarian and uterine effects. *Am J Physiol Regul Integr Comp Physiol,* 279**,** R1061-7.

IMANI, F. & SOLOSKI, M. J. 1991. Heat shock proteins can regulate expression of the Tla region-encoded class Ib molecule Qa-1. *Proc Natl Acad Sci U S A,* 88**,** 10475-9.

ISHIHARA, O., MATSUOKA, K., KINOSHITA, K., SULLIVAN, M. H. & ELDER, M. G. 1995. Interleukin-1 beta-stimulated PGE2 production from early first trimester human decidual cells is inhibited by dexamethasone and progesterone. *Prostaglandins,* 49**,** 15-26.

ISLAM, K. N. & MENDELSON, C. R. 2002. Potential role of nuclear factor kappaB and reactive oxygen species in cAMP and cytokine regulation of surfactant protein-A gene expression in lung type II cells. *Mol Endocrinol,* 16**,** 1428-40.

JENSEN, P. E., SULLIVAN, B. A., REED-LOISEL, L. M. & WEBER, D. A. 2004. Qa-1, a nonclassical class I histocompatibility molecule with roles in innate and adaptive immunity. *Immunol Res,* 29**,** 81-92.

JOBE, A. H. 2010. Lung maturation: the survival miracle of very low birth weight infants. *Pediatr Neonatol,* 51**,** 7-13.

JONES, S. A., BROOKS, A. N. & CHALLIS, J. R. 1989. Steroids modulate corticotropin-releasing hormone production in human fetal membranes and placenta. *J Clin Endocrinol Metab,* 68**,** 825-30.

KALKHOVEN, E., WISSINK, S., VAN DER SAAG, P. T. & VAN DER BURG, B. 1996. Negative interaction between the RelA(p65) subunit of NF-kappaB and the progesterone receptor. *J Biol Chem,* 271**,** 6217-24.

KAMBAYASHI, T., KRAFT-LEAVY, J. R., DAUNER, J. G., SULLIVAN, B. A., LAUR, O. & JENSEN, P. E. 2004. The nonclassical MHC class I molecule Qa-1 forms unstable peptide complexes. *J Immunol,* 172**,** 1661-9.

KARALIS, K., GOODWIN, G. & MAJZOUB, J. A. 1996. Cortisol blockade of progesterone: a possible molecular mechanism involved in the initiation of human labor. *Nat Med,* 2**,** 556-60.

KASTEN, F. H. 1975. Functional capacity of neonatal mammalian myocardial cells during aging in tissue culture. *Adv Exp Med Biol,* 53**,** 389-420.

KHVOROVA, A., REYNOLDS, A. & JAYASENA, S. D. 2003. Functional siRNAs and miRNAs exhibit strand bias. *Cell,* 115**,** 209-16.

KIM, V. N. 2004. MicroRNA precursors in motion: exportin-5 mediates their nuclear export. *Trends Cell Biol,* 14**,** 156-9.

KOBAYASHI, M., AKAHANE, M., MINAMI, K., MORO, M., AJISAWA, Y., INOUE, Y. & KAWARABAYASHI, T. 1999. Role of oxytocin in the initiation of term and preterm labor in rats: changes in oxytocin receptor density and plasma oxytocin concentration and the effect of an oxytocin antagonist, L-366,509. *Am J Obstet Gynecol,* 180**,** 621-7.

KORPAL, M., LEE, E. S., HU, G. & KANG, Y. 2008. The miR-200 family inhibits epithelial-mesenchymal transition and cancer cell migration by direct targeting of E-cadherin transcriptional repressors ZEB1 and ZEB2. *J Biol Chem,* 283**,** 14910-4.

KUMAR, N. M. & GILULA, N. B. 1996. The gap junction communication channel. *Cell,* 84**,** 381-8.

KUOKKANEN, S., CHEN, B., OJALVO, L., BENARD, L., SANTORO, N. & POLLARD, J. W. 2010. Genomic profiling of microRNAs and messenger

RNAs reveals hormonal regulation in microRNA expression in human endometrium. *Biol Reprod,* 82**,** 791-801.

KUREPA, Z., HASEMANN, C. A. & FORMAN, J. 1998. Qa-1b binds conserved class I leader peptides derived from several mammalian species. *J Exp Med,* 188**,** 973-8.

LAGOS-QUINTANA, M., RAUHUT, R., LENDECKEL, W. & TUSCHL, T. 2001. Identification of novel genes coding for small expressed RNAs. *Science,* 294**,** 853-8.

LAU, N. C., LIM, L. P., WEINSTEIN, E. G. & BARTEL, D. P. 2001. An abundant class of tiny RNAs with probable regulatory roles in Caenorhabditis elegans. *Science,* 294**,** 858-62.

LEE, J. W., CHOI, C. H., CHOI, J. J., PARK, Y. A., KIM, S. J., HWANG, S. Y., KIM, W. Y., KIM, T. J., LEE, J. H., KIM, B. G. & BAE, D. S. 2008a. Altered MicroRNA expression in cervical carcinomas. *Clin Cancer Res,* 14**,** 2535-42.

LEE, R. C. & AMBROS, V. 2001. An extensive class of small RNAs in Caenorhabditis elegans. *Science,* 294**,** 862-4.

LEE, R. H., STANCZYK, F. Z., STOLZ, A., JI, Q., YANG, G. & GOODWIN, T. M. 2008b. AKR1C1 and SRD5A1 messenger RNA expression at term in the human myometrium and chorioamniotic membranes. *Am J Perinatol,* 25**,** 577-82.

LEE, Y., AHN, C., HAN, J., CHOI, H., KIM, J., YIM, J., LEE, J., PROVOST, P., RADMARK, O., KIM, S. & KIM, V. N. 2003. The nuclear RNase III Drosha initiates microRNA processing. *Nature,* 425**,** 415-9.

LEE, Y., JEON, K., LEE, J. T., KIM, S. & KIM, V. N. 2002. MicroRNA maturation: stepwise processing and subcellular localization. *EMBO J,* 21**,** 4663-70.

LEE, Y. S., TERZIDOU, V., LINDSTROM, T., JOHNSON, M. & BENNETT, P. R. 2005. The role of CCAAT/enhancer-binding protein beta in the transcriptional regulation of COX-2 in human amnion. *Mol Hum Reprod,* 11**,** 853-8.

LEI, L., JIN, S., GONZALEZ, G., BEHRINGER, R. R. & WOODRUFF, T. K. 2010. The regulatory role of Dicer in folliculogenesis in mice. *Mol Cell Endocrinol,* 315**,** 63-73.

LEWIS, B. P., BURGE, C. B. & BARTEL, D. P. 2005. Conserved seed pairing, often flanked by adenosines, indicates that thousands of human genes are microRNA targets. *Cell,* 120**,** 15-20.

LIGGINS, G. C. 1969. Premature delivery of foetal lambs infused with glucocorticoids. *J Endocrinol,* 45**,** 515-23.

LIGGINS, G. C., FAIRCLOUGH, R. J., GRIEVES, S. A., KENDALL, J. Z. & KNOX, B. S. 1973. The mechanism of initiation of parturition in the ewe. *Recent Prog Horm Res,* 29**,** 111-59.

LIM, L. P., GLASNER, M. E., YEKTA, S., BURGE, C. B. & BARTEL, D. P. 2003a. Vertebrate microRNA genes. *Science,* 299**,** 1540.

LIM, L. P., LAU, N. C., WEINSTEIN, E. G., ABDELHAKIM, A., YEKTA, S., RHOADES, M. W., BURGE, C. B. & BARTEL, D. P. 2003b. The microRNAs of Caenorhabditis elegans. *Genes Dev,* 17**,** 991-1008.

LIPSCOMBE, D. 2005. Neuronal proteins custom designed by alternative splicing. *Curr Opin Neurobiol,* 15**,** 358-63.

LUND, E., GUTTINGER, S., CALADO, A., DAHLBERG, J. E. & KUTAY, U. 2004. Nuclear export of microRNA precursors. *Science,* 303**,** 95-8.

LYDON, J. P., DEMAYO, F. J., FUNK, C. R., MANI, S. K., HUGHES, A. R., MONTGOMERY, C. A., JR., SHYAMALA, G., CONNEELY, O. M. & O'MALLEY, B. W. 1995. Mice lacking progesterone receptor exhibit pleiotropic reproductive abnormalities. *Genes Dev,* 9**,** 2266-78.

MARSH, E. E., LIN, Z., YIN, P., MILAD, M., CHAKRAVARTI, D. & BULUN, S. E. 2008. Differential expression of microRNA species in human uterine leiomyoma versus normal myometrium. *Fertil Steril,* 89**,** 1771-6.

MARTIN, J. A., HAMILTON, B. E., SUTTON, P. D., VENTURA, S. J., MENACKER, F., KIRMEYER, S. & MUNSON, M. L. 2007. Births: final data for 2005. *Natl Vital Stat Rep,* 56**,** 1-103.

MEGRET, F., PREHAUD, C., LAFAGE, M., MOREAU, P., ROUAS-FREISS, N., CAROSELLA, E. D. & LAFON, M. 2007. Modulation of HLA-G and HLA-E expression in human neuronal cells after rabies virus or herpes virus simplex type 1 infections. *Hum Immunol,* 68**,** 294-302.

MELLOR, A. L., WEISS, E. H., KRESS, M., JAY, G. & FLAVELL, R. A. 1984. A nonpolymorphic class I gene in the murine major histocompatibility complex. *Cell,* 36**,** 139-44.

MENDELSON, C. R. 2009. Minireview: fetal-maternal hormonal signaling in pregnancy and labor. *Mol Endocrinol,* 23**,** 947-54.

MENDELSON, C. R. & BOGGARAM, V. 1990. Hormonal and developmental regulation of pulmonary surfactant synthesis in fetal lung. *Baillieres Clin Endocrinol Metab,* 4**,** 351-78.

MERLINO, A. A., WELSH, T. N., TAN, H., YI, L. J., CANNON, V., MERCER, B. M. & MESIANO, S. 2007. Nuclear progesterone receptors in the human pregnancy myometrium: evidence that parturition involves functional progesterone withdrawal mediated by increased expression of progesterone receptor-A. *J Clin Endocrinol Metab,* 92**,** 1927-33.

MESIANO, S. 2004. Myometrial progesterone responsiveness and the control of human parturition. *J Soc Gynecol Investig,* 11**,** 193-202.

MESIANO, S., CHAN, E. C., FITTER, J. T., KWEK, K., YEO, G. & SMITH, R. 2002. Progesterone withdrawal and estrogen activation in human parturition are coordinated by progesterone receptor A expression in the myometrium. *J Clin Endocrinol Metab,* 87**,** 2924-30.

MILLER, J. D., WEBER, D. A., IBEGBU, C., POHL, J., ALTMAN, J. D. & JENSEN, P. E. 2003. Analysis of HLA-E peptide-binding specificity and contact residues in bound peptide required for recognition by CD94/NKG2. *J Immunol,* 171**,** 1369-75.

MILLER, L. & HUNT, J. S. 1998. Regulation of TNF-alpha production in activated mouse macrophages by progesterone. *J Immunol,* 160**,** 5098-104.

MITCHELL, B. F. & TAGGART, M. J. 2009. Are animal models relevant to key aspects of human parturition? *Am J Physiol Regul Integr Comp Physiol,* 297**,** R525-45.

MITCHELL, M. D., MACDONALD, P. C. & CASEY, M. L. 1984. Stimulation of prostaglandin E2 synthesis in human amnion cells maintained in monolayer culture by a substance(s) in amniotic fluid. *Prostaglandins Leukot Med,* 15**,** 399-407.

MIYOSHI, T., MARUHASHI, M., VAN DE PUTTE, T., KONDOH, H., HUYLEBROECK, D. & HIGASHI, Y. 2006. Complementary expression pattern of Zfhx1 genes Sip1 and deltaEF1 in the mouse embryo and their genetic interaction revealed by compound mutants. *Dev Dyn,* 235**,** 1941-52.

MOLLARD, P., MIRONNEAU, J., AMEDEE, T. & MIRONNEAU, C. 1986. Electrophysiological characterization of single pregnant rat myometrial cells in short-term primary culture. *Am J Physiol,* 250**,** C47-54.

MUGLIA, L. J., BAE, D. S., BROWN, T. T., VOGT, S. K., ALVAREZ, J. G., SUNDAY, M. E. & MAJZOUB, J. A. 1999. Proliferation and differentiation defects during lung development in corticotropin-releasing hormone-deficient mice. *Am J Respir Cell Mol Biol,* 20**,** 181-8.

NAGARAJA, A. K., ANDREU-VIEYRA, C., FRANCO, H. L., MA, L., CHEN, R., HAN, D. Y., ZHU, H., AGNO, J. E., GUNARATNE, P. H., DEMAYO, F. J. & MATZUK, M. M. 2008. Deletion of Dicer in somatic cells of the female reproductive tract causes sterility. *Mol Endocrinol,* 22**,** 2336-52.

NELLES, L., VAN DE PUTTE, T., VAN GRUNSVEN, L., HUYLEBROECK, D. & VERSCHUEREN, K. 2003. Organization of the mouse Zfhx1b gene encoding the two-handed zinc finger repressor Smad-interacting protein-1. *Genomics,* 82**,** 460-9.

NEUMANN, H., SCHMIDT, H., CAVALIE, A., JENNE, D. & WEKERLE, H. 1997. Major histocompatibility complex (MHC) class I gene expression in single neurons of the central nervous system: differential regulation by

interferon (IFN)-gamma and tumor necrosis factor (TNF)-alpha. *J Exp Med,* 185**,** 305-16.

NISHIMORI, K., YOUNG, L. J., GUO, Q., WANG, Z., INSEL, T. R. & MATZUK, M. M. 1996. Oxytocin is required for nursing but is not essential for parturition or reproductive behavior. *Proc Natl Acad Sci U S A,* 93**,** 11699-704.

NOGUCHI, K., KUWADA, E., GOTO, S. & EGAWA, K. 2004. Tumor cell-specific transcription of a murine histocompatibility class Ib Q5 gene. *Anticancer Res,* 24**,** 3379-86.

OLIVEIRA, C. C., VAN VEELEN, P. A., QUERIDO, B., DE RU, A., SLUIJTER, M., LABAN, S., DRIJFHOUT, J. W., VAN DER BURG, S. H., OFFRINGA, R. & VAN HALL, T. 2010. The nonpolymorphic MHC Qa-1b mediates CD8+ T cell surveillance of antigen-processing defects. *J Exp Med,* 207**,** 207-21.

OLSON, D. M. 2003. The role of prostaglandins in the initiation of parturition. *Best Pract Res Clin Obstet Gynaecol,* 17**,** 717-30.

OLSON, D. M., SKINNER, K. & CHALLIS, J. R. 1983a. Estradiol-17 beta and 2-hydroxyestradiol-17 beta-induced differential production of prostaglandins by cells dispersed from human intrauterine tissues at parturition. *Prostaglandins,* 25**,** 639-51.

OLSON, D. M., SKINNER, K. & CHALLIS, J. R. 1983b. Prostaglandin output in relation to parturition by cells dispersed from human intrauterine tissues. *J Clin Endocrinol Metab,* 57**,** 694-9.

ORSINO, A., TAYLOR, C. V. & LYE, S. J. 1996. Connexin-26 and connexin-43 are differentially expressed and regulated in the rat myometrium throughout late pregnancy and with the onset of labor. *Endocrinology,* 137**,** 1545-53.

OSMAN, I., YOUNG, A., LEDINGHAM, M. A., THOMSON, A. J., JORDAN, F., GREER, I. A. & NORMAN, J. E. 2003. Leukocyte density and pro-inflammatory cytokine expression in human fetal membranes, decidua, cervix and myometrium before and during labour at term. *Mol Hum Reprod,* 9**,** 41-5.

PAN, Q., LUO, X., TOLOUBEYDOKHTI, T. & CHEGINI, N. 2007. The expression profile of micro-RNA in endometrium and endometriosis and the influence of ovarian steroids on their expression. *Mol Hum Reprod,* 13**,** 797-806.

PARK, S. M., GAUR, A. B., LENGYEL, E. & PETER, M. E. 2008. The miR-200 family determines the epithelial phenotype of cancer cells by targeting the E-cadherin repressors ZEB1 and ZEB2. *Genes Dev,* 22**,** 894-907.

PINELES, B. L., ROMERO, R., MONTENEGRO, D., TARCA, A. L., HAN, Y. M., KIM, Y. M., DRAGHICI, S., ESPINOZA, J., KUSANOVIC, J. P.,

MITTAL, P., HASSAN, S. S. & KIM, C. J. 2007. Distinct subsets of microRNAs are expressed differentially in the human placentas of patients with preeclampsia. *Am J Obstet Gynecol,* 196**,** 261 e1-6.

POMINI, F., CARUSO, A. & CHALLIS, J. R. 1999. Interleukin-10 modifies the effects of interleukin-1beta and tumor necrosis factor-alpha on the activity and expression of prostaglandin H synthase-2 and the NAD+-dependent 15-hydroxyprostaglandin dehydrogenase in cultured term human villous trophoblast and chorion trophoblast cells. *J Clin Endocrinol Metab,* 84**,** 4645-51.

POSTIGO, A. A. & DEAN, D. C. 1999. ZEB represses transcription through interaction with the corepressor CtBP. *Proc Natl Acad Sci U S A,* 96**,** 6683-8.

PYO, C. W., WILLIAMS, L. M., MOORE, Y., HYODO, H., LI, S. S., ZHAO, L. P., SAGESHIMA, N., ISHITANI, A. & GERAGHTY, D. E. 2006. HLA-E, HLA-F, and HLA-G polymorphism: genomic sequence defines haplotype structure and variation spanning the nonclassical class I genes. *Immunogenetics,* 58**,** 241-51.

REESE, J., PARIA, B. C., BROWN, N., ZHAO, X., MORROW, J. D. & DEY, S. K. 2000. Coordinated regulation of fetal and maternal prostaglandins directs successful birth and postnatal adaptation in the mouse. *Proc Natl Acad Sci U S A,* 97**,** 9759-64.

REMACLE, J. E., KRAFT, H., LERCHNER, W., WUYTENS, G., COLLART, C., VERSCHUEREN, K., SMITH, J. C. & HUYLEBROECK, D. 1999. New mode of DNA binding of multi-zinc finger transcription factors: deltaEF1 family members bind with two hands to two target sites. *EMBO J,* 18**,** 5073-84.

REYES-ENGEL, A., LE ROY, E., DIEGUES, J. L. & FERNANDEZ, N. 1993. Unusual expression pattern of the MHC class I Q5k gene in the AKR mouse: possible role in embryo development. *J Reprod Immunol,* 23**,** 73-81.

RHEE, S. & GRINNELL, F. 2007. Fibroblast mechanics in 3D collagen matrices. *Adv Drug Deliv Rev,* 59**,** 1299-305.

RIEMER, R. K. & HEYMANN, M. A. 1998. Regulation of uterine smooth muscle function during gestation. *Pediatr Res,* 44**,** 615-27.

RO, S., SONG, R., PARK, C., ZHENG, H., SANDERS, K. M. & YAN, W. 2007. Cloning and expression profiling of small RNAs expressed in the mouse ovary. *RNA,* 13**,** 2366-80.

ROBINSON, P. J., BEVEC, D., MELLOR, A. L. & WEISS, E. H. 1988. Sequence of the mouse Q4 class I gene and characterization of the gene product. *Immunogenetics,* 27**,** 79-86.

ROBINSON, P. J., TRAVERS, P. J., STACKPOOLE, A., FLAHERTY, L. & DJABALLAH, H. 1998. Maturation of Qa-1b class I molecules requires beta 2-microglobulin but is TAP independent. *J Immunol,* 160**,** 3217-24.

RODGERS, J. R. & COOK, R. G. 2005. MHC class Ib molecules bridge innate and acquired immunity. *Nat Rev Immunol,* 5**,** 459-71.

ROMERO, R., ESPINOZA, J., GONCALVES, L. F., KUSANOVIC, J. P., FRIEL, L. & HASSAN, S. 2007. The role of inflammation and infection in preterm birth. *Semin Reprod Med,* 25**,** 21-39.

SCHWARZ, D. S., HUTVAGNER, G., DU, T., XU, Z., ARONIN, N. & ZAMORE, P. D. 2003. Asymmetry in the assembly of the RNAi enzyme complex. *Cell,* 115**,** 199-208.

SCHWEMMLE, S., BEVEC, D., BREM, G., URBAN, M. B., BAEUERLE, P. A. & WEISS, E. H. 1991. Developmental and tissue-specific expression of the Q5k gene. *Immunogenetics,* 34**,** 28-38.

SEGAL, B. M. 2007. The role of natural killer cells in curbing neuroinflammation. *J Neuroimmunol,* 191**,** 2-7.

SEKIDO, R., MURAI, K., FUNAHASHI, J., KAMACHI, Y., FUJISAWA-SEHARA, A., NABESHIMA, Y. & KONDOH, H. 1994. The delta-crystallin enhancer-binding protein delta EF1 is a repressor of E2-box-mediated gene activation. *Mol Cell Biol,* 14**,** 5692-700.

SEO, N., OKAZAKI, T., NAKANISHI-ITO, C., TANINO, T., MATSUDAIRA, Y., TAKAHASHI, T. & EGAWA, K. 1992. Expression of the Qa-2k phenotype encoded by the Q5k gene on the surface of tumor cells derived from H-2k mice. *J Exp Med,* 175**,** 647-54.

SHATZ, C. J. 2009. MHC class I: an unexpected role in neuronal plasticity. *Neuron,* 64**,** 40-5.

SHAW, G. & RENFREE, M. B. 2001. Fetal control of parturition in marsupials. *Reprod Fertil Dev,* 13**,** 653-9.

SHYNLOVA, O., TSUI, P., DOROGIN, A. & LYE, S. J. 2008. Monocyte chemoattractant protein-1 (CCL-2) integrates mechanical and endocrine signals that mediate term and preterm labor. *J Immunol,* 181**,** 1470-9.

SHYNLOVA, O., TSUI, P., JAFFER, S. & LYE, S. J. 2009. Integration of endocrine and mechanical signals in the regulation of myometrial functions during pregnancy and labour. *Eur J Obstet Gynecol Reprod Biol,* 144 Suppl 1**,** S2-10.

SHYNLOVA, O. P., OLDENHOF, A. D., LIU, M., LANGILLE, L. & LYE, S. J. 2002. Regulation of c-fos expression by static stretch in rat myometrial smooth muscle cells. *Am J Obstet Gynecol,* 186**,** 1358-65.

SILER-KHODR, T. M., KANG, I. S. & KOONG, M. K. 1996. Dose-related action of estradiol on placental prostanoid prediction. *Prostaglandins,* 51**,** 387-401.

SINGER, D. S. & MAGUIRE, J. E. 1990. Regulation of the expression of class I MHC genes. *Crit Rev Immunol,* 10**,** 235-57.

SKINNER, K. A. & CHALLIS, J. R. 1985. Changes in the synthesis and metabolism of prostaglandins by human fetal membranes and decidua at labor. *Am J Obstet Gynecol,* 151**,** 519-23.

SMALHEISER, N. R. 2003. EST analyses predict the existence of a population of chimeric microRNA precursor-mRNA transcripts expressed in normal human and mouse tissues. *Genome Biol,* 4**,** 403.

SMITH, S. K. & KELLY, R. W. 1987. The effect of the antiprogestins RU 486 and ZK 98734 on the synthesis and metabolism of prostaglandins F2 alpha and E2 in separated cells from early human decidua. *J Clin Endocrinol Metab,* 65**,** 527-34.

SOLOFF, M. S., COOK, D. L., JR., JENG, Y. J. & ANDERSON, G. D. 2004. In situ analysis of interleukin-1-induced transcription of cox-2 and il-8 in cultured human myometrial cells. *Endocrinology,* 145**,** 1248-54.

SOORANNA, S. R., LEE, Y., KIM, L. U., MOHAN, A. R., BENNETT, P. R. & JOHNSON, M. R. 2004. Mechanical stretch activates type 2 cyclooxygenase via activator protein-1 transcription factor in human myometrial cells. *Mol Hum Reprod,* 10**,** 109-13.

SPITZ, I. M. & BARDIN, C. W. 1993. Mifepristone (RU 486)--a modulator of progestin and glucocorticoid action. *N Engl J Med,* 329**,** 404-12.

SPOELSTRA, N. S., MANNING, N. G., HIGASHI, Y., DARLING, D., SINGH, M., SHROYER, K. R., BROADDUS, R. R., HORWITZ, K. B. & RICHER, J. K. 2006. The transcription factor ZEB1 is aberrantly expressed in aggressive uterine cancers. *Cancer Res,* 66**,** 3893-902.

SULLIVAN, D. A. & WIRA, C. R. 1984. Hormonal regulation of immunoglobulins in the rat uterus: uterine response to multiple estradiol treatments. *Endocrinology,* 114**,** 650-8.

SYKEN, J., GRANDPRE, T., KANOLD, P. O. & SHATZ, C. J. 2006. PirB restricts ocular-dominance plasticity in visual cortex. *Science,* 313**,** 1795-800.

TAKAYANAGI, Y., YOSHIDA, M., BIELSKY, I. F., ROSS, H. E., KAWAMATA, M., ONAKA, T., YANAGISAWA, T., KIMURA, T., MATZUK, M. M., YOUNG, L. J. & NISHIMORI, K. 2005. Pervasive social deficits, but normal parturition, in oxytocin receptor-deficient mice. *Proc Natl Acad Sci U S A,* 102**,** 16096-101.

THOMSON, A. J., TELFER, J. F., YOUNG, A., CAMPBELL, S., STEWART, C. J., CAMERON, I. T., GREER, I. A. & NORMAN, J. E. 1999. Leukocytes infiltrate the myometrium during human parturition: further evidence that labour is an inflammatory process. *Hum Reprod,* 14**,** 229-36.

TIBBETTS, T. A., CONNEELY, O. M. & O'MALLEY, B. W. 1999. Progesterone via its receptor antagonizes the pro-inflammatory activity of estrogen in the mouse uterus. *Biol Reprod,* 60**,** 1158-65.

TORRICELLI, M., GIOVANNELLI, A., LEUCCI, E., DE FALCO, G., REIS, F. M., IMPERATORE, A., FLORIO, P. & PETRAGLIA, F. 2007. Labor (term and preterm) is associated with changes in the placental mRNA expression of corticotrophin-releasing factor. *Reprod Sci,* 14**,** 241-5.

TRANSY, C., NASH, S. R., DAVID-WATINE, B., COCHET, M., HUNT, S. W., 3RD, HOOD, L. E. & KOURILSKY, P. 1987. A low polymorphic mouse H-2 class I gene from the Tla complex is expressed in a broad variety of cell types. *J Exp Med,* 166**,** 341-61.

TSUBOI, K., IWANE, A., NAKAZAWA, S., SUGIMOTO, Y. & ICHIKAWA, A. 2003. Role of prostaglandin H2 synthase 2 in murine parturition: study on ovariectomy-induced parturition in prostaglandin F receptor-deficient mice. *Biol Reprod,* 69**,** 195-201.

TSUBOI, K., SUGIMOTO, Y., IWANE, A., YAMAMOTO, K., YAMAMOTO, S. & ICHIKAWA, A. 2000. Uterine expression of prostaglandin H2 synthase in late pregnancy and during parturition in prostaglandin F receptor-deficient mice. *Endocrinology,* 141**,** 315-24.

TULCHINSKY, D., HOBEL, C. J., YEAGER, E. & MARSHALL, J. R. 1972. Plasma estrone, estradiol, estriol, progesterone, and 17-hydroxyprogesterone in human pregnancy. I. Normal pregnancy. *Am J Obstet Gynecol,* 112**,** 1095-100.

VAN GRUNSVEN, L. A., SCHELLENS, A., HUYLEBROECK, D. & VERSCHUEREN, K. 2001. SIP1 (Smad interacting protein 1) and deltaEF1 (delta-crystallin enhancer binding factor) are structurally similar transcriptional repressors. *J Bone Joint Surg Am,* 83-A Suppl 1**,** S40-7.

VANCE, R. E., KRAFT, J. R., ALTMAN, J. D., JENSEN, P. E. & RAULET, D. H. 1998. Mouse CD94/NKG2A is a natural killer cell receptor for the nonclassical major histocompatibility complex (MHC) class I molecule Qa-1(b). *J Exp Med,* 188**,** 1841-8.

VANDEWALLE, C., COMIJN, J., DE CRAENE, B., VERMASSEN, P., BRUYNEEL, E., ANDERSEN, H., TULCHINSKY, E., VAN ROY, F. & BERX, G. 2005. SIP1/ZEB2 induces EMT by repressing genes of different epithelial cell-cell junctions. *Nucleic Acids Res,* 33**,** 6566-78.

VERSCHUEREN, K., REMACLE, J. E., COLLART, C., KRAFT, H., BAKER, B. S., TYLZANOWSKI, P., NELLES, L., WUYTENS, G., SU, M. T., BODMER, R., SMITH, J. C. & HUYLEBROECK, D. 1999. SIP1, a novel zinc finger/homeodomain repressor, interacts with Smad proteins and binds to 5'-CACCT sequences in candidate target genes. *J Biol Chem,* 274**,** 20489-98.

VIRGO, B. B. & BELLWARD, G. D. 1974. Serum progesterone levels in the pregnant and postpartum laboratory mouse. *Endocrinology,* 95**,** 1486-90.

WANG, J., LEE, S., TEH, C. E., BUNTING, K., MA, L. & SHANNON, M. F. 2009. The transcription repressor, ZEB1, cooperates with CtBP2 and HDAC1 to suppress IL-2 gene activation in T cells. *Int Immunol,* 21**,** 227-35.

WATTS, S., DAVIS, A. C., GAUT, B., WHEELER, C., HILL, L. & GOODENOW, R. S. 1989. Organization and structure of the Qa genes of the major histocompatibility complex of the C3H mouse: implications for Qa function and class I evolution. *Embo J,* 8**,** 1749-59.

WEISS, E. H., BEVEC, D., MESSER, G., SCHWEMMLE, S., GROSSHAUS, C., STEINMETZ, M. & SCHMIDT, W. 1989. Organization of the AKR Qa region: structure of a divergent class I sequence, Q5k. *J Immunogenet,* 16**,** 283-90.

WIENDL, H., MITSDOERFFER, M., HOFMEISTER, V., WISCHHUSEN, J., BORNEMANN, A., MEYERMANN, R., WEISS, E. H., MELMS, A. & WELLER, M. 2002. A functional role of HLA-G expression in human gliomas: an alternative strategy of immune escape. *J Immunol,* 168**,** 4772-80.

WILLECKE, K., EIBERGER, J., DEGEN, J., ECKARDT, D., ROMUALDI, A., GULDENAGEL, M., DEUTSCH, U. & SOHL, G. 2002. Structural and functional diversity of connexin genes in the mouse and human genome. *Biol Chem,* 383**,** 725-37.

WIRA, C. R. & SANDOE, C. P. 1977. Sex steroid hormone regulation of IgA and IgG in rat uterine secretions. *Nature,* 268**,** 534-6.

YI, R., QIN, Y., MACARA, I. G. & CULLEN, B. R. 2003. Exportin-5 mediates the nuclear export of pre-microRNAs and short hairpin RNAs. *Genes Dev,* 17**,** 3011-6.

YOUNG, W. S., 3RD, SHEPARD, E., AMICO, J., HENNIGHAUSEN, L., WAGNER, K. U., LAMARCA, M. E., MCKINNEY, C. & GINNS, E. I. 1996. Deficiency in mouse oxytocin prevents milk ejection, but not fertility or parturition. *J Neuroendocrinol,* 8**,** 847-53.

ZINGG, H. H., ROZEN, F., CHU, K., LARCHER, A., ARSLAN, A., RICHARD, S. & LEFEBVRE, D. 1995. Oxytocin and oxytocin receptor gene expression in the uterus. *Recent Prog Horm Res,* 50**,** 255-73.